Università degli Studi di Padova

Dipartimento di Fisica e Astronomia "Galileo Galilei"

Corso di Laurea Magistrale in

Fisica

Modeling pedestrian dynamics by means of Discrete Thermostatted Kinetic Theory methods

Relatore:
prof. Enzo Orlandini
Dip. di Fisica e Astronomia "Galileo Galilei", UniPd

Correlatore:
prof. Carlo Bianca
Laboratoire de Physique Statistique, ENS Paris

Laureando:
Caterina Mogno
Matricola:
1105565

Anno Accademico: 2015/2016

Abstract: A novel discrete thermostatted kinetic framework is derived for the modeling of complex adaptive systems subjected to external force field (non-equilibrium system). In order to model the non-equilibrium stationary states of the system, the external force field is coupled to a dissipative term (thermostat). The well-posedness of the new framework is mathematically investigated (local and global existence and uniqueness of solution of the related Cauchy problem) thus allowing the framework to be suitable for the derivation of specific models and the related computational analysis. This framework is employed for the modeling of the pedestrian dynamics at the entrance of a metro station. Specifically a model is proposed for analysing the time distribution of the pedestrians approaching at different gates (turnistiles) according to a choice dynamics which depends on the microscopic interactions among the pedestrians (internal dynamics). The microscopic interactions, assumed binary, depend on the local pedestrians density (nonlinear interactions) and follow a game theory approach based on the leader-follower dynamics. The external force field mimics different events that can affect significantly pedestrian internal dynamics (collective hurry, preferential gates recommended, periodic sound signals or evacuation alarms), and the thermostat term allows the conservation of the total number of pedestrians. Numerical simulations are addressed to analyse the system behaviour, and in particular a sensitivity analysis on the parameters and the initial conditions is performed. The results show that the model is able to reproduce qualitatively some known emerging behaviours in the metro station, e.g. flow imposed by leader dynamics, concentration of pedestrians at the central gates, and pedestrians tendency to choose progressively with time all the gates available. Moreover the simulations highlight the capability of the new model to capture non-equilibrium stationary states. Perspectives include the possibility to introduce the spatial and velocity dynamics for taking into account the geometry of the domain of interactions.

Contents

Introduction

Recently the modeling of complex systems in nature and society have been a growing object of investigations. Different approaches inspired to equilibrium and non-equilibrium statistical mechanics have been developed and employed for the description of collective behaviours and macroscopic features, as the result of microscopic (individual) interactions ([1], [2], [3], [4], [5]). Differently from the inert matter, complex phenomena in living natural systems and in society are also consequence of the ability of the individual to express purposes and develop collective strategies ([1]). The *Kinetic Theory of Active Particles* (KTAP) arises and develops in this context in order to take into account these capabilities ([7], [8], [9]). The KTAP is based on the idea that the complex systems under considerations are composed by a large number of (intelligent) individuals, called *active particles*, whose microscopic state, in addition to mechanical variables (e.g. space and velocity) is described also by an additional variable called *activity* which represents the individual capability to express a specific strategy. According to KTAP, the overall system is divided into different subsystems each of them composed by particles that collectively express the same biological/social function (functional subsystems). The evolution of each functional subsystem is described by a distribution function over the microscopic state of the particles and the time evolution of the subsystem is governed by interactions which can change both the microscopic state (conservative interactions) and the number of particles (nonconservative interactions). Various systems in life sciences are characterized by the fact that the microscopic state is identified by a *discrete* variable rather than a continuous one, in particular when the low number of individuals weakens the assumption of continuity of the distribution function. Vehicular traffic and pedestrians or animal dynamics appear the most suitable systems that can be modeled within the *Discrete* Kinetic Theory of Active Particles (DKTAP) ([7], [10], [11]). Indeed these systems are based on the assumption that the entities composing the system move in clusters identified by a discrete set of variables ([16], [17], [18]), and experiments developed to identify the parameters of the models are effectively performed looking at groups of vehicles or pedestrians with the same velocity or activity value. The discretization of microscopic variable appears worthy also for biological systems, as in models of the competition between cancer and immune system cells, where the goal is to identify the specific activities of the different cell populations interacting in a vertebrate ([7], [21]). Moreover complex living systems are usually not isolated, and they usually express their functions in situations of non equilibrium. This is expecially true for biological systems ([23], [24]), but also for social-economical systems ([25], [26]) and pedestrian dynamics ([27]). When an external force field acts on the system, the applied field does work on the system thereby moving it away from equilibrium. The excess energy needs to be removed so as to achieve a steady state. A method, is the use of *deterministic thermostats* ([31]). The use of deterministic thermostats consists in introducing a damping term into the equations of motion, and it is adjusted so as to

keep constant the mass or the kinetic energy or other quantities related to the specific real system under consideration. Systems with thermostat are called thermostatted.

This thesis work consists in the derivation of a new discrete thermostatted kinetic framework (T-DKTAP) for the modeling of complex systems subjected to an external force field. In order to model the non-equilibrium stationary states of the system, the external force field is coupled to a dumping term (thermostat). The well-posedness of the framework is mathematically investigated. The framework is then employed for the modeling of the pedestrians dynamics at the entrance of a metro station. Specifically, the model analyses the time distribution of the pedestrians approaching at different gates (turnistiles) according to a choice dynamics which depends on the microscopic interactions among the pedestrians. The microscopic interactions are assumed binary, and they depend on the local pedestrians density (nonlinear local interactions) and follow a game theory approach based on the leader-follower dynamics. The external force field in this context mimics different events that can affect significantly pedestrian internal dynamics (collective hurry, preferential gates recommended, periodic sound signals or evacuation alarms). The thermostat term allows the conservation of the total number of pedestrians. The system behaviour is analysed through numerical simulations, with special regard to the sensitivity analysis on the parameters of the model and on the initial conditions. The results show that the model is able to reproduce qualitatively some known emerging behaviours in the metro station, e.g. flow imposed by leader dynamics, concentration of pedestrians, tendency to choose progressively with time all the gates available, and ability of self-organization and adaptation in the long time limit when subjected to an external event.

More specifically, the above content is organized in five chapters:

- *Chapter 1* briefly summarizes the Kinetic Theory of Active Particles and the thermostat method. General concepts and domains of applications of the KTAP are presented, and some specific framework of the *discrete* KTAP useful for the developements in the next chapters are discussed in detail. Finally, in order to analyse also complex system subjected to external actions in the KTAP frameworks, the concept of the thermostat coupled to a system is introduced and discussed, with special focus on the isokinetic Gaussian Thermostat.

- *Chapter 2* deals with the mathematical definition of the a discrete kinetic framework for the active particles, for modeling systems whose microscopic state depends only on the activity variable (social/biological function) and that are subjected to an external force field. The external force field is coupled to a dissipative term (thermostat) that allows the system to reach a stationary state of non-equilibrium. The well-posedness of the framework is mathematically investigated (local and global existence and uniqueness of solution of the related Cauchy problem) thus allowing this new discrete thermostatted framework to be suitable for the derivation of specific models and the related computational analysis.

- *Chapter 3* develops the application of the T-DKATP framework proposed in the previous chapter for the modeling of pedestrian dynamics at the entrance of a metro station. The functional subsystems are defined, the microscopic interactions are modeled, and the thermostat term is set in order to conserve of the total number of pedestrians. Numerical simulations in this chapter are addressed to study the behaviour and the emerging features of the system when it is not subjected to an external force field, in order to focus only on the internal

dynamics. In particular the sensitivity analysis on the parameters of the model and on the initial conditions are performed.

– *Chapter 4* continues the analysis of Chapter 3, by focusing on the the analysis of the pedestrians dynamics subjected to the action of specific external force fields. The functional forms of the external force fields are defined in order to have a physical meaning for the pedestrians model under consideration (pedestrian in hurry, preferential gates, periodic sound alarm). Numerical simulations are addressed to study the behaviour and emerging features of the system under the action of the external force field. In particular, the controlling role of the thermostat and its action on the system is investigated.

Chapter 1

Kinetic Theory of Active Particles (KTAP) and Thermostats

This chapter is devoted to a brief overview o the Kinetic Theory of Active Particles, with a special focus on the aspects of the theory that will be employed in this thesis work. Specifically, in the first section the general concepts and the domains of applications of the KTAP are presented. Successively the second section develops in detail the *discrete* Kinetic Theory of Active Particles, whose frameworks class will be the reference for all the further developments in this work. Finally in order to take into account systems that are subjected to external effects, in the last section the concept of the thermostat coupled to a system is introduced and discussed.

1.1 General concepts of the KTAP

This section is devoted to the introduction of some conceptual aspects of complexity in living system, and to the discussion of the approach given by the Kinetic Theory of Active Particles for describing them ([6]), [7]). These aspects will be useful for the derivation of the specifics frameworks presented in the next section.

Contrarily to non living matter, complex living systems often give rise to phenomena that emerges from the ability of individuals to express individual and collective strategies. The *Kinetic Theory of Active Particles* (KTAP) arises and developes in this context in order to take into account these capabilities. The KTAP can be applied to systems characterized by the following common features:

- The system is constituted by a large number of (intelligent) interacting individuals called *active particles*. Each active particle is identified by a *microscopic state*, that in addition to mechanical variables (e.g. space, velocity) is described also by a scalar variable called *activity*. The activity represents the individual capability to express a specific biological or social strategy. Indeed, as already mentioned, living systems have the ability to develop behaviours that cannot only be explained by classical mechanics laws, and usually such behaviours are not simply an individual and isolated expression, but generally they depends on the interactions with other individuals. The variables can be continuous or discrete, or in some cases some of them are continuous and other are discrete, accordingly to the system under consideration.

- The system can be decomposed in *functional subsystems*. A functional subsystem is a collection of active particles which have the ability to express the same *activity*. The whole system is then constituted by several interacting functional subsystems. Generally the link between a functional subsystem and its activity depends on the specific phenomena under consideration. Therefore, the decomposition into functional subsystems is a flexible approach that can be adapted to each particular investigation. It is worth stressing that the decomposition into functional subsystems can be regarded as a method to reduce complexity. Indeed, the active particles in each functional subsystem are not identical or of the same type, but they can express the same strategy collectively, [1], [12]).

- The microscopic state of each individual is modified by interactions with other individuals. Interactions take place not only through contact, but can occur also in space. Indeed, in complex living systems an individual interact with other individual in a certain interaction domain. For example the interaction domain can be identified with the visibility zone (pedestrians), nearby cells (biological systems) or communication networks (web networks).

The mathematical frameworks of the KTAP describe complex systems by means of a *distribution function* over the microscopic states of each functional subsystem. The first step consist in the modeling of microscopic interactions at the individual level of active particle, where the output of the interaction is determined by a stochastic game. Subsequently, one derives a set of (ordinary or partial) differential equations for the evolution of the distribution functions. This mathematical framework is developed within the deterministic causality principles, unless some external noise is added. This means once interactions are given, the evolution of the system is deterministically identified.

Moreover complex systems are generally made up of many interacting components, each one of them constituted by several interacting individuals. This implies that the mathematical models need to describe the system at its typical scales. The representation scale suitable to describe each component of the system may not be the same for all of them, because living systems are characterized by a *multiscale essence*. However we can distinguish two main scales: the microscopic scale and the macroscopic scale. The *microscopic scale* corresponds to modeling the evolution of the variable that describes the state of each single element of the system. When the system is constituted by a large number of elements and it is possible to obtain suitable local averages in space of their state in an elementary space volume ideally tending to zero, the modeling refers to a *macroscopic scale*, and it describes the evolution of locally averaged quantities, called macroscopic variables. A two scales representations is largely used in biology to model multicellular systems ([15]). In many cases is useful to define also a *sub-microscopic* and a *super-macroscopic* scales. For instance, the, microscopic scale in biology corresponds to cells, and their dynamics depends on the sub-microscopic dynamics of molecules. On the contrary to describe population dynamics a super-macroscopic approach is often needed ([13], [14]). The above scaling correspond to a different classes of equations. Generally, models designed at the microscopic scale are stated in terms of ordinary differential equations, while models at the macroscopic scale are stated in terms of partial differential equations. The approach of the Kinetic Theory of Active Particles is to use the microscopic scale to model the interactive dynamics among active particles, while the overall state of the system at the macroscopic scale is described by the probability distribution over the microscopic states.

At present the KTAP has been profitably applied to model complex systems such as the onset of cancer and competition with the immune system ([1]), traffic flow ([66], [34]), social systems ([9], [35]), psychological interactions ([36], [37]), politics ([38], [39]). However the KTAP is large applied in modeling living systems, suitable developments of the KTAP's methods can be applied also to model large systems of interacting particles such as mixtures suspensions with continuous size particles distribution. Finally, it is worth stressing that the mathematical KTAP cannot be regarded as a straightforward generalization of the classical kinetic theory, because of the different way of decomposing the system and modeling interactions.

1.2 Discrete KTAP

This sections is devoted to a brief description of some discrete kinetic frameworks already existing in the literature ([6], [7]). Various systems in life sciences are characterized by the fact that the microscopic state is identified by a discrete variable rather than a continuous one, in particular when the low number of individuals weakens the assumption of continuity of the distribution function. Vehicular traffic and pedestrians or animal dynamics appear the most suitable systems that can be modeled within the *Discrete* Kinetic Theory of Active Particles (DKTAP) ([7], [10], [11]). Indeed these systems are based on the assumption that the entities composing the system move in clusters identified by a discrete set of variables ([16],[17], [18], [19],[20]). Moreover experiments developed to identify the parameters of the models are effectively performed looking at groups of vehicles or pedestrians with the same velocity or activity value. The discretization of the microscopic variable appears worthy also for biological systems, e.g. in models of the competition between tumor and immune system cells, where the goal is to identify the specific activities of the different cell populations interacting in a vertebrate. ([7]). In the following we introduce particular cases of the DKTAP frameworks, suitable for the description of homogeneous or inhomogeneous in space systems, i.e. systems for which the distribution function only depends on the biological/social state and the velocity, or can also depend on the space variable. These frameworks will be the basis for the modeling in the next chapters.

Let us first introduce some preliminary notions. Let $\mathbb{S}$ be a complex system constituted by a large number of active particles. The microscopic state of each active particle is denoted by $\mathbf{s} = (x, v, u)$, that includes the space x, the velocity v, and the activity variable u. The overall distribution of the system in the KTAP is described by the following continuous distribution function over the microscopic states:

$$f(t, \mathbf{s}) = f(t, x, v, u) : [0 + \infty[\times D_{\mathbf{s}} \to \mathbb{R}^+, \tag{1.2.1}$$

with $D_{\mathbf{s}} = D_x \times D_v \times D_u$, where $(x, v) \in D_x \times D_v$ is the mechanical microscopic state (here including only the position and velocity variables), and $u \in D_u$ represents the biological or social microscopic state. The elementary product $f(t, x, v, u)\, dx\, dv\, du$ is the number of active particles which at time t are in the elementary volume of the microscopic state $[\mathbf{s}, \mathbf{s}+d\mathbf{s}] = [x, x+dx] \times [v, v+dv] \times [u, u+du]$. Macroscopic observable quantities of the system such as mass and kinetic energy are obtained, under suitable integrability assumptions on f, as momenta of the distribution f. Assuming that the discrete variables of the microscopic state can attain only finite values, we define the following subsets

$$I_x = \{x_1, x_2, ..., x_n\}, \quad I_v = \{v_1, v_2, ..., v_m\}, \quad I_x = \{u_1, u_2, ..., u_l\},$$

where I_x, I_v, I_u, denote the domain for the space, the velocity and the activity variable, respectively. The whole domain is denoted by $I_{\mathbf{s}} = I_x \times I_v \times I_u$. If $x \in I_x$, $v \in I_v$ and $u \in I_u$, then

$$f_{ij}^k(t) = f(t, x_i, v_j, u_k) : [0, +\infty[\to \mathbb{R}^+$$

denotes the discrete distribution function of the active particles at time t located in x_i with velocity v_i and activity u_k. Consequently the distribution function f of the system $\mathbb{S}$ can be written formally as sum of Dirac delta functions:

$$f(t, \mathbf{s}) = f(t, x, v, u) = \sum_{i=1}^{n} \sum_{j=1}^{m} \sum_{k=1}^{l} f_{ij}^k(t) \delta(x_i - x) \delta(v_j - v) \delta(u_k - u). \tag{1.2.2}$$

The microscopic state of particles is modified, at time t, by *localized binary interactions* which occur at the microscopic level and refer to the mutual actions between the *candidate individual* and the *field individual*, when the candidate individual enters in the action domain of the field one. The domain is relatively small and the local density is sufficiently small so that only binary encounters are relevant. We can distinguish between *Conservative interactions* and *Proliferating or destructive interactions*. Conservative interactions modify the microscopic state $\mathbf{s}$ (mechanical and/or biological or social state) of the interacting individuals, but do not modify the size of the system, i.e. the total number of individuals. On the contrary proliferating or destructive interactions are interactions that modify the size of the system with birth or death of individuals due to pair interactions. In this work, we will consider only conservative interactions. As we have seen in the previous section, a mathematical model within the framework of the KTAP, is a system of evolution equations for the set f_{ij}^k, with $i = 1, 2, ..., n$, $j = 1, 2, ..., m$, $k = 1, 2, ..., l$. The evolution equation is obtained by considering the volume element $[\mathbf{s}, \mathbf{s} + d\mathbf{s}]$ and equating the rate of growth of individuals per unit time with microscopic state in such a volume to the inflow and the outflow of individuals per unit time in the volume due to interactions and eventually source terms. Formally such a model can be written generally as follows:

$$\mathbf{D} f_{ij}^k = \mathbf{G} f_{ij}^k - \mathbf{L} f_{ij}^k, \tag{1.2.3}$$

where $\mathbf{D}$ denotes the linear operator describing the rate of growth, while $\mathbf{G}$ and $\mathbf{L}$ denotes the non linear operators linked to the gain (inflow) and the loss (outflow) of individuals respectively. The operators $\mathbf{D}$, $\mathbf{G}$, $\mathbf{L}$ take specific form depending on the framework under consideration.

We are now ready to discuss particular frameworks of the DKTAP.

1.2.1 Discrete activity in uniform mechanical variables

In this subsection we deal with complex systems whose microscopic state is homogeneous with respect to the space variable x and the velocity variable v. So the distribution function is independent of x and v, and it depends only on the activity variable u, that can attains discrete values in the set $I_u = u_1, u_2, ..., u_n$. Accordingly, the distribution function f defined in (1.2.2) rewrites as follows:

$$f(t, u) = \sum_{i=1}^{n} f(t, u_i) \delta(u_i - u) = \sum_{i=1}^{n} f_i(t) \delta(u_i - u).$$

Therefore the mathematical model consists in a set of evolution differential equations for the $f_i(t)$. The modeling of the microscopic interactions is based on the assumption that the following quantities can be computed:

- The *Interaction rate*:

$$\eta_{hk} = \eta(u_h, u_k): \quad I_u \times I_u \to \mathbb{R}^+, \tag{1.2.4}$$

which depends on the states of the interacting pairs and gives the number of encounters per unit time between individuals with state u_h and individuals with state u_k.

- The *Transition probability density* or *Table of Games*:

$$A^i_{hk} = A(u_h, u_k, u_i): \quad I_u \times I_u \times I_u \to \mathbb{R}^+ \tag{1.2.5}$$

which is the probability density for a *candidate* individual with state u_h, to change into state u_i of a *test* individual, after an interaction with a *field* individual with state u_k. The above defined transition density function has the structure of a probability density with respect to the variable u_i:

$$\sum_{i=1}^{n} A^i_{hk} = 1 \quad \forall\, h, k. \tag{1.2.6}$$

The evolution equation for $f_i(t)$ thus reads:

$$\frac{df_i}{dt} = J_i[\mathbf{f}] = G_i[\mathbf{f}] - L_i[\mathbf{f}] = \sum_{h=1}^{n}\sum_{k=1}^{n} \eta_{hk} A^i_{hk} f_h f_k - f_i \sum_{k=1}^{n} \eta_{ik} f_k, \tag{1.2.7}$$

where $\mathbf{f} = \mathbf{f}(t) = (f_1(t), f_2(t), ..., f_n(t)) \in \mathbb{R}^n$ is the distribution function vector, $G_i[\mathbf{f}] = G_i[\mathbf{f}](t)$ and $L_i[\mathbf{f}] = L_i[\mathbf{f}](t)$ represent the gain particles term and the loss particles term, respectively. Specifically the operators $G_i[\mathbf{f}]$ and $L_i[\mathbf{f}]$ are the following positive definite bilinear operators:

$$G_i[\mathbf{f}] = \sum_{h=1}^{n}\sum_{k=1}^{n} \eta_{hk} A^i_{hk} f_h f_k \qquad L_i[\mathbf{f}] = f_i \sum_{k=1}^{n} \eta_{ik} f_k \quad \forall i \in \{1, 2, ...n\}. \tag{1.2.8}$$

The evolution equation (1.2.7) is thus a nonlinear ordinary differential equation with second order nonlinearities.

The related pth-order activity-moment of $\mathbf{f}$ is defined as follows:

$$\mathbb{E}_p[\mathbf{f}](t) = \sum_{i=1}^{n} u_i^p f_i(t), \quad p \in \mathbb{N}. \tag{1.2.9}$$

In particular the system size, the linear activity-momentum, and the activity-energy are obtained for $p = 0$, $p = 1$, and $p = 2$, respectively.

It is worth stressing that the framework (1.2.7) has been proposed as a general paradigm for the derivation of specific models in vehicular traffic, biology and opinion formation, see the main references listed in [43].

Remark 1.2.1. The global existence and uniqueness of the solution for the related Cauchy problem of the framework (1.2.7) has been proved in [9] under the assumption that the initial data $f_i(t = 0) = f_i^0$ is a discrete probability density (with the zero-order moment equal to 1) and that the interaction rate η_{hk} is uniformly bounded.

Remark 1.2.2. Further nonlinearity can be introduced in the framework (1.2.7) by imposing the dependence of the interaction rate and of the probability density function by distribution functions and moments, namely $\eta_{hk} = \eta_{hk}[\mathbf{f}, \mathbb{E}_p[\mathbf{f}]]$ and $A^i_{hk} = A^i_{hk}[\mathbf{f}, \mathbb{E}_p[\mathbf{f}]]$.

1.2.2 Discrete velocity and activity in continuous space systems

This subsection deals with the modeling of systems where the velocity variable v and the activity variable u can attain discrete values in the sets $I_v = v_1, v_2, ..., v_n$ and $I_u = u_1, u_2, ..., u_m$ respectively, while the space variable x is continuous with $x \in D_x$. By denoting $f_{ij}(t,x) = f(t,x,v_i,u_j)$, the distribution function f can be written as:

$$f(t,x,v,u) = \sum_{i=1}^{n}\sum_{j=1}^{m} f_{ij}(t,x)\delta(v_i - v)\delta(u_j - u).$$

Accordingly, if the microscopic state of the candidate individual is (x_*, v_h, u_k), the microscopic state of the field individual $(x*, v_r, u_s)$, and the microscopic state of the test individual (x, v_i, v_j), then

- $n_{hk}^{rs} = n_{hk}^{rs}(x_*, x*)$ is the interaction rate between the candidate individual and the field individual.
- $A_{hk,rs}^{ij} = A_{hk,rs}^{ij}(x_*, x*; x)$, is the probability that the canditate individual with state (x_*, v_h, u_k), interacting with the field individual with state $(x*, v_r, u_s)$ falls into the test particle state (x, v_i, v_j). Moreover the probability density $A_{hk,rs}^{ij}$ satisfies:

$$\sum_{i=1}^{n}\sum_{j=1}^{m}\int_{D_x} A_{hk,rs}^{ij}(x_* \to x|x*)dx \;=\; 1.$$

  for all $h,k \in 1,2,...,n$, $r,s \in 1,2,...,m$ and $x_*, x* \in D_x$.

The mathematical framework consists in partials integro-differential equations, which includes an advection part, and thus reads:

$$\frac{\partial f_{ij}}{\partial t} + v_i\frac{\partial f_{ij}}{\partial x} = \sum_{h,r=1}^{n}\sum_{k,s=1}^{m} G[f_{hk}, f_{rs}] - \sum_{r=1}^{n}\sum_{s=1}^{m} L[f_{ij}, f_{rs}],$$

with

$$G[f_{ij}, f_{rs}] = \int_{D_x \times D_x} \eta_{hk}^{rs}(x_*, x*) A_{hk,rs}^{ij}(x_* \to x|x*) f_{hk}(t, x_*) f_{rs}(t, x*) dx_* dx*$$
$$L[f_{hk}, f_{rs}] = f_{ij}\int_{D_x} \eta_{ij}^{rs}(x, x*) f_{rs}(t, x*) dx* .$$

Under suitable integrability assumptions of the vector function $\mathbf{f} = (f_{11}(t,x), ..., f_{nm}(t,x))$, We can define the (p,q,r)th-order moment as follow:

$$\mathbb{E}_{p,q,r}[\mathbf{f}](t) = \sum_{i=1}^{n} v_i^p \sum_{j=1}^{m} u_j^q \int_{D_x} x^r f_{ij}(t,x)dx \quad p,q,r \in \mathbb{N}.$$

The above framework can be further specialized if we assume that the probability density $A_{hk,rs}^{ij}$ is the product of the probability densities related to independent interactions of the activity and mechanical variables:

$$A_{hk,rs}^{ij} = B_{h,r}^{i} \times C_{k,s}^{j}.$$

1.2.3 Discrete velocity and activity in discrete space systems

This subsection introduces a mathematical framework for complex system characterized by a full discrete microscopic state. According to the introduction of this section, we assume that the space variable x, the velocity variable v, and the activity variable u can attain discrete values of the sets I_x, I_v, I_u respectively. Therefore the distribution function can be written formally as follow:

$$f(t,x,v,u) = \sum_{i_s}^{n}\sum_{j_s}^{m}\sum_{k_s}^{l} f_{i_s j_s k_s}(t)\delta(x_{i_s}-x)\delta(v_{j_s}-v)\delta(u_{k_s}-u),$$

where $f_{i_s j_s k_s}(t) = f(t, x_{i_s}, v_{j_s}, u_{k_s})$. The mathematical framework referes to the evolution equation for $f_{i_s j_s k_s}(t)$. Accordingly, if the microscopic state of the candidate individual is $(x_{i_1}, v_{j_1}, u_{k_1})$, the microscopic state of the field individual is $(x_{i_2}, v_{j_2}, u_{k_2})$, and the microscopic state of the test individual is $(x_{i_3}, v_{j_3}, u_{k_3})$, then

- $\eta_{i_1 j_1 k_1}^{i_2 j_2 k_2} = \eta(x_{i_1}, v_{j_1}, u_{k_1}; x_{i_2}, v_{j_2}, u_{k_2})$ is the itneraction rate between the candidate individual with microscopic state $(x_{i_1}, v_{j_1}, u_{k_1})$ and the field individual with microscopic state $(x_{i_2}, v_{j_2}, u_{k_2})$.
- $A_{i_1 j_1 k_1, i_2 j_2 k_2}^{i_3 j_3 k_3} = A(x_{i_1}, v_{j_1}, u_{k_1}; x_{i_2}, v_{j_2}, u_{k_2}; x_{i_3}, v_{j_3}, u_{k_3})$ is the probability that the candidate individual with state $(x_{i_1}, v_{j_1}, u_{k_1})$ falls into the test particle microscopic state $(x_{i_3}, v_{j_3}, u_{k_3})$, after interacting with the field individual with microscopic state $(x_{i_2}, v_{j_2}, u_{k_2})$. Moreover $A_{i_1 j_1 k_1, i_2 j_2 k_2}^{i_3 j_3 k_3}$ satisfies:

$$\sum_{i_3}^{n}\sum_{j_3}^{m}\sum_{k_3}^{l} A_{i_1 j_1 k_1, i_2 j_2 k_2}^{i_3 j_3 k_3} = 1 \quad \forall\, i_1, j_1, k_1, i_2, j_2, k_2.$$

Setting $s_1 = i_1 j_1 k_1$, $s_2 = i_2 j_2 k_2$ and $s_3 = i_3 j_3 k_3$, the mathematical framework in the totally discrete microscopic state consist in a set of nonlinear ordinary differential equation and thus reads:

$$\frac{df_{s_3}}{dt} + v_{j_s} T_{i_s j_s k_s}(\mathbf{x}, \mathbf{f}) = \sum_{i_1, i_2 = 1}^{n}\sum_{j_1, j_2 = 1}^{m}\sum_{k_1, k_2 = 1}^{l} \eta_{s_1}^{s_2} A_{s_1 s_2}^{s_3} f_{s_1} f_{s_2} - f_{s_3}\sum_{i_2=1}^{n}\sum_{j_2=1}^{m}\sum_{k_2=1}^{l} \eta_{s_3}^{s_2} f_{s_2},$$

where $v_{j_s} T_{i_s j_s k_s}(\mathbf{x}, \mathbf{f})$ approximate the transport term. More in detail $T_{i_s j_s k_s}(\mathbf{x}, \mathbf{f}$ approximates the space dericative of the distribution function by using first-order upwind point finite collocation ([49]). Under suitable integrability assumptions of the vector function $\mathbf{f} = (f_{111}(t), ..., f_{nml}(t))$, We can define the (p,q,r)th-order moment as follow:

$$\mathbb{E}_{p,q,r}[\mathbf{f}](t) = \sum_{i_s=1}^{n} v_{i_s}^p \sum_{j_s=1}^{m} u_{j_s}^q \sum_{k_s=1}^{l} x_{k_s}^r f_{i_s}(t) \quad p, q, r \in \mathbb{N}.$$

Again the framework can be further specialized if we assume that the probability density $A_{i_1 j_1 k_1, i_2 j_2 k_2}^{i_3 j_3 k_3}$ can be written as the product of the probability densities related to independent interactions of the activity and mechanical variables:

$$A_{i_1 j_1 k_1, i_2 j_2 k_2}^{i_3 j_3 k_3} = A_{i_1, i_2}^{i_3} \times A_{j_1, j_2}^{j_3} \times A_{k_1, k_2}^{k_3}.$$

It is worth stressing that mathematical model with this framework can be derived for the applications in semiconductor devices and nano-sciences.

1.3 Thermostats and KTAP

This section then aims at introducing the thermostat method in studying complex systems out of equilibrium. This brief dissertation will motivate the introduction of KTAP frameworks coupled with a Gaussian Thermostat for modeling complex systems subjected to external actions.

The frameworks proposed in the previous section consider only internal interactions among individuals of the system. However complex living systems are usually not isolated, and they usually express their functions in situations of non-equilibrium. This is especially true for biological systems ([23], [24]), but also for social-economical systems ([25], [26]) and pedestrian dynamics ([27]). When an external force field acts on the system, the applied field does work on the system thereby moving it away from equilibrium. The excess energy needs to be removed so as to achieve a steady state. A method, which is common in non-equilibrium molecular dynamics simulations, is the use of *deterministic thermostats*. Deterministic thermostats are mathematical tools used to model non-equilibrium steady states of fluids. These thermostats do not exist in nature, but non-equilibrium statistical mechanics has been used to prove that under specific circumstances thermodynamic properties and transport coefficients computed from simulations using these thermostats are essentially exact ([28], [29], [30]). More specifically, in the development of such algorithms the Hamiltonian equations of motion are augmented with fictitious driving forces used to represent the thermodynamic forces driving the system away from equilibrium. Such forces introduce energy that must be dissipated if non-equilibrium steady states are to be obtained: one therefore introduces further terms collectively called hermostat, that is adjusted to keep the kinetic energy constant (see [31] and references therein). In general then thermostats are applied in order to achieve a stationary state in non-equilibrium situations, e.g. when there is a flux of energy through the system, such as induced by external fields or by imposing temperature or velocity gradients. In this contest and for our purpose, the following general definition for thermostats can be stated:

> **Definition:** Thermostats are mechanisms by which the internal energy (or other quantities related to the specific system under consideration) of a many particle-system, can be tuned onto a specific value. Systems with thermostat are called thermostatted.

This way of thermostatting non-equilibrium molecular dynamics simulations by modifying the equations of motion was put in a theoretical framework when the connection with *Gauss principle of least constraint* (1829) was established [42]:

> **Gauss principle of least constraint:** Consider N point particles of mass m_i, subjected to frictionless bilateral constraints Φ_i and to external forces $\mathbf{F_i}$. Among all motions allowed by the constraints, the natural one minimize the curvature defined as:

$$C = \sum_{i=1}^{N} m_i \left(\ddot{\mathbf{x}} - \frac{\mathbf{F_i}}{m_i} \right)^2 = \sum_{i=1}^{N} m_i \Phi_i^2. \tag{1.3.1}$$

According to Gauss, the "Curvature" C is minimized by the accelerations of real motions or, equivalently, real motions minimize the action of the constraints. The Gauss Principle suffers from some disadvantages when compared to other common used extremal principles of variational

mechanics, such as Hamilton's Principle: it requires the calculation of accelerations, that are difficult to evaluate numerically; moreover it is not independent of coordinate transformation, and therefore not as generally applicable as Lagrangian and Hamiltonian formulations of mechanics. However, one advantage of Gauss principle, is that it applies equally to holonomic and non-holonomic constraints ([32]). In the case of holonomic constraints, Gauss principle is consistent with the principle of least action, and produces Hamiltonian equations of motion. Differently, nonholomic constraints lead to non-Hamiltonian equations of motions. The Gaussian thermostat introduced by Evans and Morris ([28]), has great interest with respect the deterministic character of the equation of motion.

Let $\dot{\mathbf{x}} = F(\mathbf{x})$ be an evolution equation in the phase space $\Gamma = (\mathbf{x}, \mathbf{v})$, where $\mathbf{x}$ is the position and $\mathbf{v}$ the velocity of the particle. A Gaussian thermostat constrains the evolution to a prescribed hypersurface Σ by projecting $F(\mathbf{x})$ for $\mathbf{x} \in \Sigma$, to the tangent plane to Σ at $\mathbf{x}$. Consider the following equations of motion for a system constituted by interacting particles with unit mass:

$$\begin{cases} \dot{\mathbf{x}} = \mathbf{v} \\ \dot{\mathbf{v}} = \mathbf{F}_1 + \mathbf{F} - \alpha(\Gamma)\mathbf{v}, \end{cases} \tag{1.3.2}$$

where $\mathbf{F}_1$ is a conservative force field (then exist a scalar potential V such that $\partial_{\mathbf{x}} V = -\mathbf{F}_1$), $\mathbf{F}$ a non conservative vector field. The term $\mathbf{F}$ mantains the system out of equilibrium, the term $-\alpha(\Gamma)\mathbf{v}$ is the thermostat and makes the dynamics dissipative, allowing the system to reach a steady state in the long time limit. Without the term $\mathbf{F} - \alpha\mathbf{v}$ the dynamic would be Hamiltonian. The *Gauss isokinetic thermostat* is obtained by choosing α such that the kinetic energy $\frac{\mathbf{v}^2}{2}$ of the system is kept constant. Accordingly, we have:

$$0 = \frac{d}{dt}\left(\frac{\mathbf{v}^2}{2}\right) = \mathbf{v} \cdot (-\partial_{\mathbf{x}} V + \mathbf{F} - \alpha(\Gamma)\mathbf{v}) = -\partial_{\mathbf{x}} V \cdot \mathbf{v} + \mathbf{F} \cdot \mathbf{v} - \alpha(\Gamma)\mathbf{v}^2.$$

namely

$$\alpha(\Gamma) = \frac{\mathbf{v} \cdot (-\partial_{\mathbf{x}} V + \mathbf{F})}{\mathbf{v}^2}.$$

The force field $\mathbf{F}_1 + \mathbf{F} - \frac{\mathbf{v}\cdot(-\partial_{\mathbf{x}} V + \mathbf{F})}{\mathbf{v}^2}\mathbf{v}$ is called Gaussian isokinetic force. The term α is just a Lagrange multiplier which implements the Gauss principle of least constraint.

The isoenergetic problem can be also briefly treated. This problem consist in keeping constant the energy function

$$H(t) = \frac{\mathbf{v}^2}{2} + V(\mathbf{x}).$$

The Gaussian isoenergetic thermostat associated with the force $-\partial_{\mathbf{x}} V + \mathbf{F}$ implies that

$$\dot{H(t)} = \mathbf{v} \cdot (-\partial_{\mathbf{x}} V + \mathbf{F} - \alpha(\Gamma)\mathbf{v}) + \partial_{\mathbf{x}} V \cdot \mathbf{v}.$$

The isoenergetic thermostat takes the form

$$\alpha(\Gamma) = \frac{\mathbf{F} \cdot \mathbf{v}}{\mathbf{v}^2}.$$

It is worth stressing that the isokinetic and the isoenergetic constraints are only two possible options. A wide range of constraint is possible (isobaric, isochoric, isoenthalpic etc.) depending on the system under consideration ([31] [33]).

1.4 Summary

In this chapter we have briefly introduced the Kinetic Theory of Active Particle (KTAP) for modeling complex living systems. The system is constituted by a large number of (intelligent) interacting individuals called *active particles*. Each active particle is identified by a *microscopic state*, that in addition to mechanical variables (space, velocity) is described also by an additional scalar variable called *activity*. The activity represents the individual capability to express a specific biological or social strategy. The microscopic state of each individual is modified by interactions with other individuals. Interaction are consider determined by a stochastic game. The system can be decomposed in *functional subsystems*, where each functional subsystem is a collection of active particles which have the ability to express the same *activity*. The whole system is then constituted by several interacting functional subsystems. In the KTAP framework the system is described by means of a *distribution function* over the microscopic states of each functional subsystem. After having set the subsystems and modeled the interactions, one derives a set of (ordinary or partial) differential equations for the evolution of the distribution function. This mathematical framework is developed within the deterministic causality principles, (unless some external noise is added), i.e. once interactions are given, the evolution of the system is deterministically identified. Many system in life science are characterized by the fact that the microscopic state is identified by a discrete variable rather than a continuous one, in particular when the low number of individuals weakens the assumption of continuity of the distribution function (animal and pedestrian dynamics, social dynamics). The dynamics for these systems can be modeled within the *Discrete* Kinetic Theory of Active Particles (DKTAP). In particular we have discussed the cases for system suitable to be described by: discrete activity in uniform mechanical variables, discrete velocity and activity in continuous space, and discrete velocity and activity in discrete space. Finally we have introduced the method of the deterministic thermostats as tool to model complex system under the action of an external force field that drives the system out of the equilibrium. The use of the deterministic thermostats consists in introducing into the equations of motion a damping term that is adjusted so as to keep constant the mass or the kinetic energy or other peculiar quantities of the system. In particular we have dealt wit the Gaussian isokinetic thermostat, that relies on the Gauss Principle of least constraint and that keeps the kinetic energy of the system constant during its time evolution.

Chapter 2

The Thermostatted Discrete Kinetic Framework

This chapter deals with the definition of a new discrete kinetic framework for active particles. Specifically this framework implements the framework (1.2.7) by introducing an external force field that is independent from the activity variable. The external force field is coupled to a dissipative term (thermostat), that is designed in order to keep constant a general p-th order moment (1.2.9) of the distribution function, and that allows the system to reach a non-equilibrium stationary state. The new thermostatted framework is then analysed in order to be suitable for the development of specific models and to perform the related computational analysis. Specifically, in the first section the new thermostatted framework is defined, and the thermostat term is derived in order to conserve a general p-th order moment. The second section is concerned with the analysis of the Cauchy Problem related to the framework, and local and global existence and uniqueness of the solutions are proved. Finally in the last section, we discuss the introduction in the new framework of nonlinear interactions, that will be useful for the derivation of the model for pedestrian dynamics proposed in Chapter 3. The results of this chapter are collected in the paper [44].

2.1 The thermostatted discrete kinetic framework

This section aims at proposing a new discrete thermostatted kinetic framework that takes into account that the system, which is composed by particles whose microscopic state u is discrete, is subjected to an external force field $\mathbf{F}$ and constrained to keep constant (bounded) a p-th order moment. Specifically the kinetic framework (1.2.7) is generalized as follows:

$$\frac{df_i}{dt}(t) = J_i[\mathbf{f}](t) + F_i(t) - \alpha f_i(t), \qquad i \in \{1, 2, \dots, n\}, \tag{2.1.1}$$

where $\mathbf{F}(t) = (F_1(t), F_2(t), \dots, F_n(t)) : [0, +\infty[\to \mathbb{R}^n_+$ is the external force field that maintains the system out of the equilibrium, the term $-\alpha f_i$ is the dumping term that makes the dynamic dissipative thus avoiding the unbounded increase of a p-th order moment and allowing the system to reach a nonequilibrium stationary state in the long-time limit. The parameter α, which is usually called the *thermostat term*, is obtained by forcing the conservation of a p-th order moment. Specifically, if the moment $\mathbb{E}_p[\mathbf{f}](t) = \mathbb{E}_p^0 \neq 0$ is constant in time, then

$$\frac{d}{dt}\left(\mathbb{E}_p[\mathbf{f}](t)\right) = \sum_{i=1}^{n} u_i^p \ \frac{df_i}{dt}(t) = 0. \tag{2.1.2}$$

By inserting (2.1.1) into (2.1.2), one obtains:

$$\alpha = \alpha(J[\mathbf{f}], \mathbb{E}_p, \mathbf{F}) = \frac{\displaystyle\sum_{i=1}^{n} u_i^p (J_i[\mathbf{f}] + F_i)}{\displaystyle\sum_{i=1}^{n} u_i^p f_i} = \frac{\mathbf{U}^p \cdot (\mathbf{J}[\mathbf{f}] + \mathbf{F})}{\mathbb{E}_p[\mathbf{f}]}, \tag{2.1.3}$$

where $\mathbf{J}[\mathbf{f}] = (J_1[\mathbf{f}], J_2[\mathbf{f}], \ldots, J_n[\mathbf{f}])$ and $\mathbf{U}^p = (u_1^p, u_2^p, \ldots, u_n^p)$. The thermostat term α is thus a dynamical parameter, which depends on the external force field $\mathbf{F}$ and on the internal dynamic of the system through $\mathbf{J}[\mathbf{f}]$. Bearing all above in mind, the thermostatted discrete kinetic framework of active particles, conserving the pth-order moment, reads:

$$\frac{df_i}{dt} = J_i[\mathbf{f}] + F_i - \left(\frac{\mathbf{U}^p \cdot (\mathbf{J}[\mathbf{f}] + \mathbf{F})}{\mathbb{E}_p[\mathbf{f}]}\right) f_i, \quad i \in \{1, 2, \ldots, n\}. \tag{2.1.4}$$

It is worth stressing that, differently from the thermostatted discrete kinetic framework proposed [6], the new framework (2.1.4) requires the definition of a discrete thermostat term, which depends on the inner dynamics of the system under consideration. In particular the derivation of the discrete thermostat term cannot be considered a straightforward discretization of the continuous thermostat term proposed in [6].

Remark 2.1.1. It is easy to see that for $p = 0$, the term $\mathbf{U}^p \cdot \mathbf{J}[\mathbf{f}]$ in (2.1.4) is null thanks to the property (1.2.6). Accordingly, for complex systems where the number of particles is conserved (conservation of the zero-order moment $\mathbb{E}_0[\mathbf{f}](t) = \mathbb{E}_0^0$ only), the thermostat term reads:

$$\alpha = \alpha(\mathbf{F}) = \frac{\displaystyle\sum_{i=1}^{n} F_i}{\mathbb{E}_0^0}. \tag{2.1.5}$$

As shown in (2.1.5), the thermostat term depends on the external field $\mathbf{F}$ only.

In general, the term $\mathbf{U}^p \cdot \mathbf{J}[\mathbf{f}]$ reads:

$$\mathbf{U}^p \cdot \mathbf{J}[\mathbf{f}] = \sum_{h=1}^{n}\sum_{k=1}^{n}\sum_{i=1}^{n} u_i^p \left[\eta_{hk} A_{hk}^i f_h f_k \ - \ \eta_{ik} A_{ik}^h f_i f_k\right]. \tag{2.1.6}$$

As the relation (2.1.6) shows, all terms with $i = h$ vanish for all k. Further simplifications of (2.1.6) can be obtained by assuming some symmetry relations on the table of games A_{hk}^i and on the encounter rate η_{nk}. A specific analysis to the case $n = 2$ and $n = 3$ follows.

- Case $n = 2$. In this case the equation (2.1.6) reads:

$$\begin{aligned}\mathbf{U}^p \cdot \mathbf{J}[\mathbf{f}] = {} & u_1^p \left[(\eta_{21} A_{21}^1 - \eta_{12} A_{12}^2) f_1 f_2 - \eta_{11} A_{11}^2 f_1^2 + \eta_{22} A_{22}^1 f_2^2\right] \\ & + u_2^p \left[(\eta_{12} A_{12}^2 - \eta_{21} A_{21}^1) f_1 f_2 + \eta_{11} A_{11}^2 f_1^2 - \eta_{22} A_{22}^1 f_2^2\right].\end{aligned} \tag{2.1.7}$$

  Assuming the following symmetries on the encounter rate and on the table of games:

$$\eta_{12} = \eta_{21} \quad \text{and} \quad A_{21}^1 = A_{12}^2,$$

the previous equation simplifies as follows:

$$\mathbf{U}^p \cdot \mathbf{J}[\mathbf{f}] = u_1^p \left[-\eta_{11} A_{11}^2 f_1^2 + \eta_{22} A_{22}^1 f_2^2 \right] \; + \; u_2^p \left[+\eta_{11} A_{11}^2 f_1^2 - \eta_{22} A_{22}^1 f_2^2 \right]$$

or, equivalently, in compact form:

$$\sum_{i=1}^{2} \sum_{\substack{h=1 \\ h \neq i}}^{2} u_i^p \left[\eta_{hh} A_{hh}^i f_h^2 \; - \; \eta_{ii} A_{ii}^h f_i^2 \right].$$

- Case $n = 3$. In this case, each of the three terms of the scalar product (2.1.6) consists in a sum of 12 terms. The first term reads:

$$\begin{aligned} (\mathbf{U}^p \cdot \mathbf{J}[\mathbf{f}])_1 = u_1^p \big[& \eta_{11}(A_{11}^1 - 1) f_1^2 \; + \; \eta_{22} A_{22}^1 f_2^2 \; + \; \eta_{33} A_{33}^1 f_3^2 \\ & - -(\eta_{12} A_{12}^2 + \eta_{12} A_{12}^3 - \eta_{21} A_{21}^1) f_1 f_2 \\ & - (\eta_{13} A_{13}^2 + \eta_{13} A_{13}^3 - \eta_{31} A_{31}^1) f_1 f_3 \; + \; (\eta_{23} A_{23}^1 + \eta_{32} A_{32}^1) f_2 f_3 \big]. \end{aligned} \tag{2.1.8}$$

If $\eta_{hk} = \eta_{kh}$ and $A_{hk}^1 = A_{kh}^1$, $\forall h, k$, then the above equation writes:

$$\begin{aligned} (\mathbf{U}^p \cdot \mathbf{J}[\mathbf{f}])_1 = \; & u_1^p \left[\eta_{11}(A_{11}^1 - 1) f_1^2 \; + \; \eta_{22} A_{22}^1 f_2^2 \; + \; \eta_{33} A_{33}^1 f_3^2 + \eta_{12}(2A_{12}^1 - 1) f_1 f_2 \right. \\ & \left. + \eta_{13}(2A_{13}^1 - 1) f_1 f_3 \; + \; 2\eta_{23} A_{23}^1 f_2 f_3 \right]. \end{aligned} \tag{2.1.9}$$

Similar expressions hold true for the other two terms $i = 2$ and $i = 3$. If the following relations on the rates encounters and on the table of games holds true:

$$\eta_{ik} = \eta_{ki} \quad \textit{and} \quad A_{hk}^i = A_{kh}^i \quad \forall i, h, k \in \{1, 2, \ldots, n\},$$

then (2.1.6) simplifies as follows:

$$\sum_{i=1}^{3} u_i^p \left(\sum_{h \neq i}^{3} \left[\eta_{hh}(A_{hh}^i - 1) f_h^2 \; + \; \eta_{ih}(2A_{ih}^i - 1) f_i f_h \right] \; + \; \eta_{ii}(A_{ii}^i - 1) f_i^2 \; + \; 2\eta_{hk} A_{hk}^i f_h f_k \right),$$

where the last term holds only for $h \neq k \neq i$. Moreover if in addition $A_{ih}^i = 1/2$, $\forall i$, and $A_{hk}^i = 0$ for $h \neq k \neq i$, the above equation rewrites:

$$\mathbf{U}^p \cdot \mathbf{J}[\mathbf{f}] = \sum_{i=1}^{3} u_i^p \left(\sum_{h \neq i}^{3} \eta_{hh}(A_{hh}^i) f_h^2 \; - \; \frac{1}{2} \eta_{ii}(A_{ii}^i - 1) f_i^2 \right).$$

It is worth stressing that the above assumptions on the encounter rates and on the table of games are not the all conceivable ones, and a priori the system could satisfy only some of them, or even none. Thus the simplification of the dynamic is strictly related to the specific model under consideration.

2.1.1 On the multiple thermostats case

This subsection is devoted to the derivation of a discrete thermostatted kinetic framework for complex systems constrained to maintain constant two moments. Specifically the subsection focuses on complex systems whose interactions among the particles do not modify the zero-order moment and the second-order moment. In order to take into account the conservation of the two moments, the framework (1.2.7) is modified by introducing two different parameters α_1 and α_2 as follows:

$$\frac{df_i}{dt} = J_i[\mathbf{f}] + \alpha_1 F_i - \alpha_2 f_i.$$

By imposing the conservation of the zero- and the second-order moment, the following system of two algebraic equations in the unknowns α_1 and α_2 is obtained:

$$\begin{cases} \displaystyle\sum_{i=1}^{n} F_i\,\alpha_1 - \mathbb{E}_0^0\,\alpha_2 = 0 \\ \\ (\mathbf{U}^2 \cdot \mathbf{F})\,\alpha_1 - \mathbb{E}_2^0\,\alpha_2 = 0 \end{cases} \tag{2.1.10}$$

where $\mathbb{E}_0^0$ and $\mathbb{E}_2^0$ denote the initial values of the zero-order moment and the second-order moment, respectively. Accordingly:

$$\begin{cases} \alpha_1 = \dfrac{\mathbf{U}^2 \cdot \mathbf{J}}{\mathbf{F} \cdot \left(\frac{\mathbb{E}_2^0}{\mathbb{E}_0^0} - \mathbf{U}^2\right)} \\ \\ \alpha_2 = \dfrac{\displaystyle\sum_{i=1}^{n} F_i}{\mathbb{E}_0^0} \left(\dfrac{\mathbf{U}^2 \cdot \mathbf{J}}{\mathbf{F} \cdot \left(\frac{\mathbb{E}_2^0}{\mathbb{E}_0^0} - \mathbf{U}^2\right)} \right) \end{cases} \tag{2.1.11}$$

It is worth pointing out that in the partial discrete kinetic framework proposed in [6], only one thermostat α has been introduced to ensure the total conservation of the zero- and the second-order moment, respectively. Indeed, as shown in [6], the introduction of one thermostat is sufficient to ensure the conservation of $\mathbb{E}_0[\mathbf{f}]$ and $\mathbb{E}_2[\mathbf{f}]$, considering that the activity variable has been assumed continuous. Indeed the conservation of the total kinetic energy ensures automatically the conservation of the total density, under the assumption that border effects are negligible. In the total discrete kinetic framework proposed here, the introduction of one thermostat is not sufficient, because an analogue condition for the border effects cannot be found. However further assumptions can be considered in order to reduce the number of thermostats. These assumptions can refer to the dynamics of the system. In particular, it could be possible to require the conservation of both the zero- and the second-order moment by keeping in the evolution equation only one dynamical parameter. In this case, the thermostat term writes as in (2.1.5), under the following condition:

$$\mathbf{F} \cdot \left(\frac{\mathbb{E}_2^0}{\mathbb{E}_0^0}\,\hat{\mathbf{f}} - \mathbf{U}^2 \right) = \mathbf{U}^2 \cdot \mathbf{J},$$

where $\hat{\mathbf{f}}$ is the unit vector in the $\mathbf{F}$ direction. The physical meaning of this relation depends on the specific model under consideration.

2.2 The Cauchy problem: Existence and uniqueness of solution

This section is concerned with the analysis of the Cauchy problem for the discrete thermostatted kinetic framework (2.1.4), which consists in a system of n nonlinear ordinary differential equations in the unknown vector $\mathbf{f}(t) = (f_1(t), f_2(t), \dots, f_n(t))$ where $f_i : [0, +\infty[\to \mathbb{R}_+$, for all $i \in \{1, 2, \dots, n\}$.

Let $C = C([0, +\infty[; \mathbb{R}^n_+)$ be the space of the continuous vector function $\mathbf{f} = \mathbf{f}(t) : [0, +\infty[\to \mathbb{R}^n_+$, and $\mathfrak{K}^p_{\mathbf{f}} = \mathfrak{K}^p_{\mathbf{f}}(\mathbb{R}_+; \mathbb{E}^0_p)$ the following function set:

$$\mathfrak{K}^p_{\mathbf{f}}(\mathbb{R}_+; \mathbb{E}^0_p) = \{\mathbf{f} \in C([0, +\infty[; \mathbb{R}^n_+) : \mathbb{E}_p[\mathbf{f}](t) = \mathbb{E}^0_p\}. \tag{2.2.1}$$

The set $\mathfrak{K}^p_{\mathbf{f}}$ is composed of vector functions $\mathbf{f}$ whose components are positive continuous functions and such that $\mathbf{f}$ conserves the pth-order moment. In particular the set $\mathfrak{K}^p_{\mathbf{f}}$ is closed in C. The Cauchy problem for the discrete thermostatted kinetic framework (2.1.4) thus reads:

$$(CP) : \begin{cases} \dfrac{d\mathbf{f}}{dt} = \mathbf{J}[\mathbf{f}] + T_{\mathbf{F}}[\mathbf{f}] \\ \\ \mathbf{f}(0) = \mathbf{f}^0 \end{cases} \tag{2.2.2}$$

where $\mathbf{f}^0 \in \mathfrak{K}^p_{\mathbf{f}}$ is the initial condition, $\mathbf{J}[\mathbf{f}] = (J_1[\mathbf{f}], J_2[\mathbf{f}], \dots, J_n[\mathbf{f}])$, with $J_i[\mathbf{f}]$ defined in (1.2.7), and $T_{\mathbf{F}}[\mathbf{f}]$ is the thermostat operator:

$$T_{\mathbf{F}}[\mathbf{f}] = \mathbf{F} - \left(\frac{\mathbf{U}^p \cdot (\mathbf{J}[\mathbf{f}] + \mathbf{F})}{\mathbb{E}_p[\mathbf{f}]} \right) \mathbf{f}. \tag{2.2.3}$$

Definition 2.2.1. Let $\mathbf{U} = (u_1, u_2, \dots, u_n) \in ([1, +\infty[)^n$ be the discrete activity vector; $\eta_{hk} = \eta(u_h, u_k) : I_u \times I_u \to \mathbb{R}_+$, for $h, k \in \{1, 2, \dots, n\}$, the interaction rate between the particles with state u_h and u_k; $A^i_{hk} = A(u_h, u_k, u_i) : I_u \times I_u \times I_u \to \mathbb{R}_+$, for all $i, h, k \in \{1, 2, \dots, n\}$, the transition probability density satisfying the property (1.2.6), and $F_i(t) : \mathbb{R}_+ \to \mathbb{R}_+$, for all $i \in \{1, 2, \dots, n\}$, the ith external force. The vector function $\mathbf{f} = (f_1, f_2, \dots, f_n)$ is said to be solution of the Cauchy problem (2.2.2) in the interval $[0, +\infty[$ if:

i f is differentiable with respect to the variable t, namely f_i, for all $i \in \{1, 2, \dots, n\}$, is differentiable with respect to the variable t;

ii $\mathbf{f} \in \mathfrak{K}^p_{\mathbf{f}}$

iii $\mathbf{f}$ satisfies the following vector equation:

$$\frac{d\mathbf{f}}{dt}(t) = \mathbf{J}[\mathbf{f}](t) + T_F[\mathbf{f}](t), \quad \forall t \in [0, +\infty[, \tag{2.2.4}$$

and $\mathbf{f}(0) = \mathbf{f}^0$.

Remark 2.2.1. Straightforward computations show that $\mathbf{f} = (0, 0, \dots, 0) \in \mathbb{R}^n$ is not solution of (2.2.2). Thus, in what follows, the condition $\mathbb{E}_p[\mathbf{f}] = \mathbb{E}^0_p \neq 0$ can be assumed without loss of generality.

Let $p \in \mathbb{N} \setminus \{0\}$ and $x = (x_1, x_2, \ldots, x_n) \in \mathbb{R}^n$. In what follows, the set $\mathbb{R}^n$ is endowed with the ℓ_p norm $\|x\|_p$:

$$\|x\|_p = \left(\sum_{i=1}^{n} |x_i|^p \right)^{1/p} \qquad x \in \mathbb{R}^n.$$

Moreover the real Banach space $(C, \|\cdot\|_\infty)$, where $\|\mathbf{f}\|_\infty = \sup_{t\in[0,+\infty[} \|\mathbf{f}(t)\|_p$, will be considered in the sequel.
The following Lemmas hold true.

Lemma 2.2.1. *Let $\mathbf{U} = (u_1, u_2, \ldots, u_n) \in ([1, +\infty[)^n$ be the discrete activity vector, $\eta_{hk} = \eta(u_h, u_k) : I_u \times I_u \to \mathbb{R}^+$, for $h, k \in \{1, 2, \ldots, n\}$, a bounded function with upper-bound M, and $A^i_{hk} = A(u_h, u_k, u_i) : I_u \times I_u \times I_u \to \mathbb{R}^+$, for all $i, h, k \in \{1, 2, \ldots, n\}$, the transition probability density satisfying the property (1.2.6). Then*

$$\|\mathbf{J}[\mathbf{f}] - \mathbf{J}[\mathbf{g}]\|_1 \leq 4M\mathbb{E}^0_p \|\mathbf{f} - \mathbf{g}\|_1, \qquad \forall \mathbf{f}, \mathbf{g} \in \mathfrak{K}^p_{\mathbf{f}}(\mathbb{R}_+; \mathbb{E}^0_p). \tag{2.2.5}$$

Proof. The operator $\mathbf{J}[\mathbf{f}]$ can be written as the sum of the gain operator and the loss operator:

$$\mathbf{J}[\mathbf{f}] = \mathbf{G}[\mathbf{f}] - \mathbf{L}[\mathbf{f}].$$

Let $\mathbf{f}, \mathbf{g} \in \mathfrak{K}^p_{\mathbf{f}}(\mathbb{R}_+; \mathbb{E}^0_p)$. For the gain operator $\mathbf{G}[\mathbf{f}]$ one has:

$$\begin{aligned}
\|\mathbf{G}[\mathbf{f}] - \mathbf{G}[\mathbf{g}]\|_1 &= \sum_{i=1}^{n} \big| G_i[f] - G_i[g] \big| \\
&= \sum_{i=1}^{n} \left| \sum_{h=1}^{n}\sum_{k=1}^{n} \eta_{hk} A^i_{hk} f_h f_k \; - \; \sum_{h=1}^{n}\sum_{k=1}^{n} \eta_{hk} A^i_{hk} g_h g_k \right| \\
&= \sum_{i=1}^{n} \left| \sum_{h=1}^{n}\sum_{k=1}^{n} \eta_{hk} A^i_{hk} \big[f_h f_k \; - \; g_h g_k \big] \right|.
\end{aligned}$$

By employing the triangular inequality, the assumption that $\eta_{hk} \leq M$, $\forall h, k$ and the assumption (1.2.6), one obtains:

$$\|\mathbf{G}[\mathbf{f}] - \mathbf{G}[\mathbf{g}]]\|_1 \leq M \sum_{h=1}^{n}\sum_{k=1}^{n} \big| f_h f_k \; - \; g_h g_k \big|.$$

By adding and subtracting the term $f_h g_k$ and rearranging the terms in the sum, one has:

$$\begin{aligned}
\|\mathbf{G}[\mathbf{f}] - \mathbf{G}[\mathbf{g}]\|_1 &\leq M \sum_{h=1}^{n}\sum_{k=1}^{n} \big| f_h (f_k - g_k) \; + \; g_k (f_h - g_h) \big| \\
&\leq M \sum_{h=1}^{n}\sum_{k=1}^{n} \big[|f_h| |(f_k - g_k)| \; + \; |g_k| |(f_h - g_h)| \big] \\
&= M \left[\sum_{h=1}^{n} |f_h| \; + \; \sum_{h=1}^{n} |g_h| \right] \sum_{k=1}^{n} |(f_k - g_k)| \\
&= M \big(\|\mathbf{f}\|_1 \; + \; \|\mathbf{g}\|_1 \big) \|\mathbf{f} - \mathbf{g}\|_1,
\end{aligned}$$

and bearing in mind the definition of the p-th order momentum $\mathbb{E}_p$, see (1.2.9), the norm $\|\mathbf{f}\|_1$ represents the zero-order momentum $\mathbb{E}_0$ (remember that the f_i is a positive function). Bearing all above in mind, the following inequality for the operator $\mathbf{G}[\mathbf{f}]$ holds true:

$$\|\mathbf{G}[\mathbf{f}] - \mathbf{G}[\mathbf{g}]\|_1 \leq M \big(\mathbb{E}_0[\mathbf{f}] \; + \; \mathbb{E}_0[\mathbf{g}] \big) \|\mathbf{f} - \mathbf{g}\|_1. \tag{2.2.6}$$

Similarly, for the loss operator $L[\mathbf{f}]$, one has:

$$\begin{aligned}\|\mathbf{L}[\mathbf{f}]-\mathbf{L}[\mathbf{g}]\|_1 &= \sum_{i=1}^{n}\left|f_i\sum_{k=1}^{n}\eta_{ik}f_k \,+\, g_i\sum_{k=1}^{n}\eta_{ik}g_k\right| \\ &\leq M\sum_{i=1}^{n}\sum_{k=1}^{n}\left|f_if_k \,-\, g_ig_k\right| \\ &\leq M\Big[\sum_{k=1}^{n}\left|f_k\right| \,+\, \sum_{k=1}^{n}\left|g_k\right|\Big]\sum_{i=1}^{n}\left|(f_i-g_i)\right| \\ &= M\big(\|\mathbf{f}\|_1 \,+\, \|\mathbf{g}\|_1\big)\|\mathbf{f}-\mathbf{g}\|_1,\end{aligned}$$

and thus

$$\|\mathbf{G}[\mathbf{f}]-\mathbf{G}[\mathbf{g}]\|_1 \leq M\big(\mathbb{E}_0[\mathbf{f}] \,+\, \mathbb{E}_0[\mathbf{g}]\big)\|\mathbf{f}-\mathbf{g}\|_1. \tag{2.2.7}$$

Finally by summing the (2.2.6) and the (2.2.7), one obtains for the operator $J[\mathbf{f}]$:

$$\|\mathbf{J}[\mathbf{f}]-\mathbf{J}[\mathbf{g}]\|_1 \leq 2M\left(\mathbb{E}_0[\mathbf{f}] \,+\, \mathbb{E}_0[\mathbf{g}]\right)\|\mathbf{f}-\mathbf{g}\|_1. \tag{2.2.8}$$

Since $u_i \geq 1$ and $f_i \geq 0$, then $\mathbb{E}_0[\mathbf{f}] \leq \mathbb{E}_p[\mathbf{f}]$. The proof is concluded. □

Lemma 2.2.2. *Let* $\mathbf{U}=(u_1,u_2,\ldots,u_n)\in([1,+\infty[)^n$ *be the discrete activity vector;* $F_i(t):\mathbb{R}_+\to\mathbb{R}_+$*, for all* $i\in\{1,2,\ldots,n\}$*, a bounded function with upper-bound* F*;* $\eta_{hk}=\eta(u_h,u_k):I_u\times I_u\to\mathbb{R}^+$*, for* $h,k\in\{1,2,\ldots,n\}$*, a bounded function with upper-bound* M*, and* $A^i_{hk}=A(u_h,u_k,u_i):I_u\times I_u\times I_u\to\mathbb{R}^+$*, for all* $i,h,k\in\{1,2,\ldots,n\}$*, the transition probability density satisfying the property (1.2.6). If* $\mathbf{f},\mathbf{g}\in\mathfrak{K}^p_{\mathbf{f}}(\mathbb{R}_+;\mathbb{E}^0_p)$*, then*

$$\|T[\mathbf{f}]-T[\mathbf{g}]\|_1 \leq \left(\frac{F\|\mathbf{U}^p\|_1}{\mathbb{E}^0_p}+2M\mathbb{E}^0_p+4M\mathbb{E}^0_p\|\mathbf{U}^p\|_1\right)\|\mathbf{f}-\mathbf{g}\|_1. \tag{2.2.9}$$

Proof. Let $\mathbf{f},\mathbf{g}\in\mathfrak{K}^p_{\mathbf{f}}(\mathbb{R}_+;\mathbb{E}^0_p)$. For the thermostat operator $T[\mathbf{f}]$ one has:

$$\begin{aligned}\|T[\mathbf{f}]-T[\mathbf{g}]\|_1 &= \sum_{i=1}^{n}|T_i[\mathbf{f}]-T_i[\mathbf{g}]| \\ &= \sum_{i=1}^{n}\left|F_i-\left(\frac{\mathbf{U}^p\cdot(\mathbf{J}[\mathbf{f}]+\mathbf{F})}{\mathbb{E}_p[\mathbf{f}]}\right)f_i-F_i+\left(\frac{\mathbf{U}^p\cdot(\mathbf{J}[\mathbf{g}]+\mathbf{F})}{\mathbb{E}_p[\mathbf{g}]}\right)g_i\right|.\end{aligned}$$

Since $\mathbf{f},\mathbf{g}\in\mathfrak{K}^p_{\mathbf{f}}(\mathbb{R}_+;\mathbb{E}^0_p)$, then $\mathbb{E}_p[\mathbf{f}]=\mathbb{E}_p[\mathbf{g}]=\mathbb{E}^0_p$, and one has:

$$\begin{aligned}\|T[\mathbf{f}]-T[\mathbf{g}]\|_1 &= \sum_{i=1}^{n}\left|-\left(\frac{\mathbf{U}^p\cdot\mathbf{F}}{\mathbb{E}^0_p}\right)(f_i-g_i)-\left(\frac{\mathbf{U}^p\cdot\mathbf{J}[\mathbf{f}]}{\mathbb{E}^0_p}\right)f_i+\left(\frac{\mathbf{U}^p\cdot\mathbf{J}[\mathbf{g}]}{\mathbb{E}^0_p}\right)g_i\right| \\ &\leq \sum_{i=1}^{n}\left(\frac{\mathbf{U}^p\cdot\mathbf{F}}{\mathbb{E}^0_p}\right)|f_i-g_i|+\sum_{i=1}^{n}\left|\left(\frac{\mathbf{U}^p\cdot\mathbf{J}[\mathbf{f}]}{\mathbb{E}^0_p}\right)f_i-\left(\frac{\mathbf{U}^p\cdot\mathbf{J}[\mathbf{g}]}{\mathbb{E}^0_p}\right)g_i\right|.\end{aligned} \tag{2.2.10}$$

The first sum writes:

$$\sum_{i=1}^{n}\left(\frac{\mathbf{U}^p\cdot\mathbf{F}}{\mathbb{E}^0_p}\right)|f_i-g_i|=\left(\frac{\mathbf{U}^p\cdot\mathbf{F}}{\mathbb{E}^0_p}\right)\|\mathbf{f}-\mathbf{g}\|_1. \tag{2.2.11}$$

For the second sum in (2.2.10), recalling that $\sum_{l=1}^{n} u_l^p f_l = \sum_{l=1}^{n} u_l^p g_l = \mathbb{E}_p^0$, we have:

$$\sum_{i=1}^{n}\left|\left(\frac{\mathbf{U}^p\cdot\mathbf{J}[\mathbf{f}]}{\mathbb{E}_p^0}\right)f_i-\left(\frac{\mathbf{U}^p\cdot\mathbf{J}[\mathbf{g}]}{\mathbb{E}_p^0}\right)g_i\right| = \sum_{i=1}^{n}\left|\frac{1}{\mathbb{E}_p^0}\sum_{l=1}^{n}u_l^p J_l[\mathbf{f}]f_i-\frac{1}{\mathbb{E}_p^0}\sum_{l=1}^{n}u_l^p J_l[\mathbf{g}]g_i\right| \tag{2.2.12}$$

$$\begin{aligned}
&= \sum_{i=1}^{n}\left|\frac{1}{\mathbb{E}_p^0}\sum_{l=1}^{n}u_l^p\sum_{h=1}^{n}\sum_{k=1}^{n}\eta_{hk}A_{hk}^l f_h f_k f_i-\frac{1}{\mathbb{E}_p^0}\sum_{l=1}^{n}u_l^p f_l\sum_{k=1}^{n}\eta_{lk}f_k f_i-\right.\\
&\left.-\frac{1}{\mathbb{E}_p^0}\sum_{l=1}^{n}u_l^p\sum_{h=1}^{n}\sum_{k=1}^{n}\eta_{hk}A_{hk}^l g_h g_k g_i+\frac{1}{\mathbb{E}_p^0}\sum_{l=1}^{n}u_l^p g_l\sum_{k=1}^{n}\eta_{lk}g_k g_i\right|\\
&= \sum_{i=1}^{n}\left|\frac{1}{\mathbb{E}_p^0}\sum_{l=1}^{n}u_l^p\sum_{h=1}^{n}\sum_{k=1}^{n}\eta_{hk}A_{hk}^l\left[f_h f_k f_i-g_h g_k g_i\right]-\sum_{k=1}^{n}\eta_{lk}\left[f_k f_i-g_k g_i\right]\right|.
\end{aligned} \tag{2.2.13}$$

Bearing in mind that $\eta_{hk}\leq M$, $0<A_{hk}^l\leq 1$, $\forall l,h,k$, and by employing the triangular inequality, one has:

$$\begin{aligned}
&\sum_{i=1}^{n}\left|\frac{1}{\mathbb{E}_p^0}\sum_{l=1}^{n}u_l^p\sum_{h=1}^{n}\sum_{k=1}^{n}\eta_{hk}A_{hk}^l\left[f_h f_k f_i-g_h g_k g_i\right]-\sum_{k=1}^{n}\eta_{lk}\left[f_k f_i-g_k g_i\right]\right|\\
&\leq \frac{1}{\mathbb{E}_p^0}\sum_{i=1}^{n}\sum_{l=1}^{n}\left|u_l^p\right|\sum_{h=1}^{n}\sum_{k=1}^{n}\eta_{hk}A_{hk}^l\left|f_h f_k f_i-g_h g_k g_i\right|+\sum_{i=1}^{n}\sum_{k=1}^{n}\eta_{lk}\left|f_k f_i-g_k g_i\right|\\
&\leq \frac{M}{\mathbb{E}_p^0}\|\mathbf{U}^p\|_1\sum_{i=1}^{n}\sum_{h=1}^{n}\sum_{k=1}^{n}\left|f_h f_k f_i-g_h g_k g_i\right|+M\sum_{i=1}^{n}\sum_{k=1}^{n}\left|f_k f_i-g_k g_i\right|
\end{aligned} \tag{2.2.14}$$

By following the same procedure for the operator $\mathbf{J}[\mathbf{f}]$ (see Lemma 2.2.1), the first term in (2.2.14) can be rewritten as follows:

$$\begin{aligned}
&\frac{M}{\mathbb{E}_p^0}\|\mathbf{U}^p\|_1\sum_{i=1}^{n}\sum_{h=1}^{n}\sum_{k=1}^{n}\left|f_h f_k f_i-g_h g_k g_i\right| =\\
&\frac{M}{\mathbb{E}_p^0}\|\mathbf{U}^p\|_1\sum_{i=1}^{n}\sum_{h=1}^{n}\sum_{k=1}^{n}\left|f_h f_k(f_i-g_i)+g_i g_h(f_k-g_k)+g_i f_k(f_h-g_h)\right|\\
&\frac{M}{\mathbb{E}_p^0}\|\mathbf{U}^p\|_1\sum_{i=1}^{n}\sum_{h=1}^{n}\sum_{k=1}^{n}\left|f_h f_k(f_i-g_i)+g_i g_h(f_k-g_k)+g_i f_k(f_h-g_h)\right|\\
&\leq \frac{M}{\mathbb{E}_p^0}\|\mathbf{U}^p\|_1\sum_{i=1}^{n}\sum_{h=1}^{n}\sum_{k=1}^{n}\left[\left|f_h f_k(f_i-g_i)\right|+\left|g_i g_h(f_k-g_k)\right|+\left|g_i f_k(f_h-g_h)\right|\right]\\
&= \frac{M}{\mathbb{E}_p^0}\|\mathbf{U}^p\|_1\left[\sum_{h=1}^{n}\sum_{k=1}^{n}\left|f_h\right|\left|f_k\right|+\left|g_i\right|\left|g_h\right|+\left|g_i\right|\left|f_k\right|\right]\sum_{i=1}^{n}\left|f_i-g_i\right|\\
&= \frac{M}{\mathbb{E}_p^0}\|\mathbf{U}^p\|_1\left[\|\mathbf{f}\|_1^2+\|\mathbf{g}\|_1^2+\|\mathbf{f}\|_1\|\mathbf{g}\|_1\right]\|\mathbf{f}-\mathbf{g}\|_1\\
&\leq \frac{M}{\mathbb{E}_p^0}\|\mathbf{U}^p\|_1\left[\|\mathbf{f}\|_1^2+\|\mathbf{g}\|_1^2+2\|\mathbf{f}\|_1\|\mathbf{g}\|_1\right]\|\mathbf{f}-\mathbf{g}\|_1\\
&= \frac{M}{\mathbb{E}_p^0}\|\mathbf{U}^p\|_1\left[\|\mathbf{f}\|_+\|\mathbf{g}\|_1\right]^2\|\mathbf{f}-\mathbf{g}\|_1\\
&= \frac{M}{\mathbb{E}_p^0}\|\mathbf{U}^p\|_1\left[\mathbb{E}_0[\mathbf{f}]+\mathbb{E}_0[\mathbf{g}]\right]^2\|\mathbf{f}-\mathbf{g}\|_1.
\end{aligned} \tag{2.2.15}$$

Thus for the first term in (2.2.14) we have:

$$\sum_{i=1}^{n}\left|\left(\frac{\mathbf{U}^p\cdot\mathbf{J}[\mathbf{f}]}{\mathbb{E}_p^0}\right)f_i-\left(\frac{\mathbf{U}^p\cdot\mathbf{J}[\mathbf{g}]}{\mathbb{E}_p^0}\right)g_i\right|\leq\frac{M}{\mathbb{E}_p^0}\|\mathbf{U}^p\|_1\left[\mathbb{E}_0[\mathbf{f}]+\mathbb{E}_0[\mathbf{g}]\right]^2\|\mathbf{f}-\mathbf{g}\|_1. \tag{2.2.16}$$

By employing the same procedure for $\mathbf{G}[\mathbf{f}]$ and $\mathbf{L}[\mathbf{f}]$, for the second term in (2.2.14) one has:

$$M\sum_{i=1}^{n}\sum_{k=1}^{n}|f_kf_i-g_kg_i|\leq M\left[\mathbb{E}_0[\mathbf{f}]+\mathbb{E}_0[\mathbf{g}]\right]\|\mathbf{f}-\mathbf{g}\|_1. \tag{2.2.17}$$

Finally by summing (2.2.11), (2.2.16) and (2.2.17), one has:

$$\|T[\mathbf{f}]-T[\mathbf{g}]\|_1\leq\left[\left(\frac{\mathbf{U}^p\cdot\mathbf{F}}{\mathbb{E}_p^0}\right)+M\left(\mathbb{E}_0[\mathbf{f}]+\mathbb{E}_0[\mathbf{g}]\right)+\frac{M}{\mathbb{E}_p^0}\|\mathbf{U}^p\|_1\left(\mathbb{E}_0[\mathbf{f}]+\mathbb{E}_0[\mathbf{g}]\right)^2\right]\|\mathbf{f}-\mathbf{g}\|_1. \tag{2.2.18}$$

Since $u_i\geq 1$, $f_i\geq 0$ and $F_i\leq F$, then $\mathbb{E}_0[\mathbf{f}]\leq\mathbb{E}_p[\mathbf{f}]$. The proof is concluded. □

Remark 2.2.2. If $\mathbf{f},\mathbf{g}\in\mathfrak{K}_{\mathbf{f}}^0(\mathbb{R}_+;\mathbb{E}_0^0)$ (the zero-order moment is conserved), then

$$\|\mathbf{J}[\mathbf{f}]-\mathbf{J}[\mathbf{g}]\|_1\leq 4M\mathbb{E}_0^0\|\mathbf{f}-\mathbf{g}\|_1, \tag{2.2.19}$$

$$\|T[\mathbf{f}]-T[\mathbf{g}]\|_1\leq\left(\frac{\mathbf{U}^p\cdot\mathbf{F}}{\mathbb{E}_0^0}+2M\mathbb{E}_0^0+4M\mathbb{E}_0^0\|\mathbf{U}^p\|_1\right)\|\mathbf{f}-\mathbf{g}\|_1. \tag{2.2.20}$$

The main result of this chapter, concerning the existence and uniqueness solution of the Cauchy problem (2.2.2), follows:

Theorem 2.2.1. *Let* $\mathbf{U}=(u_1,u_2,\dots,u_n)\in([1,+\infty[)^n$ *be the discrete activity vector;* $F_i(t):\mathbb{R}_+\to\mathbb{R}_+$*, for all* $i\in\{1,2,\dots,n\}$*, a bounded function;* η_{hk}*, for* $h,k\in\{1,2,\dots,n\}$*, a bounded positive function;* A_{hk}^i*, for all* $i,h,k\in\{1,2,\dots,n\}$*, the positive function satisfying the property (??), and* $\mathbf{f}^0\in\mathfrak{K}_{\mathbf{f}}^p(\mathbb{R}_+;\mathbb{E}_p^0)$ *a given function. Then there exists a unique nonnegative vector function* $\mathbf{f}\in C([0,+\infty[;\mathbb{R}_+^n)\cap\mathfrak{K}_{\mathbf{f}}^p(\mathbb{R}_+;\mathbb{E}_p^0)$ *solution of the Cauchy problem (2.2.2).*

Proof. The results gained in the previous two Lemmas ensure the local existence and uniqueness of the solution of (2.2.2). Indeed the operators $\mathbf{J}[\mathbf{f}]$ and $T_{\mathbf{F}}[\mathbf{f}]$ are locally Lipschitz in the variable $\mathbf{f}$, uniformly with respect to the variable t.
In order to prove that $\mathbf{f}\in\mathfrak{K}_{\mathbf{f}}^p(\mathbb{R}_+;\mathbb{E}_p^0)$, the Cauchy problem (2.2.2) is rewritten in the following Volterra integral vectorial equation:

$$\begin{aligned}\mathbf{f}(t)&=\mathbf{f}(0)+\int_0^t\frac{d\mathbf{f}}{ds}(s)ds\\&=\mathbf{f}(0)+\int_0^t\left[J[\mathbf{f}](s)+\mathbf{F}(s)-\left(\frac{\mathbf{U}^p\cdot(\mathbf{J}[\mathbf{f}](s)+\mathbf{F}(s))}{\mathbb{E}_p[\mathbf{f}](s)}\right)\mathbf{f}(s)\right]ds.\end{aligned}$$

Considering the above vectorial equation componentwise, multiplying both sides for u_i^p and summing over i, yields:

$$\begin{aligned}\sum_i^n u_i^pf_i(t)&=\sum_{i=1}^n u_i^pf_i(0)\\&\quad+\int_0^t\left[\sum_{i=1}^n u_i^p(J_i[\mathbf{f}](s)+F_i(s))-\left(\frac{\mathbf{U}^p\cdot(\mathbf{J}[\mathbf{f}](s)+\mathbf{F}(s))}{\mathbb{E}_p[\mathbf{f}](s)}\right)\sum_{i=1}^n u_i^pf_i(s)\right]ds.\end{aligned}$$

Recalling the (1.2.9), the above equation rewrites:

$$\sum_{i=1}^{n} u_i^p f_i(t) = \mathbb{E}_p^0 + \int_0^t \left[\sum_{i=1}^{n} u_i^p (J_i[\mathbf{f}](s) + F_i(s)) - (\mathbf{u}^p \cdot (\mathbf{J}[\mathbf{f}](s) + \mathbf{F}(s)) \right] ds.$$

Since the integrand function of the above equation vanishes for all s, finally one has:

$$\sum_{i=1}^{n} u_i^p f_i(t) = \mathbb{E}_p[\mathbf{f}](s) = \mathbb{E}_p^0.$$

Setting

$$Q^i[\mathbf{f}, F_i](t) = G_i[\mathbf{f}](t) + F_i(t), \quad P_i[\mathbf{f}, \alpha](t) = \sum_{i=1}^{n} \eta_{ik} f_k(t) + \alpha(J[\mathbf{f}], \mathbb{E}_p, \mathbf{F}), \tag{2.2.21}$$

the equation (2.2.2) can be rewritten as follows:

$$\frac{df_i}{dt}(t) + f_i(t) P_i[\mathbf{f}, \alpha](t) = Q^i[\mathbf{f}, F_i](t), \tag{2.2.22}$$

which is a first-order nonhomogeneous differential equation in the unknown f_i. Let $\gamma_i(t)$ be the formal primitive of $P_i[\mathbf{f}, \alpha](t)$ vanishing for $t = 0$:

$$\gamma_i(t) = \int_0^t P_i[\mathbf{f}, \alpha](s)\, ds.$$

Then equation (2.2.22) writes:

$$f_i(t) = f_i^0 \exp(-\gamma_i(t)) + \int_0^t \exp((\gamma_i(s) - \gamma_i(t)))\, Q^i[\mathbf{f}, F_i](s)\, ds.$$

Let $\mathcal{T} : \mathfrak{K}_{\mathbf{f}}^p \to C$ the functional operator whose ith component reads:

$$(\mathcal{T}[\mathbf{f}])_i(t) = f_i^0 \exp(-\gamma_i(t)) + \int_0^t \exp((\gamma_i(s) - \gamma_i(t)))\, Q^i[\mathbf{f}, F_i](s)\, ds. \tag{2.2.23}$$

Every fixed point of $\mathcal{T}$, i.e. every vector function $\mathbf{f}$ such that $\mathcal{T}[\mathbf{f}] = \mathbf{f}$, in $\mathfrak{K}_{\mathbf{f}}^p$ is solution of the Cauchy problem (2.2.2). It is easy to see that $\mathcal{T}$ maps $\mathfrak{K}_{\mathbf{f}}^p$ into itself, i.e. $\mathcal{T}[\mathfrak{K}_{\mathbf{f}}^p] \subseteq \mathfrak{K}_{\mathbf{f}}^p$; indeed the positivity of the exponential function, the positivity of $Q^i[\mathbf{f}, F_i]$, and $f_i^0 \geq 0$ for all $i \in \{1, 2, \ldots, n\}$, ensure that the relation $f_i(t) \geq 0$ holds true for all $t \in [0, +\infty[$.

The global existence of solution is easily gained. Indeed the occurrence of the global existence of a solution $\mathbf{f}(t)$ on the interval $t \in [0, +\infty[$ would be violated only if $|\mathbf{f}(\mathbf{t})| \to +\infty$ as $t \to t^*$ for some $t^* \leq +\infty$. Since $f_i(t) \geq 0$ and

$$\sum_{i=1}^{n} f_i(t) \leq \sum_{i=1}^{n} u_i^p f_i(t) = \mathbb{E}_p^0 < +\infty,$$

the solution is bounded. Accordingly $\mathbf{f} \in C([0, +\infty[; \mathbb{R}_+^n)$. The proof of the theorem is thus concluded. □

Remark 2.2.3. The set $\mathfrak{K}_{\mathbf{f}}^p(\mathbb{R}_+; \mathbb{E}_p^0)$ is positively invariant for the system (2.2.2). Indeed if $\mathbf{f}^0 \in \mathfrak{K}_{\mathbf{f}}^p(\mathbb{R}_+; \mathbb{E}_p^0)$ then $\mathbf{f}(t) \in \mathfrak{K}_{\mathbf{f}}^p(\mathbb{R}_+; \mathbb{E}_p^0)$.

Remark 2.2.4. In general, if $D_u \subset \mathbb{R}$ (discrete activity), the pth-order moment can be zero even if the distribution vector $\mathbf{f} \neq 0$.

2.3 The introduction of nonlinear interactions

The aim of this subsection is to briefly discuss the role of nonlinear interactions in the KTAP frameworks. Nonlinear interactions will be employed in the next chapter for the derivation of a specific model for pedestrian dynamics in a metro station. The framework proposed in (2.1) is based on the assumption that interactions at the microscopic scale are linearly additive and conservative. However many living systems show complex behaviours that cannot be modeled and simulated simply by linear interactions (see [6] [7]). The introduction of nonlinear interactions consist in assuming that rate η_{hk} and/or the table of games A^i_{hk} depends explicitly on the values of the activity variable u, on the distribution functions f_i and the momenta $\mathbb{E}_p$. In this contest the introduction of a *distance* d_{hk} between the active particles of the h-th and the k-th functional subsystems is needed. The following functions are the most common for modeling the distance d_{hk}:

- $d_{hk} = \eta^0_{hk} \in \mathbb{R}^+$ is simply a real positive constant that depends on the encounter rate of the interacting functional subsystems.
- $d_{hk} = d_{hk}(u_h, u_k)$ depends on the microscopic states of the two interacting particles. The most common case is when d_{hk} depends on the relative difference between the microscopic states of interacting particles:

$$d_{hk} = |u_h - u_k|^\alpha \quad \alpha \in \mathbb{R}.$$

- $d_{hk} = d_{hk}[f_h, f_k](t)$ depends on the distribution functions of the two interacting particles. For example the Euclidean distance between f_h and f_k:

$$d_{hk} = d_{hk}[f_h, f_k](t) = |f_h - f_k|.$$

Additional models and examples can be proposed according to the specific characteristic of the system under consideration. In particular the modeling of the encounter rate η_{hk} can be achieved in a fashion such that increasing values of the distance d_{hk} correspond to decreasing values of the encounter rate η_{hk}. A high level of nonlinearity is introduced when the probability transition A^i_{hk} is conditioned by the microscopic states pf the particles or by the distributions functions, or by the momenta:

$$A^i_{hk} = A^i_{hk}(u_h, u_k, u_i, f_h, f_k, f_i, \mathbb{E}_p[\mathbf{f}]).$$

Moreover the role of the *local interactions* need to be defined. Specifically the interaction domain of the candidate particle with state u_h is not the whole domain D_u, but a subset I_{u_k} which contains the particle $u_k \in I_{u_k}$ that are able to interact with the candidate particle. Bearing all above in mind the thermostatted kinetic framework (2.1.4) that takes into account the nonlinear interactions can be rewritten as follows:

$$\begin{aligned}\frac{df_i}{dt} =& \sum_{h=1}^{n}\sum_{k=1}^{n} \eta_{hk}(d_{hk}) A^i_{hk}(u_h, u_k, u_i, f_h, f_k, f_i, \mathbb{E}_p[\mathbf{f}]) f_h f_k - f_i \sum_{k=1}^{n} \eta_{ik}(d_{ik}) f_k + \\ &+ F_i - \left(\frac{\mathbf{u}^p \cdot (\mathbf{J}[\mathbf{f}] + \mathbf{F})}{\mathbb{E}_p}\right) f_i,\end{aligned} \tag{2.3.1}$$

where the time dependence has been omitted for simplicity. It is worth stressing that the well-posedness of the framework (2.3.1) with nonlinear interactions can be technically proved as an extension of Theorem (2.2.1). The framework (2.3.1) will be employed in the next chapter for the derivation of a specific model for pedestrian dynamic in a metro station.

2.4 Summary

In this chapter we have defined a new discrete kinetic framework for active particles subjected to an external force field and whose microscopic state depends only on the activity variable. The external force field is independent from the activity variable, and it is coupled to a dumping term (thermostat), that is designed in order to keep constant a general p-th order moment $\mathbb{E}_p[\mathbf{f}](t) = \sum_{i=1}^n u_i^p f_i(t)$ of the distribution function. The new framework reads:

$$\frac{df_i(t)}{dt} = \sum_{h=1}^{n}\sum_{k=1}^{n} \eta_{hk} A_{hk}^i f_h(t) f_k(t) - f_i(t) \sum_{k=1}^{n} \eta_{ik} f_k(t) + F_i(t) - \left(\frac{\mathbf{u}^p \cdot (\mathbf{J}[\mathbf{f}] + \mathbf{F})}{\mathbb{E}_p} \right) f_i(t),$$

where:

- $\mathbf{f}(t) = (f_1(t), f_2(t), \ldots, f_n(t))$ is the vector of the distribution functions, where each f_i is the distribution function of the i-th functional subsystem with activity variable u_i.
- η_{hk} is the interaction rate (1.2.4) and A_{hk}^i the probability density (1.2.5)
- $\mathbf{F}(t) = (F_1(t), F_2(t), \ldots, F_n(t))$ is the external force field.
- $\mathbf{J}[\mathbf{f}] = (J_1[\mathbf{f}], J_2[\mathbf{f}], \ldots, J_n[\mathbf{f}])$ is the vector of the internal interactions, where $J_i[\mathbf{f}]$ is given by the RHS of (1.2.7).
- $\mathbf{U}^p = (u_1^p, u_2^p, \ldots, u_n^p)$ is the vector of the activity variable.

The first two terms in the R.H.S. represent the internal interactions among active particles, the second term is the external force field acting on the ith subsystem, and the last term is the thermostat term. It is worth stressing that the thermostat term generally depends on the inner dynamics of the system, the external force field and the p-th order moment, but it has the same functional form given by α for all the functional subsystems. This new framework is suitable to describe complex systems subjected to an external force field where the low number of individuals weakens the assumption of continuity of the distribution function. The main results of this chapter is the prove of local and global existence of solutions for the Cauchy Problem related to the new thermostatted framework.

Chapter 3

Modeling pedestrian dynamics in a metro station

This chapter aims at developing an application of the general thermostatted kinetic framework proposed in the previous chapter. This new framework is be employed for the modeling of pedestrian dynamics at the entrance of a metro station when an external event (sound signals, collective hurry, evacuation alarm) can affect significantly their internal dynamics. The model is proposed for analysing the time distribution of the pedestrians approaching at different gates (turnistiles). In particular the pedestrian dynamics is analysed in absence of the external force field acting on the system, in order to focus only on the internal dynamics of the system (the analysis with the external force field is developed in Chapter 4). Specifically, the chapter is organized in three sections. The first section deals with the derivation of the model, in particular with the characterization of the functional subsystems, the derivation of the evolution equations and the modeling of the microscopic interactions. The second section concerns the analytical analysis of the equilibrium solutions by means of the classical stability theory of perturbations for two specific cases. Finally the last section is addressed to the numerical analysis of the system, which aims at depicting the dynamics and the emerging behaviours described by the model. In particular a sensitivity analysis on the parameters and the initial conditions is performed.

3.1 The Model

This section deals with the derivation of a model for pedestrian dynamics in a metro station in the framework of the thermostatted kinetic theory for active particles proposed in Chapter 2. The section is presented through five sequential subsections. First we deal with a schematic phenomenological analysis of the system (pedestrians in a metro station), then with the characterization of the functional subsystems and the derivation of the evolution equations, and then with the modeling of the internal microscopic interactions. Finally we discuss few initial conditions that have a phenomenological meaning for this model, and that will be employed for the computational analysis.

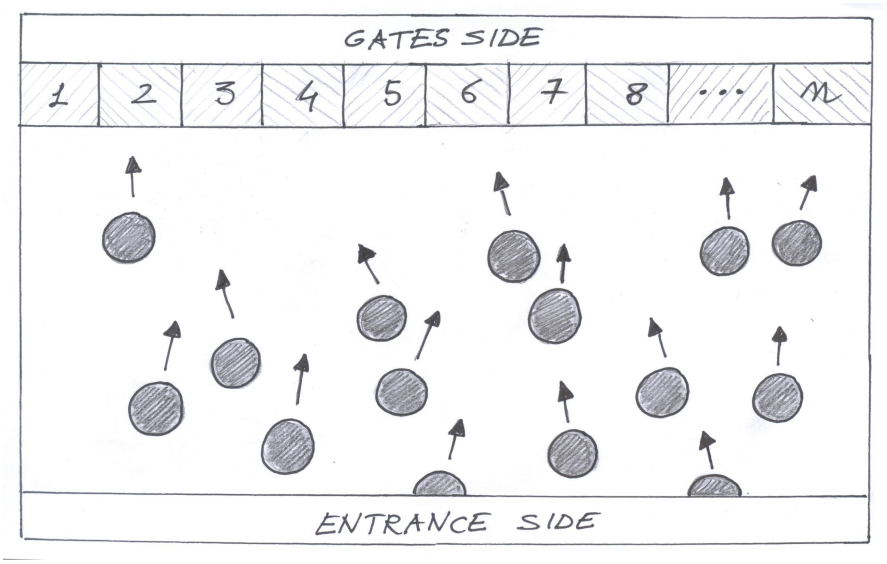

Figure 3.1: Sketch of the metro gates zone.

3.1.1 The system

Let G be a set of N pedestrian that enters [1] in a metro station composed of n gates. The entrance area is assume a rectangle. Gates occupy one side of the rectangle, and they are ordered in ascending way from left to right, while pedestrians come towards them from the opposite side. For simplicity in what follows these two zones are called the *gates side* and the *enter side*, respectively. See Figure 3.1. The number of pedestrians N is supposed to be fixed and constant in time. The last assumption takes into account either the dynamics of a finite group of pedestrians or the dynamics of a constant flux of pedestrians, considering N as the number of pedestrians per unit time entering in the metro station.
Bearing all above in mind, how do pedestrians distributed themselves in time in the n gates, in presence or not of some external factors that influence their internal dynamics in normal situations, such as collective hurry in the early morning, sound signal for fast evacuation or visual signal that recommend some preferential gates? The aim of the proposed model derived with the thermostatted discrete framework (2.1.4) is then to reproduce the main features of this dynamics, once fixed the initial distribution f_i^0 of pedestrians, the interactions among individuals through the design of the interaction rate η_{hk} and the table of games A_{hk}^i, and the definition of an external force field $\mathbf{F}$ coupled with the thermostat term.

3.1.2 The activity variable and the functional subsystems

As already mentioned in Chapter 2, the general thermostatted structure defined in (2.1) is a paradigm for the derivation of a specific model in homogeneous space and velocity, and depends only on the activity variable u. In the pedestrian modeling we are dealing with the activity variable represents the *pedestrian choices*. Specifically the activity variable u_i denotes the *choice of ith gate* by a generic pedestrian. Consequently the system is divided into n functional subsystems, one associated to each gate choice, and the distribution function $f_i(t)$ represents the number of

[1] The case where pedestrians exit the metro through the gates can be represented exactly by the same model. For simplicity, here we focus only on pedestrians who enter a metro station.

pedestrians that at time t has chosen the ith gate to enter. As already mentioned, the model is based on the assumption that the number N of pedestrians is kept constant, then the zero-order moment $\mathbb{E}_0$ is conserved:

$$\mathbb{E}_0[\mathbf{f}](t) = \mathbb{E}_0 \sum_{i=1}^{n} f_i(t) = N. \tag{3.1.1}$$

Bearing in mind the thermostat term (2.1.5) in the case of the conservation of the zero-order momentum $\mathbb{E}_0$, the evolution equations of the model coupled to the initial values (2.2.2) writes:

$$\begin{cases} \dfrac{df}{dt} = J_i[\mathbf{f}] + F_i - \left(\dfrac{\sum_{i=1}^{n} F_i}{\mathbb{E}_0} \right) f_i \\ \\ f(0) = f^0 \end{cases} \tag{3.1.2}$$

where the term of the internal interactions $J_i[\mathbf{f}]$ reads:

$$J_i[\mathbf{f}] = \sum_{h=1}^{n} \sum_{k=1}^{n} \eta_{hk} A^i_{hk} f_h f_k - f_i \sum_{k=1}^{n} \eta_{ik} f_k. \tag{3.1.3}$$

Is easy to see that, the number of equation of the system is equal to the number of gates n under consideration, that will be taken into account as an additional parameter of the model. It is worth stressing that the thermostat term (2.1.5), that allows the conservation of the zero-order momentum, is proportional to the magnitude of the total external force.

3.1.3 The microscopic interaction terms

Referring to the model (3.1.2), the next step is the modeling of the interactions among individuals of the various subsystems and the definition of the related external force field $\mathbf{F}$. Thus in the sequel the interaction rate η_{hk}, the table of games A^i_{hk} and the external force field $\mathbf{F}$ are designed for the specific model. It is worth stressing that for the internal interactions, only binary interactions are taken into account.

- *The Interaction Rate*

  The interaction rate η_{hk} is modeled by considering the *local interactions*. Specifically it is assumed that a pedestrian can interact with pedestrians allocated in a certain number m of gates, that will be referred to as the *interaction range*. The interaction range m is assumed to be a function of the number n of total gates:

$$m(n) = \begin{cases} n & if \;\; n \leq 5 \\ [\frac{1}{3}n + \frac{10}{3}] & if \;\; n > 5, \end{cases} \tag{3.1.4}$$

  where $[a]$ denotes the integer part of a. The above choice reproduces the fact that if the total number of gates is low, then a pedestrian can interact with all the other pedestrians within the entire extension of the gates side; as the total number of gates increases, a pedestrian

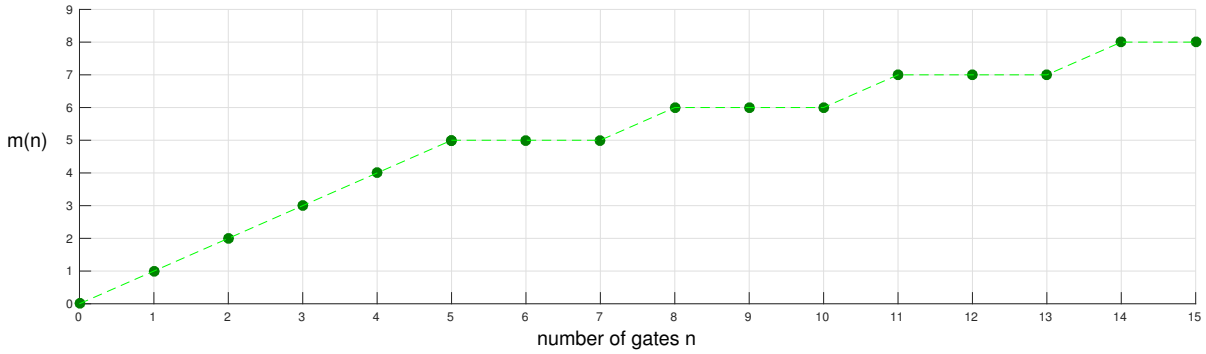

(a) interaction range $m(n)$

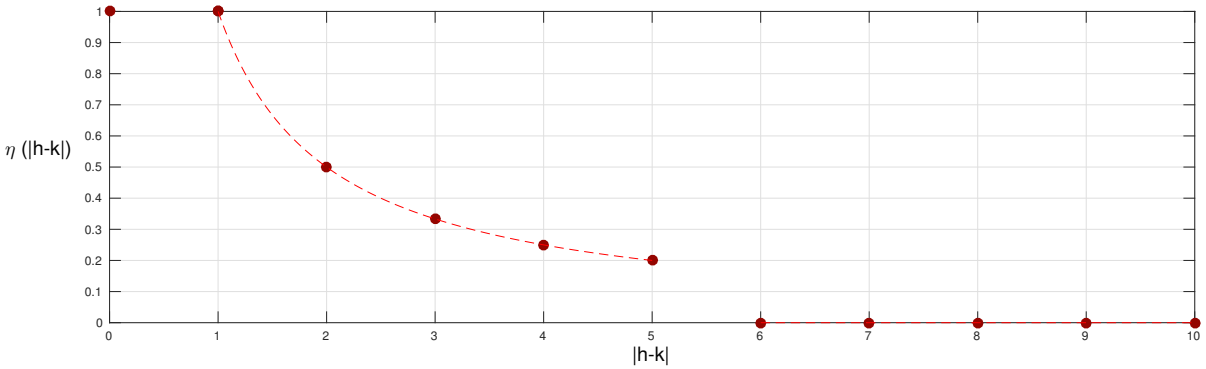

(b) interaction rate η_{hk} for $n = 6$

Figure 3.2: Discrete functions of interaction range and interaction rate.

can physically interact with pedestrians that find themselves in a limited range of gates. In both cases the dependence is modeled as linear, but with different slopes. Moreover for the second subcase we take the integer part to be coherent with the discretization of the activity variable chose in the previous subsection. The cut-off between these two different linear behaviours has been chosen at $m = 5$.
The interaction rate η_{hk} is then designed assuming that it depends only on the relative distance between two gates $|h - k|$ and on m. Specifically:

if $h \neq k$:

$$\eta_{hk} = \eta(|h-k|) = \begin{cases} \frac{1}{|h-k|} & if \ \ |h-k| \leq m \\ 0 & if \ \ |h-k| > m, \end{cases} \tag{3.1.5}$$

if $h = k$:

$$\eta_{hh} = 1. \tag{3.1.6}$$

The Eq. (3.1.4) shows that the probability of interaction decreases as the relative distance between the gates within the interaction range m, while beyond this limit no interaction is allowed. Figure 3.2 shows the two functions $m(n)$ and η_{hk}.

- *The table of games*

  The table of game A^i_{hk} is derived according to a local *leader-follower dynamic* [2] which is function of the *local density*. This is obtained by introducing in the dynamics an explicit dependence on the distribution functions f_i, and non-linear interactions as discussed at the end of Chapter 2. For sake of simplicity, the pedestrian that at time t chooses the ith gate, is identified as the ith pedestrian. For designing the table of games the following assumptions are taken into account:

  A1) The candidate pedestrian h can interact only with a pedestrian k within the range of interaction m according to Eq.(3.1.4) and the choice of the new gate is within this range (*locality*).

  A2) The new gate i chosen by the pedestrian h after the encounter with the pedestrian k belongs to the range $h < i \leq k$ if gate $h < k$, or $k \leq i < h$ if gate $k > h$. Moreover the probability to choose the i-th gate decreases with the distance between the hth and the ith gate. These hypothesis want to reproduce a leader-following dynamic: the candidate h is influenced by the choice of the pedestrian k in the sense that the pedestrian h partially follows the choice of the leader pedestrian k. In brief, when the candidate h encounters the pedestrian k, he follows the direction of the pedestrian k. This fact allows the pedestrian h to visualize the gates between him and the pedestrian k, and to take into consideration this range of gates for a possible new choice. Moreover in general the candidate h considers a new gate that is not too far from his position.

  A3) The probability to choose the new ith gate is proportional to a *local density* ρ_h defined as $\rho_h = \frac{f_h}{N}$, that is a measure of how many pedestrians are queuing, at time t, in the hth gate. This assumption simply models the fact that a pedestrian tends to choose a new gate if there is a lot of queue forming in the one he has chosen (leader).

  A4) The probability to choose the new i-th gate is be proportional to a normalized *fluidity parameter* S. This parameter takes into account the pedestrian flow fluidity, that can be influenced by different factors, e.g. age of pedestrians, mechanical quality of the gates, pedestrians with luggages.

  A5) The pedestrian h that interacts with another pedestrian h, keeps his current choice to gate h.

  Let ϵ_{ih} be a transition probability defined as follows:

$$\epsilon_{ih}(t) = \frac{S\rho_h(t)}{|h-i|^p} \qquad \text{with} \quad \rho_h = \frac{f_h(t)}{\mathbb{E}_0}, \quad S \in]0,1], \quad p \geq 0, \tag{3.1.7}$$

  where $\mathbb{E}_0 = N$ is the conserved zero-order momentum. The parameter p is the fit-best parameter that we denote as the *leader parameter* because it controls how strong is the leader-follower term. The term $\epsilon_{ih}(t)$ partially takes into account assumptions A2), A3), A4). It is worth stressing that the dynamic is symmetric in the left and in the right directions, in the sense that there is no difference if the candidate h encounters the pedestrian k coming from the left or from the right, because in the transition probability ϵ_{ih} the new gate i that

[2] The reader interested in a more deeper understanding about *leader-follower dynamics is referred to* [45]

	$i<h$	$h<i\leq k$	$i>k$	$i=h$	$i<k$	$k\leq i<h$	$i>h$
				$\lvert h-k\rvert > m$			
$\forall\, h,k$	0	0	0	1	0	0	0
				$\lvert h-k\rvert \leq m$			
$k<h$	/	/	/	$1-\sum_{k\leq i<h}\epsilon_{ih}$	0	ϵ_{ih}	0
$k>h$	0	ϵ_{ih}	0	$1-\sum_{h<i\leq k}\epsilon_{ih}$	/	/	/
$k=h$	0	0	0	1	0	0	0

Table 3.1: The table of game for the model (3.1.2) of pedestrian dynamics in a metro station.

the candidate h can choose depends only on the absolute difference of gates. According to all the above assumptions, Table 3.1 summarizes the table of games. It is easy to see that the table of games A^i_{hk} is conservative, i.e. it respects the completeness property:

$$\sum_{i=1}^{n} A^i_{hk} = 1 \quad \forall h,k \in \{1,2,...,n\}.$$

3.1.4 The External Force Field

As mentioned in the introduction of the chapter, the external force field $\mathbf{F}$ can represent collective hurry in the early morning, sound signals or visual signals, or evacuation alarms, that can affect significantly the internal dynamics of pedestrian. The explicit definition of the external force field will be give casewise, and will be analyzed in the next Chapter, that is devoted to the study of the system under the action of the external force field coupled with the thermostat term.

3.1.5 The Initial Conditions

The numerical analysis is based on the definition of five different initial conditions f^0 which specifically are (see Figure 3.3):

Initial condition U : uniform distribution

$$f^0_i = N/n \quad \forall i, \tag{3.1.8}$$

. This initial condition reproduces the case in which pedestrians enter uniformly from the entrance side. Such a situation can be found in big metro stations, where the bigger available space allows people to move freely and arrange themselves uniformly in the gates zone.

Initial condition L : all pedestrians are allocated in the first (left) gate

$$f^0_i = \begin{cases} N & if \;\; i=1 \\ 0 & otherwise. \end{cases} \tag{3.1.9}$$

This initial condition correspond to the case in which all pedestrians reach the gates zone from the left side of the entrance zone. In terms of f_i^0 this is translated into the fact that, at $t = 0$, pedestrians all choose the first gate.

Initial condition R : all pedestrians are allocated in the last (right) gate

$$f_i^0 = \begin{cases} N & if \;\; i = n \\ 0 & otherwise. \end{cases} \tag{3.1.10}$$

This condition is the analogous of the previous one, but now all the pedestrians enter from the right side of the entrance zone. In terms of f_i^0 this is translated into the fact that, at $t = 0$, pedestrians are all choose the last gate n.

Initial condition C : all pedestrians are allocated in the central gate

$$\text{if } n \text{ is a even number} \quad f_i^0 = \begin{cases} \frac{N}{2} & if \;\; i = n/2 \vee i = n/2 + 1. \\ 0 & otherwise, \end{cases} \tag{3.1.11}$$

$$\text{if } n \text{ is an odd number} \quad f_i^0 = \begin{cases} N & if \;\; i = n/2 + 1/2 \\ 0 & otherwise. \end{cases} \tag{3.1.12}$$

This initial condition corresponds to the case where all the pedestrians enter from the center of the entrance zone. In the case of odd number n of gates, this is translated into the fact that, at $t = 0$, all pedestrians choose the only central gate. In the case of even number n of gates, pedestrians choose the two central gates with equal probability.

Initial condition H : pedestrians are allocated in the first gate (left) and in the last gate (right)

$$f_i^0 = \begin{cases} \frac{N}{2} & if \;\; i = 1 \vee i = n \\ 0 & otherwise. \end{cases} \tag{3.1.13}$$

This initial condition corresponds to the case in which $N/2$ pedestrians enter from the left side of the entrance zone, and the other $N/2$ pedestrians enter from the right side of the entrance zone. In terms of f_i^0 this is translated into the fact that, at $t = 0$, $N/2$ pedestrians choose the first gate, and the other $N/2$ choose the last gate.

In all the sets of the numerical simulations the number N of total pedestrians is kept constant. This choice is in agreement with the problem under consideration. In fact according to the table of games we have built up, the dynamic depends only by a local density in (3.1.7) through the candidate local density $\rho_h = \frac{f_h}{N}$, and not on a global density, then N does not affect the qualitative results of simulations. Since the model aims at describing the dynamic of a constant group of pedestrians, the number of total pedestrians is set $N = 100$. This choice is coherent with real data in Paris metro stations: 100 is the mean number of pedestrians passing through each metro station every 10 minutes (rough evaluation). [3]

[3] Paris Metro counts 303 metro stations and the annual ridership in 2012 counted over 1.5 billion passengers (daily 4.21 billion). References: *The Network - The Metro: a Parisian institution*, RATP. Retrieved 2014-01-29. `http://www.ratp.fr/en/ratp/c_10556/the-metro-a-parisian-institution/`.

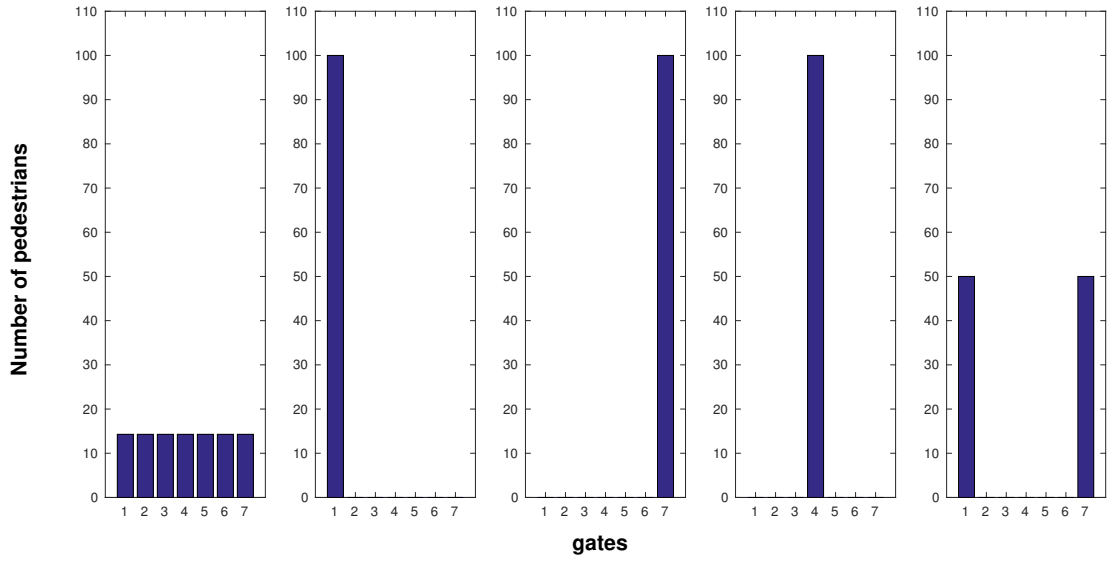

Figure 3.3: The Five initial conditions for the case $n = 7$, $N = 100$. From left to right: U, L, R, C, H.

3.2 A qualitative analysis for the case F = 0: equilibrium solutions

This section is concerned with a qualitative analysis of the model introduced in the previous section. The external force field, and consequently the thermostat term, are assumed to be equals to zero, and then the analysis is focused only on the internal dynamics of the system given by the term $\mathbf{J}[\mathbf{f}]$ in (3.1.2). The study is limited to the case of low number of gates $n = 2$ and $n = 3$, for which an analytical analysis on the equilibrium solutions is feasible by means of the classical stability theory of perturbations. The analysis aims understanding explicitly the equations of the thermostatted framework (3.1.2), and to obtain a first qualitative insight on some general features of the system and of the parameters of the model S, and p. Indeed, the analysis of the asymptotic behaviour of the system allows a deeper comprehension of the transient behaviour, that has a fundamental role in the current application to pedestrian dynamics.

3.2.1 The case $n = 2$

In the case of $n = 2$ gates without external force field, the model (3.1.2) consists of the following two equations:

$$\begin{cases} \dfrac{df_1(t)}{dt} = \eta_{11}A^1_{11}f_1^2 + \eta_{12}A^1_{12}f_1f_2 + \eta_{21}A^1_{21}f_1f_2 + \eta_{22}A^1_{22}f_2^2 \\ \\ \dfrac{df_2(t)}{dt} = \eta_{11}A^2_{11}f_1^2 + \eta_{12}A^2_{12}f_1f_2 + \eta_{21}A^2_{21}f_1f_2 + \eta_{22}A^2_{22}f_2^2. \end{cases} \tag{3.2.1}$$

The interaction range (3.1.4) is given by $m = 2$, and as consequence the interaction rate is simply given by $\eta_{hk} = 1, \quad \forall h, k \in \{1, 2\}$, according to (3.1.5). The table of games is given by the matrices A^1, A^2 that explicitly take the form:

$$A^1 = \begin{pmatrix} 1 & 1-\epsilon_{21} \\ \epsilon_{12} & 0 \end{pmatrix} \qquad A^2 = \begin{pmatrix} 0 & \epsilon_{21} \\ 1-\epsilon_{12} & 1 \end{pmatrix} \tag{3.2.2}$$

where each ϵ_{hk} is given by (3.1.7). Bearing all above in mind, the model (3.2.1) reads:

$$\begin{cases} \frac{df_1(t)}{dt} = f_1^2 + (1-\epsilon_{21})f_1 f_2 + \epsilon_{12} f_1 f_2 - f_1^2 - f_1 f_2 \\ \\ \frac{df_2(t)}{dt} = \epsilon_{12} f_1 f_2 + (1-\epsilon_{12}) f_1 f_2 + f_2^2 - f_1 f_2 - f_2^2, \end{cases} \tag{3.2.3}$$

and considering the transition probability ϵ_{hk} (3.1.7), then the direct computation gives the final system of two nonlinear differential equations:

$$\begin{cases} \frac{df_1(t)}{dt} = \frac{S}{N} f_1 f_2 (f_2 - f_1) \\ \\ \frac{df_2(t)}{dt} = \frac{S}{N} f_1 f_2 (f_1 - f_2). \end{cases} \tag{3.2.4}$$

As one can easily see, the ratio S/N governs the speed of the evolution of the system. The fact that the ratio S/N is linked to the speed of the evolution is in agreement with what one could expect: the more pedestrian are in the gates zone, the less fast they can move because of their high global density that is proportional to N and vice versa. Pedestrians move less fast also if there is a slow (small $S \approx 0$) or a fast (high $S \approx 1$) pedestrian flow. Moreover in this case the equations are independent of the parameter p, because the leader-follower term in Eq.(3.1.7) is equal to 1. This is in agreement with the fact that with only two gates the realization of a leader-following dynamic is not really possible. It is important to notice that $df_2(t)/dt = -df_1(t)/dt$, that is consistent with the conservation of total number of pedestrians N, that in this case means $f_1 + f_2 = N$ (recall that for the discrete framework without thermostat, the conservation of the zero-order momentum $\mathbb{E}_0$ is automatically assured, as previously demonstrated in section (2.1). Thus a model with n gates is described by a system of $n-1$ coupled differential equations. Then by using the substitution $f_2 = N - f_1$, the stability analysis is limited to the equation:

$$\frac{df_1(t)}{dt} = \frac{S}{N} f_1 (N - f_1)(N - 2f_1). \tag{3.2.5}$$

It is easy to see that there are three positive equilibrium points $\bar{f}_1$:

$$\text{A) } \bar{f}_1 = 0 \qquad \text{B) } \bar{f}_1 = N \qquad \text{C) } \bar{f}_1 = N/2. \tag{3.2.6}$$

In order to test the linear stability of these solutions we need to study the evolution in time of the perturbations. Let $\bar{f}_1$ be the equilibrium configurations and δf a small perturbation around it. The evolution problem (3.1.2) relative to $(\bar{f} + \delta f)$ is obtained by developing Eq. (3.2.5) up to the first order in δf, and taking into account that $\bar{f}$ is a solution of this equation, one obtains:

$$\frac{\delta f_1(t)}{dt} = (N^2 - 6N\bar{f}_1 + 6\bar{f}_1{}^2)\, \delta f_1. \tag{3.2.7}$$

By evaluating the r.h.s. of Eq. (3.2.7) in each equilibrium, perturbations grows with time for equilibrium A) and equilibrium C), while they decrease for equilibrium B). Equilibrium $\bar{f}_1 = N/2$ then turns out to be the only stable equilibrium for any initial condition. Recalling the expression for f_2, the whole equilibrium for the system is:

$$(\bar{f}_1, \bar{f}_2) = \left(\frac{N}{2}, \frac{N}{2}\right), \tag{3.2.8}$$

that is a uniform distribution. The asymptotic behaviour of the system is then to fill partially all the available gates. We will see in the next subsection that this behaviour holds true also for the case $n = 3$.

3.2.2 The case $n = 3$

In the case of $n = 3$ gates the analysis follows the same steps of the case $n = 2$. The interaction range is $m = 3$, and the interaction rate η_{hk} is always non zero. The table of Ggmes is given by the three matrices A^1, A^2, A^3, that take the following form:

$$A^1 = \begin{pmatrix} 1 & 1-\epsilon_{21} & 1-\epsilon_{21}-\epsilon_{31} \\ \epsilon_{12} & 0 & 0 \\ \epsilon_{13} & 0 & 0 \end{pmatrix} \qquad A^2 = \begin{pmatrix} 0 & \epsilon_{21} & \epsilon_{21} \\ 1-\epsilon_{12} & 1 & 1-\epsilon_{32} \\ \epsilon_{23} & \epsilon_{23} & 0 \end{pmatrix}$$
$$A^3 = \begin{pmatrix} 0 & 0 & \epsilon_{31} \\ 0 & 0 & \epsilon_{32} \\ 1-\epsilon_{13}-\epsilon_{23} & 1-\epsilon_{23} & 1 \end{pmatrix} \tag{3.2.9}$$

where each ϵ_{hk} is given again by Eq. (3.1.7). It is easy to see that the matrices (3.2.2) for $n = 2$ are the upper-left sub-matrices 2×2 of this case. This is a recurrent relation that holds true in the general dimension n, i.e. the table of game matrices in the case $n-1$ are the upper-left $(n-1) \times (n-1)$ sub-matrices of the case n. By replacing the explicit expression of the table of games and of ϵ_{hk} in (3.1.2), the system of equations for three gates reads:

$$\begin{cases} \frac{df_1(t)}{dt} = \frac{S}{N} \cdot (f_1 f_2 (f_2 - f_1) + \frac{1}{2} f_1 f_3 (\frac{1}{2^p}(f_3 - f_1) - f_1)) \\ \\ \frac{df_2(t)}{dt} = \frac{S}{N} \cdot (f_1 f_2 (f_1 - f_2) + \frac{1}{2}(f_1 + f_3) + f_2 f_3 (f_3 - f_2)) \\ \\ \frac{df_3(t)}{dt} = \frac{S}{N} \cdot (f_2 f_3 (f_2 - f_3) + \frac{1}{2} f_1 f_3 (\frac{1}{2^p}(f_1 - f_3) - f_3)). \end{cases} \tag{3.2.10}$$

The ratio S/N governs again the speed of the dynamical evolution, but unlike the case $n = 2$, in this case the dynamic depends on the parameter p. Indeed with $n = 3$ a leader-follower dynamics can take place more likely. The zero-order moment $\mathbb{E}_0 = N$ is conserved, then the problem is reduced to a system of two coupled differential equations. By means of the substitution $f_3 = N - f_1 - f_2$, the system (3.2.10) then writes:

$$\begin{cases} \frac{df_1(t)}{dt} = \frac{S}{N} \cdot (f_1 f_2 (f_2 - f_1) + \frac{1}{2^{p+1}} f_1 (f_1 + f_2 - N)(f_1(2 + 2^p) + f_2 - N)) \\ \\ \frac{df_2(t)}{dt} = \frac{S}{N} \cdot (f_1 f_2 (f_1 - f_2) + \frac{1}{2}(N - f_2)(N - f_1 - f_2) + f_2 (N - f_1 - f_2)(N - f_1 - 2f_2)). \end{cases} \tag{3.2.11}$$

By equating to zero the r.h.s. of (3.2.11), the following nine equilibrium configurations are obtained:

equilibrium point	TrM	DetM	stability
A)	> 0	> 0	unstable
B)	> 0	< 0	unstable
C)	> 0	> 0	unstable
D)	< 0	< 0	unstable
E)	< 0	< 0	unstable
G)	< 0	> 0	stable

Table 3.2: Stability of the equilibrium points for the case of $n = 3$.

$$
\begin{aligned}
&\text{A) } (0,0) \qquad \text{B) } (N,0) \qquad \text{C) } (0,N) \qquad \text{D) } (N/2,N/2) \qquad \text{E) } (0,N/2) \\
&\text{F) } \left(\frac{N}{11}(5+\sqrt{3}), \frac{N}{11}(1-2\sqrt{3})\right) \qquad \text{G) } \left(\frac{N}{11}(5-\sqrt{3}), \frac{N}{11}(1+2\sqrt{3})\right) \\
&\text{H) } = \left(N\frac{2^p\sqrt{2+2^p}+\sqrt{2^p(4^p-2-2^{p+1})}}{\sqrt{2+2^p}(2^{p+1}-1)}, \frac{N}{1-2^{p+1}}\right) \\
&\text{I) } = \left(N\frac{2^p\sqrt{(2+2^p)}-\sqrt{2^p(4^p-2-2^{p+1})}}{\sqrt{2+2^p}(2^{p+1}-1)}, \frac{N}{1-2^{p+1}}\right).
\end{aligned}
\tag{3.2.12}
$$

Under the model constraints $N > 0$, $0 < S \leq 1$ and $f_i \geq 0$, $\forall i$, all the equilibrium points are acceptable except the points F), H), and I) for which $f_2 < 0$ for all $N > 0$ and $p \geq 0$.
It is worth stressing that all equilibrium points depends on N as expected, but only two equilibrium points, H) and I), show a dependence on p. In order to test the linear stability of the above solutions, the evolution problem (3.1.2) relative to $(\bar{\mathbf{f}} + \delta\mathbf{f})$ is derived as follows:

$$
\frac{d(\bar{f}_i + \delta f_i)}{dt} = G_i[\bar{\mathbf{f}}_\mathbf{i} + \delta\mathbf{f}_\mathbf{i}] - L_i[\bar{\mathbf{f}}_\mathbf{i} + \delta\mathbf{f}_\mathbf{i}] \quad i \in \{1,2,3\}. \tag{3.2.13}
$$

By expanding Eq. (3.2.11) up to the first order in $\delta\mathbf{f}$, and taking into account that $\bar{\mathbf{f}}$ is a solution of it, after some straightforward computing, the following linear system for the perturbations evolution is obtained:

$$
\dot{\delta\mathbf{f}} = M(\bar{f}_1, \bar{f}_2)\delta\mathbf{f}, \tag{3.2.14}
$$

where dotted $\dot{\delta\mathbf{f}}$ in the l.h.s. of Eq. (3.2.14) stays for derivative respect to time, matrix M is evaluated at the equilibrium point $(\bar{f}_1, \bar{f}_2)$ and its explicit expression is given by:

$$
M = \frac{S}{N} \cdot \begin{pmatrix} M_{11} & M_{12} \\ M_{21} & M_{22} \end{pmatrix} \tag{3.2.15}
$$

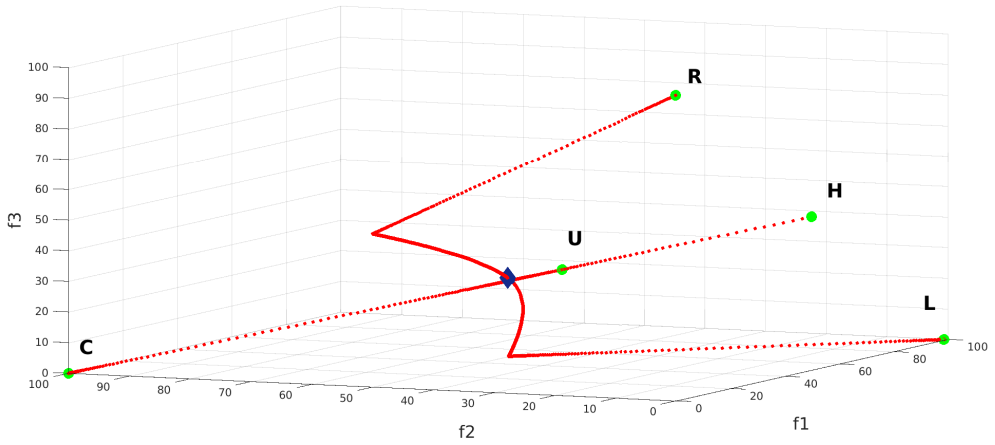

Figure 3.4: Trajectory in the 3D space of the system evolution. The initial conditions (3.1.5) are labeled and marked as green points. Asymptotic state is given by the blue diamond. For $N = 100$ the asymptotic state is given by $(\bar{f}_1 = 29.7, \bar{f}_2 = 40.6, \bar{f}_3 = 29.7)$.

where:

$$M_{11} = \bar{f}_2{}^2 - 2\bar{f}_1\bar{f}_2 + \frac{1}{2^{p+1}}(\bar{f}_1{}^2(4 + 2^{p+1}) + (\bar{f}_2 - N)(\bar{f}_2 - N + \bar{f}_1(4 + 2^p))) \tag{3.2.16}$$

$$M_{12} = 2\bar{f}_1\bar{f}_2 - \bar{f}_1{}^2 + \frac{\bar{f}_1}{2^p}(\bar{f}_2 - N) + \frac{\bar{f}_1{}^2}{2^{p+1}}(3 - 2^p) \tag{3.2.17}$$

$$M_{21} = N^2 + 5\bar{f}_2{}^2 + 10\bar{f}_1\bar{f}_2 - 2N\bar{f}_1 - 6N\bar{f}_2 \tag{3.2.18}$$

$$M_{22} = N^2 + \frac{5}{2}\bar{f}_1{}^2 + 6\bar{f}_2{}^2 + 5\bar{f}_1\bar{f}_2 - 3N\bar{f}_1 - 6N\bar{f}_2. \tag{3.2.19}$$

Because of the complex form of the matrix M, the stability analysis of equilibriums will be performed through the evaluation of the determinant $\mathrm{Det}M$ and the trace $\mathrm{Tr}M$. An equilibrium point is stable if and only if $\mathrm{Det}M > 0$ and $\mathrm{Tr}M < 0$ ([48]). Table 3.2 sums up this quite simple but long analysis. The only stable equilibrium point is G). Then, taking into account also f_3, the asymptotic configuration for the system with $n = 3$ reads:

$$(\bar{f}_1, \bar{f}_2, \bar{f}_3) = \left(\frac{N}{11}(5 - \sqrt{3}), \frac{N}{11}(1 + 2\sqrt{3}), \frac{N}{11}(5 - \sqrt{3})\right). \tag{3.2.20}$$

It is worth stressing that the only equilibrium point of the system, as for the case $n = 2$, depends only on the macro-parameter N, and not on S or p that are exclusively linked to the microscopic dynamic. Being the only stable point, the equilibrium (3.2.20) is the attractor for all the initial conditions. Moreover the steady state is a symmetric distribution, centred at the middle gate $n = 2$. Figure 3.4 shows the numerical solution $\mathbf{f}$ in the 3D space for the different initial condition in (3.1.5). Parameters are fixed at $p = 1$, $S = 1$, $N = 100$. All the trajectories end at the same asymptotic state, and this is in agreement with the previous analytical analysis. It is worth stressing that the trajectories in the 3D space for initial conditions **R** and **L** are symmetric. It is clear from Figure 3.4 that the trajectory starting from the initial condition **U** is part of the trajectory for the initial condition **H**. It means that for $n = 3$, the dynamics for pedestrian entering in the metro with a uniform initial condition **U**, is a subcase of the dynamics of pedestrian entering in the metro

with initial condition $\mathbf{H}$. In the next subsection we will see that the two last facts hold true also for higher values of n.

3.3 Simulations and analysis of emerging behaviours (the case $\mathbf{F} = \mathbf{0}$)

This section deals with numerical simulations addressed to give an insight both to the transient dynamics and to the asymptotic dynamics described by the model, in cases in which no analytical results are available or expensive to obtain. The computational analysis aims at depicting the emerging behaviours described by the model when varying the parameters' magnitude, the number n of the initial distribution functions f_i and their shape, i.e. initial conditions for the Cauchy Problem (3.1.2). Simulations give a complete insight into the system dynamics in order to to show the typical pedestrians' behaviours on the macroscale that emerge from the dynamics at the microscale: pedestrian flow imposed by the leader-follower dynamics, changes in pedestrian flow velocity, concentration of pedestrians, stuck periods at the gates side, and tendency to fill progressively in time all the gates available. In particular, as objectives of the computational analysis, we focus on the sensitivity of parameters S, p and on the initial conditions described in (3.1.5); finally on the analysis of the dynamics for increasing value of gates n.
The sensitivity analysis is developed through four sequential subsections, while the last subsection is devoted to a final discussion that sums up the results of the computational analysis. As in the previous section, the system is not subjected to an external force field, and then we focus only on the internal interactions of the system. In this case with $\mathbf{F} = \mathbf{0}$ the model (3.1.2) simply reads:

$$\begin{cases} \dfrac{df}{dt} = J_i[\mathbf{f}] = \displaystyle\sum_{h=1}^{n}\sum_{k=1}^{n} \eta_{hk} A^i_{hk} f_h f_k - f_i \sum_{k=1}^{n} \eta_{ik} f_k. \\ \\ f(0) = f^0 \end{cases} \tag{3.3.1}$$

It is worth recalling that the conservation of the zero-order momentum $\mathbb{E}_0 = N$ in the case with only internal interaction is automatically assured, as previously demonstrated in Sec.2.1. For what concerns simulations, it is worth stressing that simulations refer to the evolution and the behaviour of the distribution functions in Eq.(3.3.1). Since the model is a system of ordinary differential equations for the distribution functions, the general computational scheme adopted is that of the well-known iterative method. Specifically simulations are performed by means of a Runge-Kutta $(4, 5)$ formula, on the programming language and numerical analysis environment MATLAB ([50], [51]). In all the performed simulations, the only parameter kept constant is the number N of pedestrians, that we set at $N = 100$ as mentioned in subsection 3.1.5. On the contrary the values of the other parameters S, p and n are set casewise as detailed in the next subsections. Moreover time scales and comparison between different times that will be done throughout the chapter have to be consider relatively, because they are simulations times. The rescaling to real situation has to be done in the moment of the validation of the model. It is important to underline that the simulations developed in this section, with their phenomenological interpretations do not cover the whole variety of conceivable pedestrian dynamical situations that can be observed at the entrance of a metro station.

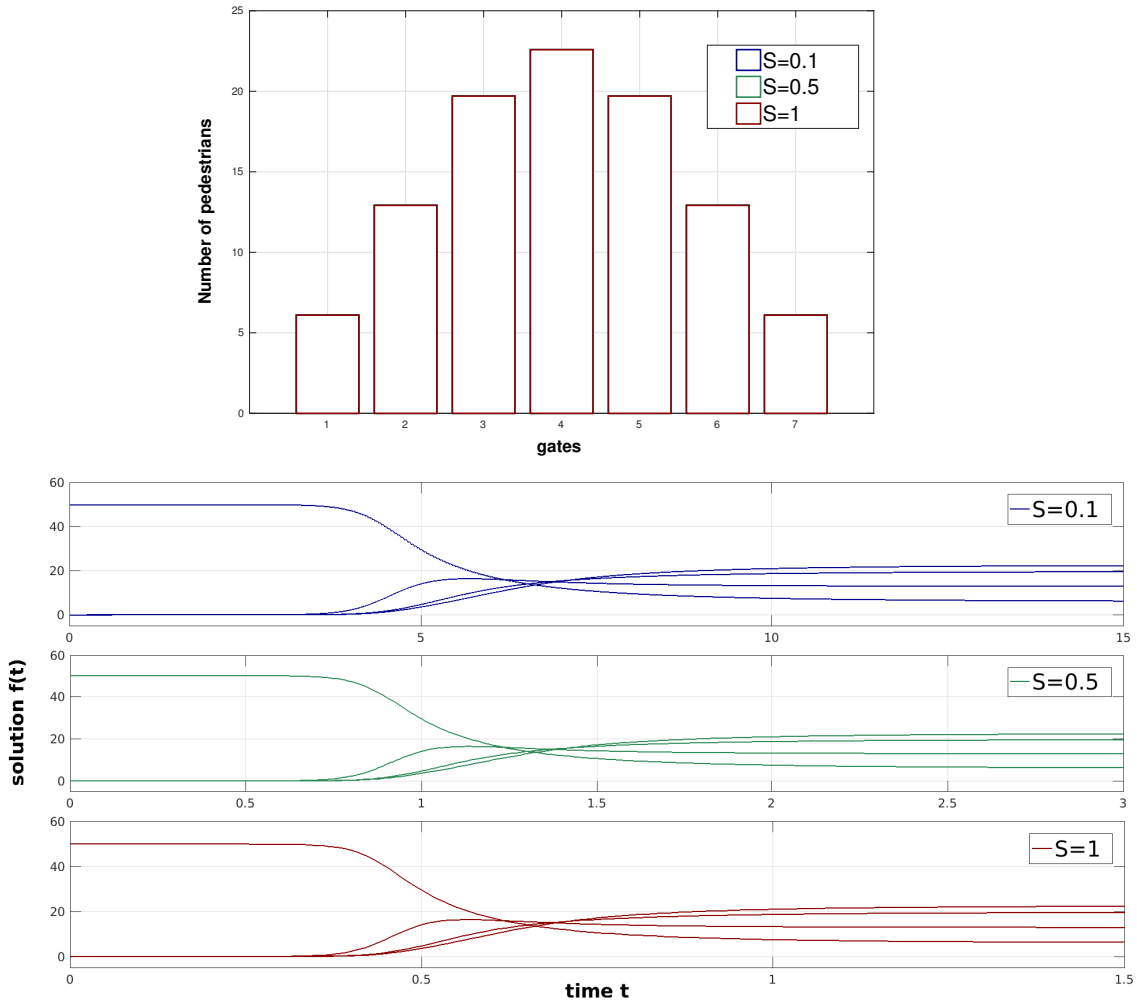

Figure 3.5: Analysis of the parameter S. Asymptotic distribution (upper panel), and whole dynamic evolution (lower panel) for the initial condition **H** for the three different values of S: $S = 0.1$,$S = 0.5$, $S = 1$.

3.3.1 The sensitivity analysis of the *fluidity parameter S*

In this subsection we analyse how the emerging behaviours change when we increase the fluidity parameter S, introduced in the table of games (3.1) in the transition probability ϵ_{ih} of Eq.(3.1.7). Specifically, after fixing the parameter N, we set $n = 7$ (number of gates) and $p = 1$ (leader parameter). Then we fix an initial condition among (3.1.5), and we let S vary in the interval $]0, 1]$. The system dynamics is analysed for three representative values of S:

- $S = 0.1$ (*low fluidity*)
- $S = 0.5$ (*intermediate fluidity*)
- $S = 1$ (*high fluidity*).

Letting S vary from low to high values, we expect an increase in pedestrian flow velocity.
For each simulation, we depict the dynamical evolution in time of the the whole system, and the asymptotic distribution. For the dynamical evolution of the whole system for fixed S, we show in the same figure the evolution in time of each $f_i(t)$, represented by a single line. The asymptotic

distribution is represented by an histogram, where the bars are enumerated in ascending order from left to right as the gates are. The ith bar then shows the number of pedestrian that at finite time has chosen the ith gate. A general discussion on the asymptotic distribution is not reported here, but it is postponed to subsection 3.3.5 where we discuss the results of the whole sensitivity analysis.

The results of the simulations indeed show that by varying the magnitude of the parameter S, time convergence towards the asymptotic distribution decreases for increasing values of S. The evolution dynamics remains instead the same, as shown in the right panel of Figure 3.5, that depicts the time evolution for the initial condition $\mathbf{H}$ (3.1.13). The fact that by varying S the same dynamic takes place on shorter time scale, is further confirmed by the independence of the asymptotic distribution from S (see the left panel of Figure 3.5). Further simulations show that the convergence time towards the asymptotic distribution varies continuously with S, and the scenario just described is qualitative the same for all the initial condition (3.1.5).

The above results are in agreement with the role of the parameter S as indicator for the pedestrian fluidity. Indeed, the less fluid is the people flow (small values of S), the slow the dynamic is and the time needed for reach the gates increases. This fact can be explained also from a mathematical point of view. Actually S in ϵ_{ih} (3.1.7) tunes the probability of transition to other gates. The less probable the change is, the more time is needed for the system to evolve and reach the asymptotic distribution.

3.3.2 The sensitivity analysis of the *leader parameter p*

In this subsection we let vary the leader parameter p introduced in the table of game via ϵ_{ih} in Eq. (3.1.7). Similar simulations performed for the fluidity parameter S are done also for investigating the effects of the leader parameter p.

As before we fix $N = 100$ and $n = 7$, and we set $S = 1$ and an initial condition among (3.1.5), and we let then p vary from low to higher values. As for parameter S, we expect that p affects time convergence towards the asymptotic distribution, i.e. pedestrian flow velocity. For each simulation, we depict the dynamical evolution in time of the the whole system, and the asymptotic distribution.

Before discussing simulation, we perform a preliminary asymptotic analysis on parameter p. By referring to Eq.(3.1.7), if we let $p \to +\infty$ the term ϵ_{ih} goes towards zero, and The table of games (3.1) then depicts a scenario where pedestrians do not move, but on the contrary they rather prefer the gate choice they have done (all term equal zero except for $i = h$). Consequently, the possible dynamics is reduced, and the interactions are quite fixed. On the contrary, in the other limit as $p \to 0$ the transition probability ϵ_{ih} will not depend on the leader-follower term, and all the gates admitted by the interaction range $m(n)$ will be all equiprobable. Then for $p = 0$ there are the maximum interaction possibilities for the dynamics.

The results of the simulations performed on the leader parameter p are summarized as follow: for *low values of the parameter* p ($p <\sim 7$), simulations show that the convergence time towards the asymptotic state grows with p (see right panel of Figure 3.6). Actually by recalling the modeling of the microscopic interactions in the table of games, as p increases the probability of displacement in ϵ_{ih} (3.1.7) to new gates decreases. This simulation results can represent the leader influence in determining the velocity of pedestrian flow: if there are strong leaders that take the initiative to move to other gates, the dynamic is more various and the pedestrians reach faster

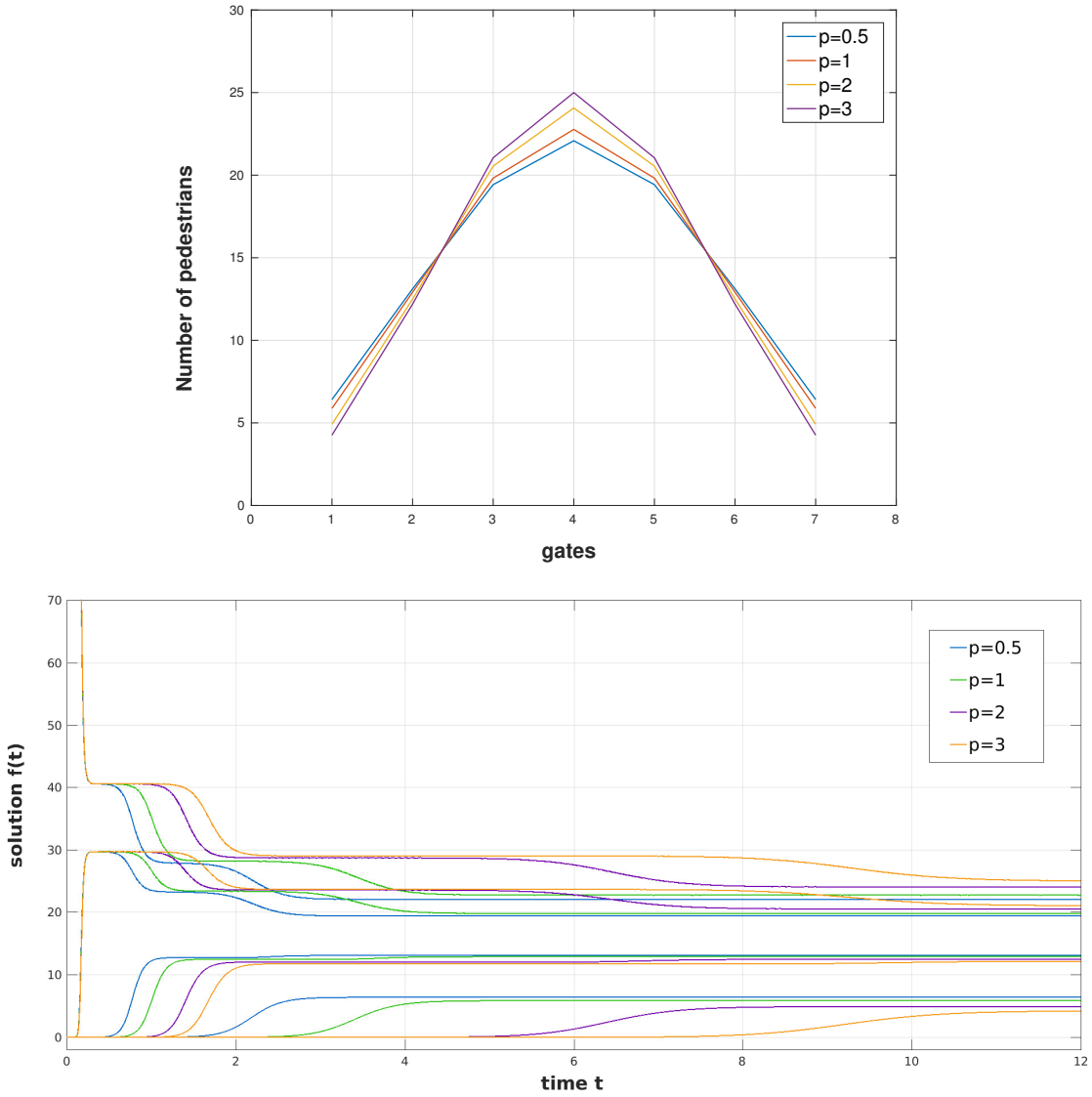

Figure 3.6: Analysis of the parameter p. Stationary distribution (upper panel) and dynamic evolution (lower panel) for the initial condition **C**, for four different low values of p: $p = 0.5 \quad p = 1 \quad p = 2 \quad p = 3$.

their asymptotic distribution. On the contrary if there are weak leaders the dynamics struggles to evolve. Moreover, as shown in the left panel of Figure 3.6, the parameter p has a role in tuning the dispersion σ of the asymptotic distribution. Simulations show that the dispersion σ of the stationary distribution decreases as p increases. If the leader parameter p grows within a range of low values of p, pedestrian tends to be more concentrate in their asymptotic behaviour. The concentration of pedestrians in their asymptotic distribution obtained by increasing p, can not be predicted a priori from the interactions at the microscale of the table of games, but it is an emerging characteristic of the system. It is worth stressing that the asymptotic distribution always fills all the gates available.

For *higher values of the parameter* p ($p >\sim 7$) the simulations shows that neither the convergence time towards the asymptotic distribution nor σ of the asymptotic distribution changes after a certain value of the parameter p, as shown in the panel (a) and in the panel (b) of Figure 3.7 respectively. The effects on the dynamics for increasing p reach then a saturation point. These

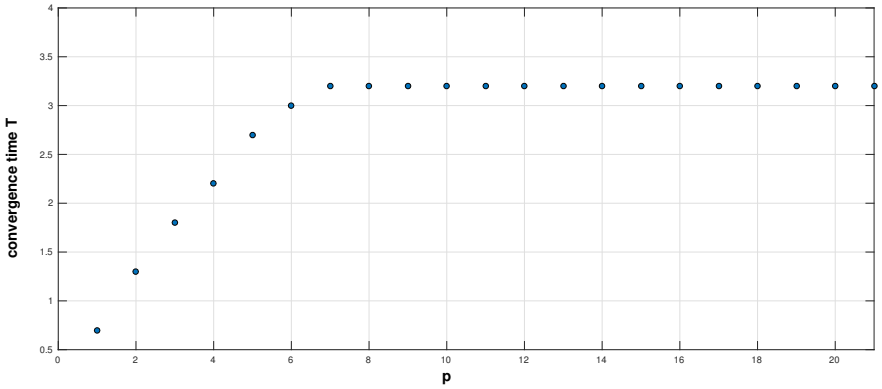

(a) Saturation of the convergence time towards the asymptotic distribution.

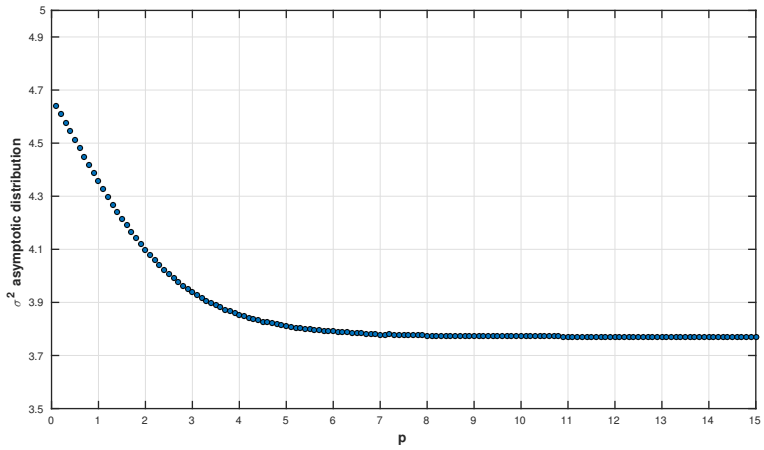

(b) Saturation of the dispersion σ of the asymptotic distribution. The dispersion σ^2 is computed as the dispersion of a discrete distribution: $\sigma^2 = \sum_{i=1}^{n} p_i(i-\mu)^2$, with probability weight p_i for each gate i given by the relative frequency $p_i = f_i/N$, and with mean μ given by $\mu = n/2$ for even number of gates n and $\mu = n/2 + 1/2$ for odd number of gates.

Figure 3.7: The p effects on the dynamics for the initial condition $\mathbf{U}$.

saturation effects can be explained by taking into account the asymptotic analysis on parameter p performed above, the fact that the system reaches a stationary state that involves all gates, and to conservation of total number of pedestrians N. The combination of these three results, gives rise to a sort of incompressibility effect on the asymptotic distribution of pedestrians for high values of p. The saturations effects are important because we can impose a significant upper-bound in changing the parameter p. It is worth noting that the stationary distribution reach the maximum dispersion σ for $p = 0$. Indeed, as previously mentioned, for $p = 0$ there are the maximum interaction possibilities for the dynamics. The dispersion of the stationary distribution is then linked to the *interaction possibilities* for the dynamics: high values of the dispersion means high interactions among the pedestrians. Moreover the fact that p is an indicator of the dispersion asymptotic distribution of pedestrians, allows in principle to obtain the value of p from empirical data.

3.3.3 The sensitivity analysis of the initial conditions

In this subsection we analyse how the different initial conditions mentioned in (3.1.5) give rise to a very heterogeneous dynamics and we investigate the behaviour of the asymptotic distribution. In particular the simulations should visualize the emergent behaviours in the system dynamics that the interactions at the microscale given by the table of games (3.1) give rise to. Specifically, we fix $N = 100$ (total number of pedestrians), we select $n = 7$ (number of gates) and we set $p = 1$ (leader parameter) and $S = 1$ (fluidity parameter). The case $n = 7$ selects a small number of gates that allows to have a better comprehension of the graphics and of the detailed dynamics. Moreover this is a common number of gates in many metro stations as order of magnitude. It is worth stressing that the interaction range (3.1.4) for the case $n = 7$ is equal to $m = 5$, then the interactions involve nearly the whole gates side. We will see the importance of the interaction range m, especially when we will analyse the dynamics for the initial condition **H**.
The sensitivity analysis of the initial condition is performed as follow: for each one of the initial conditions in (3.1.5) we perform a simulation and the we discuss the obtained results. We depict the results of each simulation with two figures. The first figure is a sequence of histograms that represents the pedestrians distribution at consecutive instants of time. In each histogram, at fixed time t, the ith bar shows $f_i(t)$, i.e. the number of pedestrians that at time t chooses the ith gate. The distribution at fixed time t can be interpreted as the distribution with which all pedestrians (or the flux of pedestrians) pass the gates side if they have t time available. The second figure instead represents the whole dynamical evolution $\mathbf{f}(t)$ in time of the system. Each coloured line in the graph represents the evolution in time of each $f_i(t)$. The results of the simulations are summarized for each initial condition as follow:

Initial condition U. As shown in Figure 3.8 (a), for the dynamics where pedestrians come uniformly from the entrance side (initial condition (3.1.8)), we can identify a leader at the central gate $i = 4$. Indeed, from the beginning of the evolution, pedestrians tend to choose the central gates and concentrate simmetrically around the central gate. The evolution continues until pedestrians reach a symmetric asymptotic distribution (see the last histogram of Figure 3.8 (a)). For what concerns the speed of the pedestrians flux during the evolution, the dynamics is faster at the beginning and then converges slowly in a strictly monotonically ascending way to the asymptotic distribution, see Figure 3.8 (b). During the evolution there are no short time intervals in which pedestrians keep the same distribution (i.e. the system does not evolve during this short time intervals). We can define these time intervals *periods of stuck in time*. We underling the absence of periods of stuck in time for the dynamics with the initial condition **U** in contrast to other cases (see below the dynamics for initial condition **L**, **R** and **C**). It is worth stressing that the symmetry in the evolution respect to the central gate $i = 4$, is clear from the fact that only four lines are distinguishable in Figure 3.8 (b). Indeed pedestrians at gates $i = 1$ and $i = 7$ follow the same dynamics, as well as pedestrians at gate $i = 2$ and $i = 6$, and finally as pedestrians at gate $i = 3$ and $i = 5$.

Initial condition L. When all pedestrians enter in the metro station all from the left side of the gates zone (initial condition 3.1.9), at the beginning there are no interactions among first-neighbours, because all pedestrians find themselves in front of a single gate (see the first histogram of Figure 3.9 (a)). Then what allows the dynamic to start is the high local density

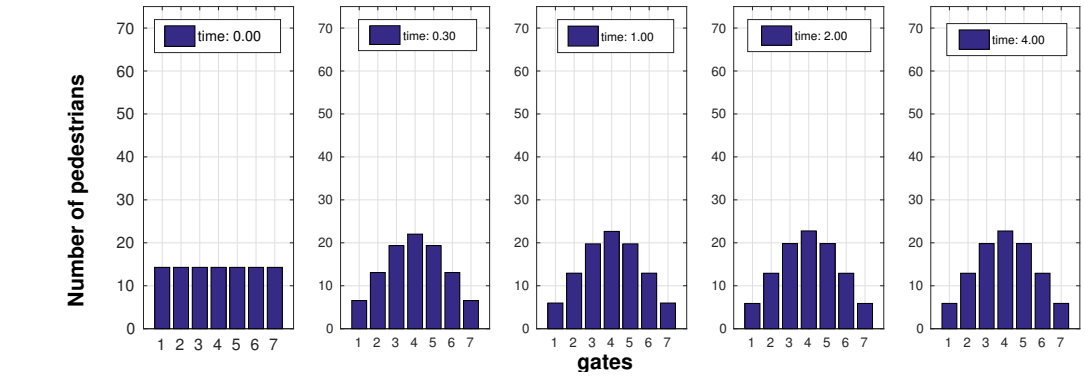

(a)

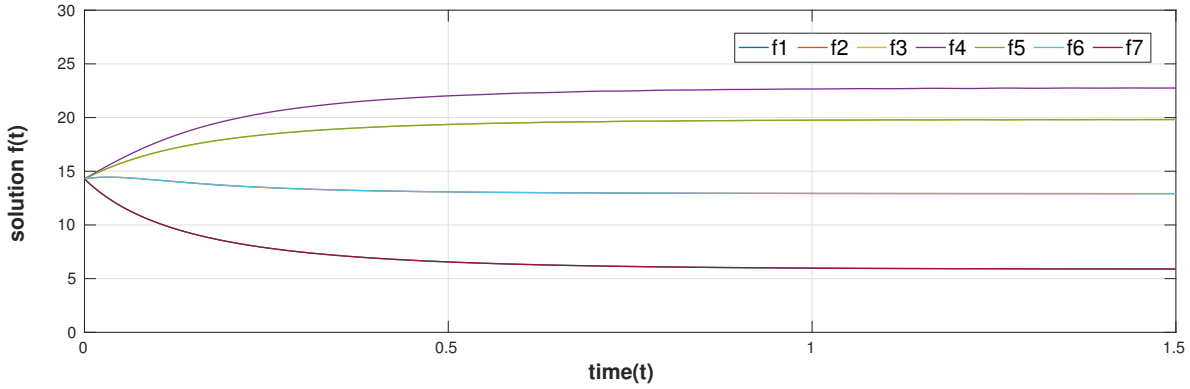

(b)

Figure 3.8: The pedestrians distribution at consecutive fixed instants of time (a), and the whole time evolution of $\mathbf{f}(t)$ for the initial condition $\mathbf{U}$ (b).

ρ_h (recall the probability transition ϵ_{ih} defined in Eq.(3.1.7)). Indeed the high number of pedestrian queuing at gate $i = 1$, induces some leaders to choose the second gate. Other pedestrians follow the leaders choice of gate $i = 2$, and the dynamics evolves until pedestrians reach a distribution where half of them choose the gate $i = 1$, and the other half the gate $i = 2$, as shown in the second histogram of Figure 3.9 (a). The described scenario is a likely situation in a real metro station: when pedestrians enter all from one side of the gates zone (say left), many of them choose as their first choice the second gate and not the first gate closest to them. The distribution where half of the pedestrians choose the gate $i = 1$ and the other half the gate $i = 2$, stabilises for a short time. It is exactly a period of stuck in time, that we have mentioned when we analysed the dynamics for the initial condition $\mathbf{U}$. The behaviour is clear in Figure 3.9(b) at $t \sim 0.3$, where dynamics stops for a short time. The dynamics then restarts when some new leaders move from gates $i = 1$ and $i = 2$ to gate $i = 3$. As shown in the third histogram of Figure 3.9 (a), there are more pedestrians moving from gate $i = 1$ to gate $i = 3$ than pedestrian moving from gate $i = 2$ to gate $i = 3$ (see also Figure 3.9 (b) at $t \sim 0.5$: f_1 decrease more than f_2). This scenario where there is a notable flux of pedestrians moving from gate $i = 1$ to gate $i = 3$, can be explained as follow: some leaders queuing at gate $i = 1$ decide to pass over gate $i = 2$ and reach directly gate $i = 3$, that is the nearest empty gate. Consequently other pedestrians are influenced by the choice

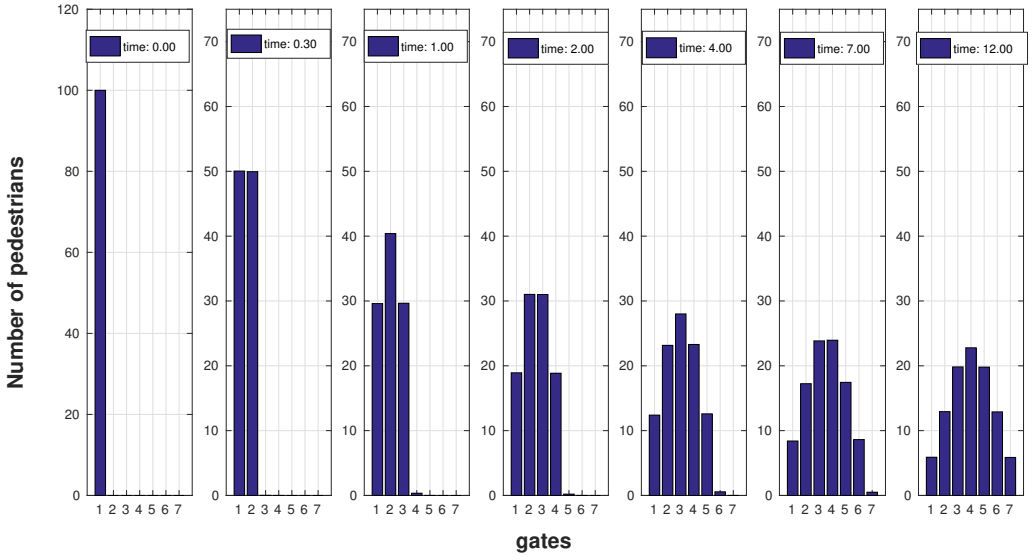

(a)

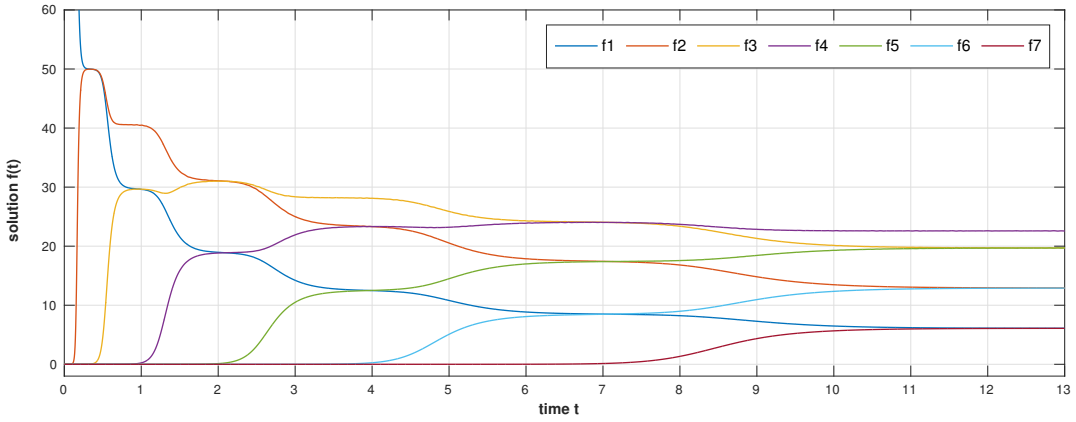

(b)

Figure 3.9: The pedestrians distribution at different instants of time (a), and the whole time evolution of $\mathbf{f}(t)$ for the initial condition $\mathbf{L}$ (b).

of these leaders, and they choose to move from gate $i = 1$ to gate $i = 3$ too. Gradually pedestrian reaches a new metastable distribution, symmetrically centred at gate $i = 2$, as shown in the third histogram of Figure 3.9 (a). The dynamic then restarts again when a new leaders decides to move from gate $i = 1$ and $i = 2$ to gate $i = 4$, a similar dynamics of the one just described take place again. This trend continues until the system reaches the stationary distribution, where all the 7 gates are partially filled, as shown in the last four histogram of Figure 3.9 (b). The dynamics for the initial condition $\mathbf{L}$ then depicts a scenario where the pedestrians tend to choose gradually all the gates from gate $i = 1$ up to gate $i = 7$, giving rise to a global pedestrian flow in this direction. As shown in Figure 3.9 (a), the pedestrian flow is realised through local symmetric metastable distributions, that include increasing number of gates. The last histogram in Figure 3.9 (a) is the configuration that coincides with the asymptotic distribution. The symmetry of local metastable distributions

can find an explanation in the symmetry of the interaction in the table of games. For what concerns the speed of the pedestrians' flow, as for the initial condition **U**, at the beginning the dynamic is faster, and the lifetime of metastable configurations is then shorter; as the time goes on, the dynamics becomes slower and the lifetime of metastable states increases as the more number of gates is filled. The progressive filling of the gates that emerges in the dynamics, can be explained by the leader-follower dynamic in the table of games (3.1) allows pedestrians to choose a new gate in the range thto the gate chosen by the leader. Moreover, the leader chooses as new gate the nearest empty gate. The combination of the two results generates this progressive filling of the gates.

It is worth clarifying that the dynamic just described can be thought also as the dynamic of a single line of pedestrians, and no only as the dynamic for the initial condition **L**. From this point of view then, the analysis focus on the internal interactions of the pedestrian line. This analysis allows to isolate and better understand the single pedestrian line behaviour, in fact the whole dynamics is not the sum of the single lines dynamics, then it clarifies why it is a complex system.

Initial condition R. As Figure 3.10 shows, the dynamics where all pedestrians comes from the right side of the gates zone (initial condition (3.1.10)) is completely symmetric to the dynamics where all pedestrians coming from the left side of the gates zone that we have previous analysed. This behaviour is due to the symmetry in the interactions of the table of games and in the interaction rate η_{hk}. Then it is not surprising that Figure 3.10 (b) and Figure 3.9 (b) are identical.

Initial condition C. When pedestrians enter in the metro station all from the center of the gates zone (initial condition (3.1.12)), simulations show an inverse trend with respect to the dynamics for the initial condition **U**. Indeed as in Figure 3.11 (a) shows, there is a symmetric flow of pedestrians moving from the gate $i = 4$ towards the external gates $i = 1$ and $i = 7$. It is possible to recognize two groups of leaders, one that leads pedestrian from the central gate towards the left part of the gates side, and the other one leads pedestrians to the right part of the gates side. The symmetric behaviour of the flow of pedestrians is again consequence of the fact that the transition probability ϵ_{ih} in (3.1.7) and the interaction rate η_{hk} depends only on the absolute distances between gates $|h - k|$. As for the dynamics in the case of the initials conditions **L** and **R**, the systems evolves through local symmetric metastable states with increasing life time. The metastable states are always symmetric distributions (with respect to the gate $i = 4$) involving only increasing *odd* number of gates (1,3,5,7), while the symmetric distributions with even number of gates are not stable (see Figure 3.11 (b)). The local symmetric metastable distributions are then the ones that keep the symmetry with respect to the central gate $i = 4$. On the contrary as we have previously seen, the dynamics for the initials conditions **L** and **R** allows local symmetric metastable distributions involving increasingly all the number of gates, from $i = 1$ to $i = 7$. This behaviour is due to the fact that initial conditions **L** and **R** are not symmetric respect to the central gate $i = 4$, while the initial condition **C** is symmetric with respect to gate $i = 4$, and the systems in this last case keeps this symmetry during the evolution. Moreover this symmetric evolution is clear in Figure 3.11 (b), where, as for the dynamic in the case of initial condition **U**, we can distinguish only 4 lines. As for all the previous cases, the dynamic is fast at the beginning

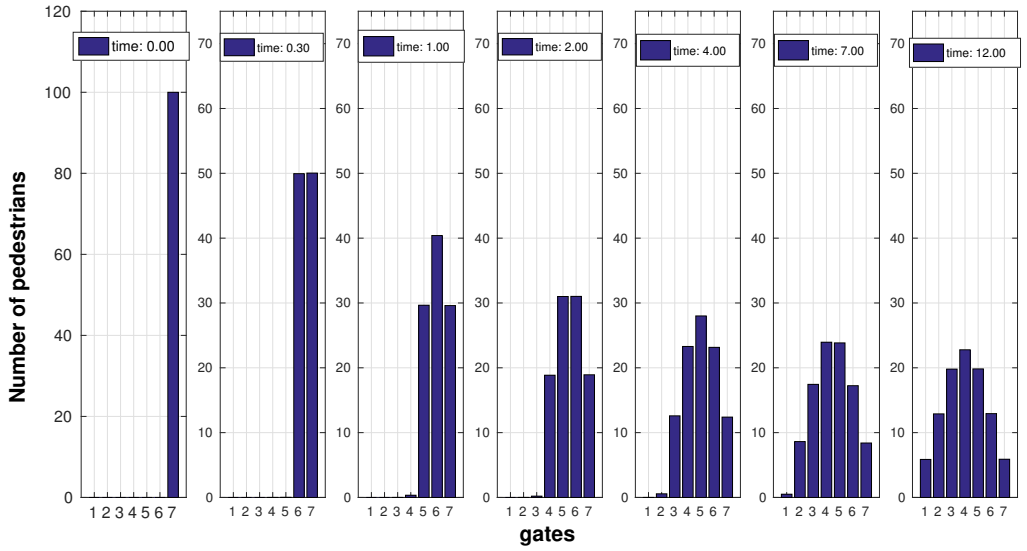

(a)

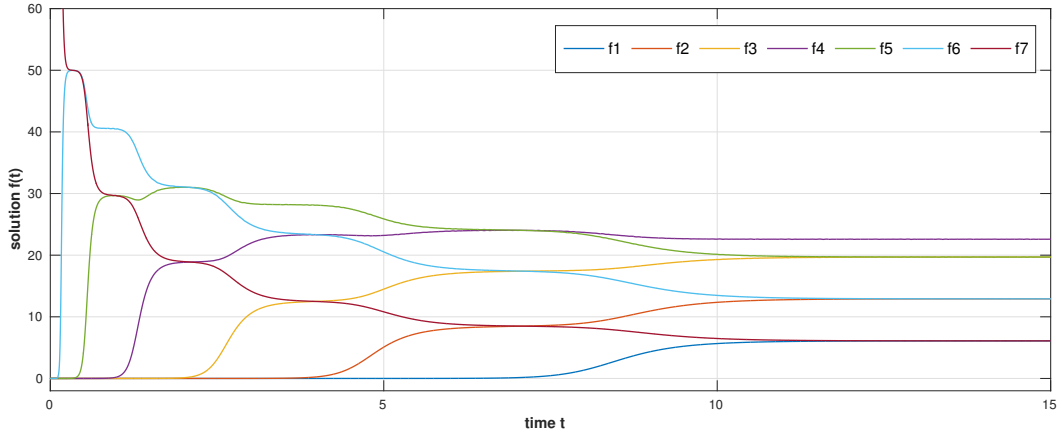

(b)

Figure 3.10: The pedestrians distribution at different instants of time (a), and the whole time evolution of $\mathbf{f}(t)$ for the initial condition $\mathbf{R}$ (b).

and then it tends to stabilize as the time goes on and all gates are progressively chosen.

Initial condition H. When half of the group of the pedestrians enters in the metro station from the left side of the gates zone, and the other half enters from the right side of the gates zone (initial condition (3.1.13)), simulations show that the dynamics does not start at $t = 0$ as in the previous cases, but a bit later (see Figure 3.12 (b)). The delay in the starting time of the dynamics is due to two distinct facts: from one side the neighbour interactions are not possible (recall that for $n = 7$ the interaction range is $m = 5$) then the two groups of pedestrians, one at gate $i = 1$ and the other one at gate $i = 7$, can not interact one with another immediately. From the other side, the probability to choose a new gate ϵ_{ih} is lower with respect to the cases of initial condition $\mathbf{L}$ and $\mathbf{R}$, because the local density ρ_h at gates $i = 1$ and gate $i = 7$ is lower (it is equal to $\rho_h = 1/2$, while for the other two cases is $\rho_h = 1$).

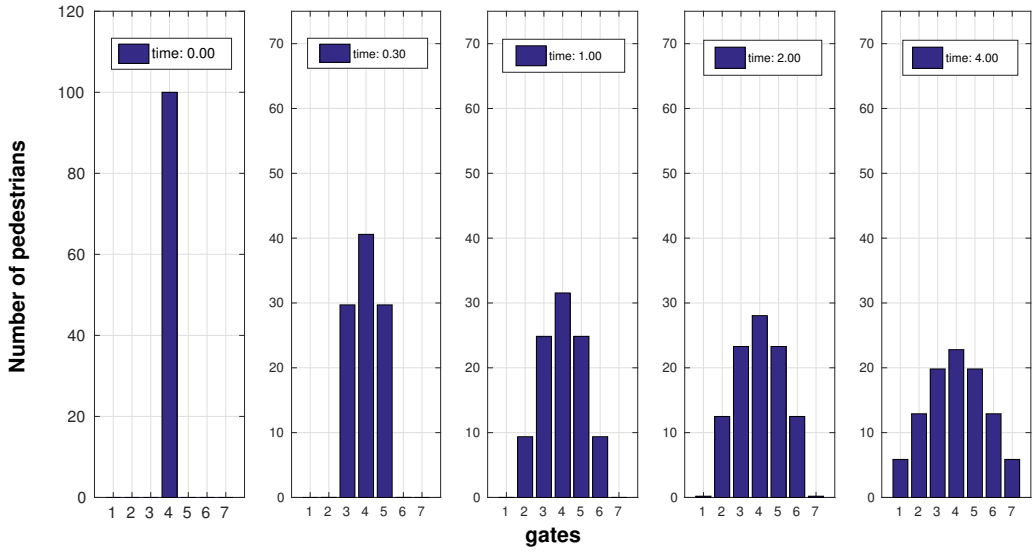

(a)

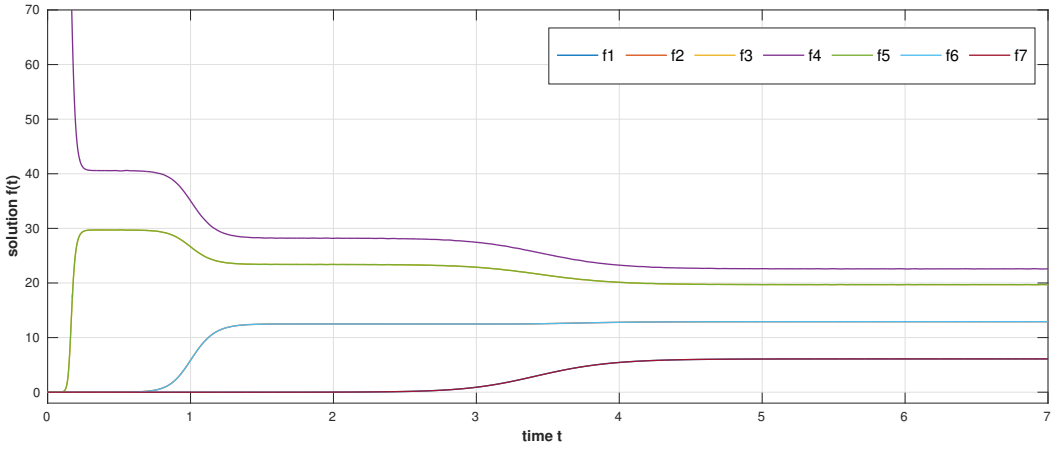

(b)

Figure 3.11: The pedestrians distribution at different instants of time (a), and the whole time evolution of $\mathbf{f}(t)$ for the initial condition $\mathbf{C}$ (b).

What allows the dynamics to start, is then the leader-follower effect: a leader decides to change gate, and is followed by other pedestrians. As shown in Figure 3.12 (a) and (b), there is a fast symmetric decreasing flow of pedestrians going from the gate $i = 1$ and gate $i = 7$ to the center central gate $i = 4$, followed by a slower concentration towards the center with a dynamic similar to the case with initial condition $\mathbf{U}$ (compare Figure 3.12(b)) after $t \sim 0.65$ with Figure 3.8 (b). Indeed as shown in Figure 3.12(b), the system never pass through the uniform distribution, because there is no time at witch all lines intersect at the same point, even though they are very close at $t \sim .0.65$. The dynamics develops always in a symmetric way towards the center. One could expect that the evolution with the initial condition $\mathbf{H}$ could be the superposition of the dynamics with initial conditions $\mathbf{L}$ and $\mathbf{R}$, i.e. the system could evolve through two separated sequences of metastable distributions, one evolving from

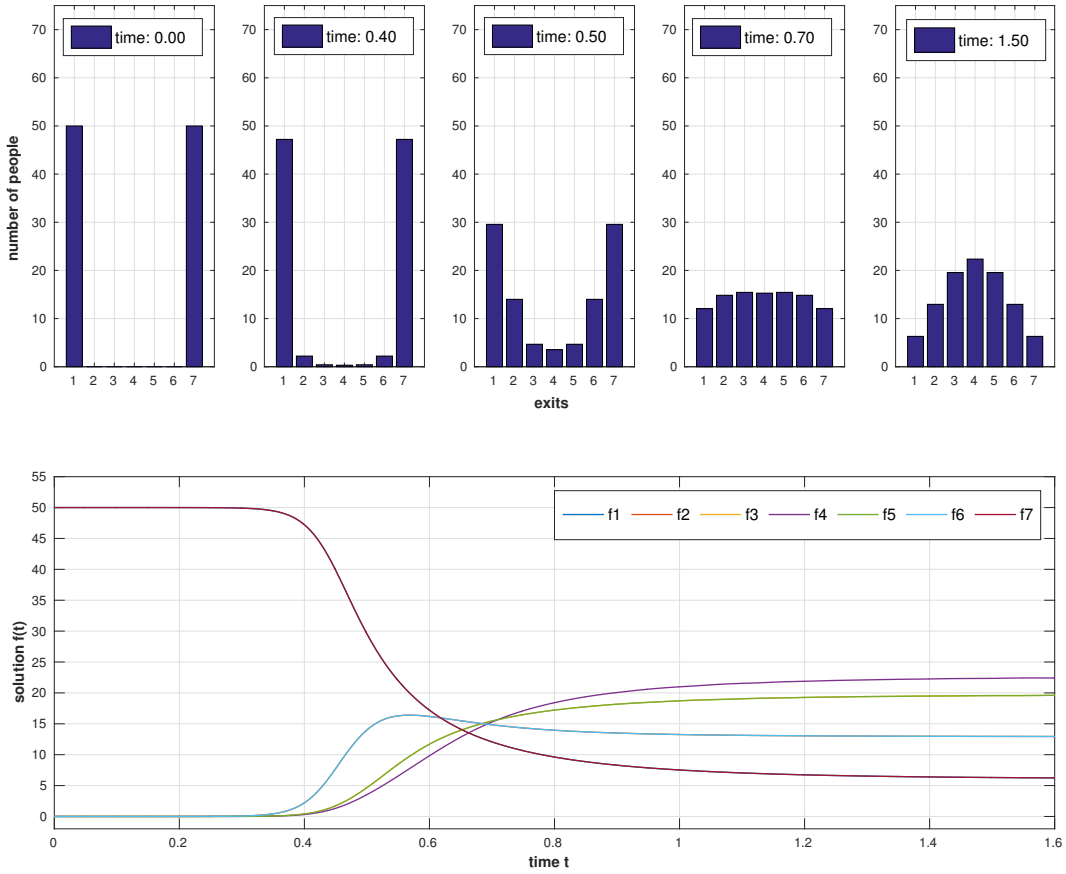

Figure 3.12: The pedestrians distribution at different instants of time (a), and the whole time evolution of $\mathbf{f}(t)$ for the initial condition $\mathbf{H}$ (b).

the left side and one from the right side, until they join together to reach the asymptotic distribution. The scenario is not possible for the case $n = 7$, because the role of interactions between neighbours prevents this type of dynamics. Indeed since values of gates $i = 2$ and gate $i = 6$ start to be partially filled, the two group of pedestrians can start to interact (recall $m = 5$ and then η_{hk} is always different from zero), giving rise to the flow towards the center and then to the concentration in the middle of the gates side, with a continuous evolution without meta-stable states.

3.3.4 Analysis for increasing number of gates n

In this subsection we focus on the analysis of the system dynamics when varying the number of gates n. It is worth stressing that n is not an intrinsic parameter of the model. Indeed the dynamical system (3.1.2) is properly defined when we fix the number of subsystems n and the initial condition. Nevertheless, for the aims of the model to pedestrian dynamics in a metro station, is also important to analyse the pedestrians distribution when varying the number n of gates available in the gates zone. Accordingly, after fixing the parameters $N = 100$, $S = 1$, $p = 1$, we let vary the number of gates n from $n = 2$ up to $n = 25$ (number n of gates higher then this value are not significant for real applications to pedestrian dynamics in metro station). The results of the simulations show that increasing values of the number n of gates depict the following

behaviours:

1. The importance of the local interactions clearly emerges in the dynamics when we let n increase. As shown in Figure 3.13 (a) (case $n = 20$ gates), the dynamics for the initial condition **H** (3.1.13) starts as the dynamics of two independent groups of pedestrians, one entering from the left side and one from the right side. Indeed the group of pedestrians entering from left locally behaves as an entire group of pedestrians entering from left (compare the first three histograms of Figure 3.13 (a) with Figure 3.9 (a)), and similarly the group of pedestrians entering from right locally behaves as an entire group of pedestrians entering from right (compare the first three histograms of Figure 3.13 (a) with Figure 3.10(a)). This behaviour is clearly due to the local interaction structure of the table of games (3.1). Indeed the interaction range $m(n)$ introduced in (3.1.4) marks a limit in the number of gates involved in the interactions between pedestrians. For the case $n = 20$ this limit is $m = 10$. Then at the beginning of the system evolution the number of gates between the two groups of pedestrians is too big (equal to 18) in order to develop mutual interactions. The two groups of pedestrians continue to evolve independently as described above until the number of empty gates that divides them is less than $m = 10$. As shown in the last three histograms of Figure 3.13 (a), when this threshold is passed, the two groups start to interact, and the arising dynamics is analogue to the dynamics for the case $n = 7$ for the initial condition **H** depicted in Figure 3.12 (b): there is no more the formation of metastable states, and the distribution converges monotonically increasing towards its asymptotic state. One can clearly see in Figure 3.13(b) the two different dynamical behaviour just described, the first phase of independent evolutions and then the second phase that concerns the interaction of the two groups. For the initial conditions **U**, **C**, **L**, **R**, simulations show that the dynamics is qualitatively the same as in the case for $n = 7$ described in the previous subsection. Indeed the dynamics in these cases starts from a single nucleus of pedestrians, so interactions are always within this group, and then nothing changes in the dynamical behaviour from the analogue cases for $n = 7$.

2. Simulations show that the convergence time towards the asymptotic distribution grows exponentially-like as n increases, as shown in Figure 3.14. The Figure refers to the convergence time for the initial condition **U**, but the behaviour of the convergence time is qualitatively the same for all the other four initial conditions. Indeed, as seen in the analysis of the previous subsection, what changes among the different initial conditions is the convergence time at fixed n. Then the behaviour of the convergence time versus n for each initial condition will be the same, but on different timescales. The growing in the convergence time can be explained as follow: as the number n of gates increases, the number of gates that a single pedestrian can choose grows with the interaction range $m(n)$ (and η_{hk} grows as consequence). Then pedestrian a priori have more choice and more time for deciding the gate, i.e. the dynamics becomes more heterogeneous during the evolution of the system. Moreover the stationary distribution fills partially always all the gates (see Figure 3.15), and for filling a higher number of gates more time is obviously needed.

3. As shown in Figure 3.15, as we let vary the number n, of gates the asymptotic distribution is always a Gaussian distribution centred in the middle of the gates side, but with a greater

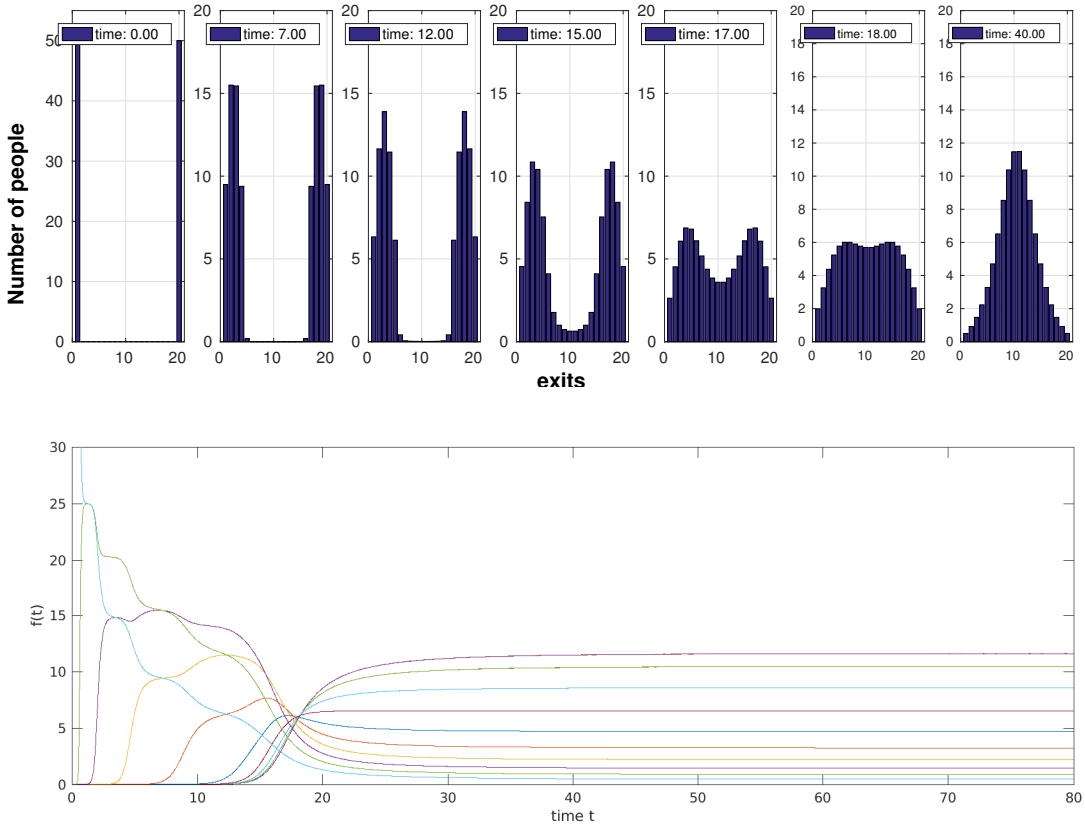

Figure 3.13: The pedestrians distribution at different instants of time (a), and the whole time evolution of $\mathbf{f}(t)$ for the initial condition $\mathbf{H}$ (b) for $n = 20$ number of gates.

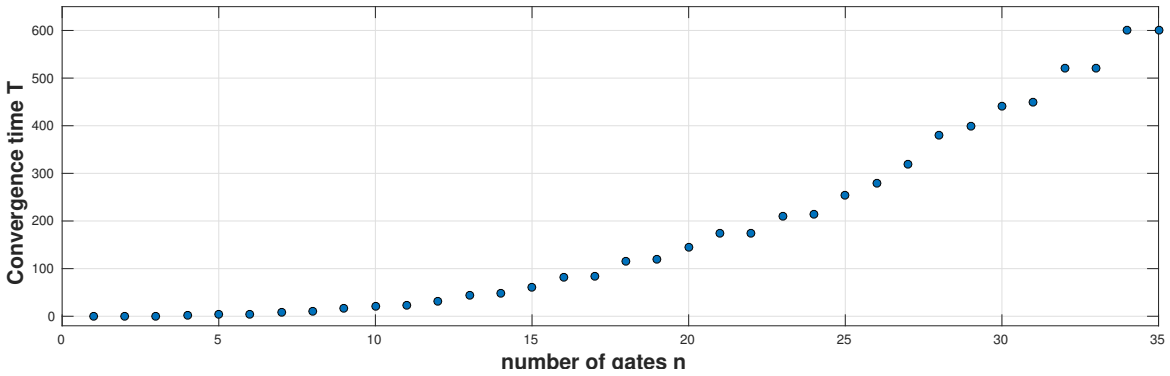

Figure 3.14: Convergence time versus n towards the asymptotic distribution. The system evolves from the initial condition $\mathbf{U}$ fro all n.

dispersion σ for increasing n. Then pedestrians tends to distribute asymptotically in a more uniform way if there are more gates available. This behaviour of the asymptotic distribution can be seen as a direct consequence of the conservation of the total the number N of pedestrians (or the flux of pedestrians per unit time) and of the fact that the stationary distribution fills all the gates. Indeed if the asymptotic distribution must involve all the gates but always with the same fixed number of pedestrian N, its dispersion σ must increase with increasing n. Notice that for odd number of gates the stationary distribution is centred

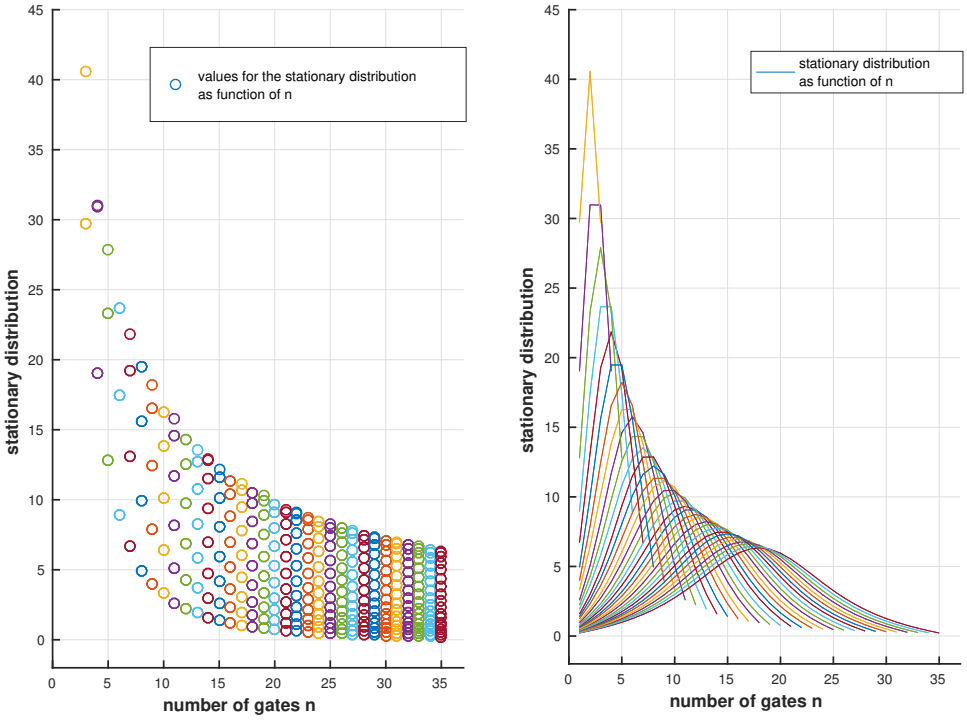

Figure 3.15: Asymptotic distribution for different values of n

at one gate, while for even a the two central gates. It can be seen from the shape of the maximum of the Gaussian: it is picked for odd n while flat for even.

3.3.5 Discussion of the computational analysis results

This last subsection contains some general and conclusive observations on the emerging dynamics caught by the previous analysis:

- According to the table of games (3.1), to the interaction range m and the interaction rate η_{hk}, the pedestrian dynamics is driven by a leader-follower dynamics based on the local density. Simulations performed in this chapter show that the macro dynamics that arises from the microscales interactions reproduces qualitatively some known behaviours of pedestrians distribution in time at the entrance of the metro station: the flow imposed by the leader dynamics, concentration of pedestrians, stuck periods and tendency to fill progressively with time all the gates available.

- As expected, the conservation of the zero-order momentum $\mathbb{E}_0$, i.e. the total number of pedestrians N is ensured in each simulation. Figure 3.16 show the conservations of N for the case $n = 7$ and initial condition $\mathbf{U}$.

- The time evolution of the pedestrians distribution shows for all the initial conditions in (3.1.5), a symmetric or locally symmetric structure, with respect to the gate order. This symmetry property holds true also for the asymptotic distribution. This behaviour is in agreement with the modeling of the Table of Game and in the encounter rate η_{hk}. Indeed interactions depend only on the relative distance between gates.

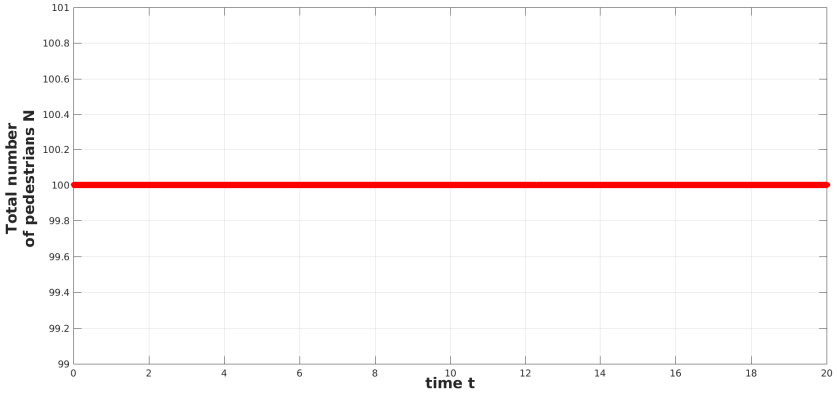

Figure 3.16: Conservation of total number of pedestrians N for $n = 7$, $S = 1$, $p = 1$ with initial condition **U**.

- The local metastable states that arise for some initial conditions, that we called periods of stuck in time, can be thought as instants where pedestrians are thinking what to do, or just waiting to see if the situation in front of the gates changes. The dynamics then restarts when a new leader decides to move to another gate. The stuck periods are more and more longer as the system approaches to the asymptotic configuration, because when almost all the gates are partially filled, pedestrians tends to keep their current gate choice instead of choose a new gate. Simulations show that only the initial conditions depicting situations where pedestrians enter in the metro coming all from one specific point (**L**, **R**, **C**) show this stuck periods. On the contrary the initial conditions that depict situations where more pedestrians enter in the metro gates zone from more than one point do not show this behaviour (**U**, **H**), but they exhibit a continue evolution. The model give rise to these two different scenarios because in the first case the dynamics evolves from a single group of pedestrians where interaction are always internal to the group, that then tends to locally stabilizes itself; in the second case, there are interactions among different groups of pedestrians that prevent local stability. The modeling of local interactions are fundamental for the formation or not of meta-stable states during the evolution.

- The performed simulations show that the asymptotic distribution has always the shape of a Gaussian centred in the central gate of the gates side. The asymptotic distribution can be seen as the distribution that pedestrians will have if they had an ïnfinite timeẗo choose the gates. It is worth stressing that the asymptotic distribution always fills partially all the gates available (say n). This fact is in agreement with the real situation in the metro station, i.e. when pedestrians have long time to choose, all the gates will be chosen.

- The simulations show that the asymptotic distribution is not only qualitative but quantitative the same for all the tested initial condition. Moreover from the sensitivity analysis for the parameters S and p, we can deduce that there is just one asymptotic state depending on p. Mathematically, this means that all these initial conditions belongs to the same attractor field. However from a mathematical point of view we cannot say if it is just the only asymptotic state for the system or if it is just one of the possible attractors. For the asymptotic state of the model then, there is no memory of the initial condition. This likely reproduces

the fact that if pedestrians have a lot of time to enter in the metro, it does not really matter from where they come from. Nevertheless in a more realistic case, there is a limited time for pedestrians to pass through the metro gates. Then initial conditions and the transient dynamics that follows become really determinant in the effective distribution of pedestrians, as we have seen in the sensitivity analysis of the initial conditions. The stationary distribution then is not so important itself for the aim of the model (which is more interested in the dynamic of people in finite time), but however it is central to understand the transient part of the evolution.

- The convergence time towards the asymptotic distribution depends strongly on initial conditions. Because the stationary distribution is always a Gaussian centred at the central gate of the gates side that fills (partially) all the gates, the system that starts from an asymmetric initial conditions respect to the center takes more time to reach the stationary distribution. Compared to the other four cases, then the evolution in time for the uniform initial distribution (initial condition **U**) is faster to converge to the stationary state, because is the only initial condition we have tested with all gates partially filled from the beginning. On the contrary the slowest situations to reach the asymptotic distributions are the situations where pedestrians enter the metro or all from the left side (initial condition **L**) or all from right side (initial condition **R**). The case with the initial conditions **C** and **L** places in the middle of these two cases (see the time scales of figures 3.8, 3.9, 3.10, 3.11, 3.12).

3.4 Summary

In this chapter we have derived a specific model for pedestrian dynamics in a metro station in the framework of the thermostatted kinetic theory proposed in Chapter 2. In particular the model is proposed for analysing the time distribution of a finite group of N pedestrians at approaching different gates (turnistiles) at the entrance of a metro station when an external event can affect significantly their internal dynamics (sound signals, collective hurry, evacuation alarm). The aim of the model is to reproduce the main features of this dynamics, once fixed the initial distribution f_i^0 of pedestrians, the interactions among individuals through the design of the interaction rate η_{hk} and the table of games A_{hk}^i, and the definition of an external force field $\mathbf{F}$ coupled with the thermostat term. Accordingly with the new thermostatted framework developed in Section (2.1), in the pedestrian modeling we are dealing with the activity variable represents the *pedestrian choices*. Specifically the activity variable u_i denotes the *choice of ith gate* by a generic pedestrian. Consequently the system is divided into n functional subsystems, one associated to each gate choice, and the distribution function $f_i(t)$ represents the number of pedestrians that at time t has chosen the ith gate to enter. The model keeps the number N of pedestrians constant (the zero-order moment $\mathbb{E}_0$ is conserved). The evolution equations of the model coupled to the initial values are given by (3.3.1). The microscopic interactions are considered binary, and modelized as follow: the interaction rate η_{hk} (3.1.5) considers only local interactions, through the definition of an interaction range m (3.1.4); the table of games (3.1) is derived according to a local leader-follower dynamics that depends on the local density of pedestrians. The model depends on two free parameters, S (fluidity parameter) and p (leader parameter), introduced in the table of games in the transition probability term (3.1.7). The numerical analysis is based on the definition of five

initial conditions f_i^0 (3.1.5), that have a specific meaning for the model and its applications. In the computational analysis performed in this chapter the external force field, and consequently the thermostat term, are assumed to be equal to zero, in order to focus only on the internal dynamics of the system. In particular the simulations have been addressed to the sensitivity analysis of the parameters S and p, on the sensitivity analysis on the initial conditions (3.1.5) and on the analysis of the dynamics for increasing values of gates n. The results of the simulations are summarized as follows:

- The fluidity parameter S controls the convergence time towards the asymptotic distribution, that decreases for increasing values of S. This is in agreement with the role of the parameter S as indicator of pedestrian fluidity as defined in (3.1.7).

- The leader parameter p represents the leader influence in determining the velocity of the pedestrian flow. Indeed p controls the convergence time towards the asymptotic distribution: as p increases (weaker leader), the convergence time increases. Moreover p has a role in tuning the dispersion of the asymptotic distribution, that decreases as p increases. In both cases the effect of increasing p reaches a saturation point.

- The time evolution of the pedestrians distribution shows a symmetric or locally symmetric evolution. This behaviour is in agreement with the modeling of microscopic interactions, that depend only on the relative distance between gates.

- The asymptotic distribution (that can be seen as the distribution that pedestrians will have if they had infinite time to choose the gates) has always the shape of a Gaussian centred in the central gate of the gates side, and it is quantitative the same for all the tested initial condition. The asymptotic distribution always fills partially all the n gates available. This fact is in agreement with the real situation in the metro station: when pedestrians have long time to choose, all the gates will be chosen.

- The convergence time towards the asymptotic distribution depends strongly on the initial conditions. Because the stationary distribution is always a Gaussian centred at the central gate of the gates side that fills (partially) all the n gates available, the system that starts from an asymmetric initial condition respect to the center takes more time to reach the stationary distribution.

- Local metastable states arise during the evolution in time for some initial conditions (periods of stuck in time). This phenomenon arises only when the dynamics evolves from a single group of pedestrians (initial conditions 3.1.9, 3.1.10, 3.1.12), because interaction are always internal to the group, and the group tends to locally stabilizes itself. On the contrary when the dynamics evolves from an initial condition with more than one local group of pedestrians (initial conditions 3.1.8, 3.1.13), the interactions among different groups prevent local stability. The modeling of local interactions are then fundamental for the formation of meta-stable states during the evolution of the system.

- By increasing the number of gates n, the role of local interactions clearly emerges. The asymptotic distribution is always a Gaussian that involves all the gates available. From this fact, and from the conservation of the total number N of pedestrians, the dispersion of the

asymptotic distribution increases as n increases. Moreover the convergence time towards the asymptotic distribution grows with n, because the asymptotic state always involves all the gates available, and then the system takes more time to choose all the gates.

The simulations performed and the above considerations show that the dynamics that arises from the microscales interactions reproduces qualitatively some known behaviours of pedestrians distribution in time at the entrance of the metro station: the flow imposed by the leader dynamics, the concentration of pedestrians in time, the tendency to choose progressively with time all the gates available and periods of stuck in time, i.e. instants where pedestrians are thinking what to do, or just waiting to see if the situation in front of the gates changes.

Chapter 4

Pedestrian dynamics under the action of an external force field

This chapter is devoted to the analysis of the pedestrian dynamics when subjected to an external event. In particular, the analysis focuses on the model (3.1.2) for specific external force fields acting on the systems, whose functional forms are defined in order to have a physical meaning for the pedestrians model under consideration (pedestrian in hurry, preferential gates, sound alarm and so on). The investigation on the system dynamics is performed through numerical simulations that focus on how the internal dynamics of the system is affected by the presence of an external force field (changes in the asymptotic distribution and in convergence time, symmetry breaking of the internal dynamics). In particular the emergent features of the dynamics are stressed out, and the role of the thermostat in allowing the system to reach a stationary state is underlined. The analysis of the model follows the same outline and style of the analysis presented in Chapter 3 for the internal dynamics of pedestrians. Specifically in the first section the model is analysed in the case of a constant an uniform external force field, in the second section in the case of a constant non uniform external force field, and in the third section in the case of a uniform time dependent force field.

4.1 The case of a constant uniform external force field

This section is concerned with a qualitative analysis of the pedestrian dynamics subjected to a *constant* and *uniform* external force field. Specifically the external force field $\mathbf{F}$ is constant and acts with the same magnitude on all the gates, i.e. $F_i = F > 0$, $\forall i$. For the system depicting the dynamics of pedestrians in a metro station, the constant uniform external force field can represent an event where pedestrians are in a hurry to reach the gate (think about metro station at 8 a.m. in the morning, when pedestrians are pushed for going to work), or some audio announcement to evacuate the metro as soon as possible. The thermostat term (2.1.1) in this case simply reads $\alpha = \frac{nF}{N}$, and the related Cauchy problem for the pedestrian dynamics in a metro station (3.1.2) rewrites:

$$\begin{cases} \dfrac{df}{dt} = J_i[\mathbf{f}] + F - \left(\dfrac{n}{N}F\right) f_i \\ \\ f(0) = f^0 \end{cases} \tag{4.1.1}$$

The analysis of the system (4.1.1) follows the same outline and style of the analysis presented in Chapter 3 for the internal dynamics of pedestrians in Section 3.3. Firstly for a fixed magnitude F of the external field $\mathbf{F}$ we investigate the case of low number of gates analytically, and then we perform a sensitivity analysis on the initial conditions (3.1.5) and an analysis for increasing number of gates. Finally the system dynamics is analyzed for increasing values of the magnitude F of the external force field, and we investigate the role of the force magnitude in affecting the emergent behaviours of pedestrians.

4.1.1 Analytical analysis for the case $n = 2$

In this simple case of $n = 2$ gates with uniform force field the model4.1.1) is explicitly given by the two following equations system:

$$\begin{cases} \frac{df_1(t)}{dt} = \frac{S}{N} f_1 f_2 (f_2 - f_1) + F - \frac{2F}{N} f_1 \\ \\ \frac{df_2(t)}{dt} = \frac{S}{N} f_1 f_2 (f_1 - f_2) + F - \frac{2F}{N} f_2 \end{cases} \tag{4.1.2}$$

where for the first term of each equation we have simply rewritten the terms in (3.2.4) for the case without external force field. The total number of pedestrian N is conserved, then recalling $f_2 = N - f_1$, the system analysis is limited to the equation:

$$\frac{df_1(t)}{dt} = 2\frac{S}{N} f_1^3 - 3S f_1^2 + \left(SN - 2\frac{F}{N} \right) f_1 + F. \tag{4.1.3}$$

In order to find a stationary solution the following equation must be solved:

$$2\frac{S}{N} f_1^3 - 3S f_1^2 + \left(SN - 2\frac{F}{N} \right) f_1 + F = 0, \tag{4.1.4}$$

which is a polynomium of degree 3 in the variable f_1 and with real coefficients. The stationary solution problem of (4.1.2) then reduces to find out the real roots of the polynomium (4.1.4). Straightforward computation gives the following roots:

$$A)\ \bar{f}_1 = \frac{N}{2} \quad B)\ \bar{f}_1 = \frac{A}{2} + \frac{1}{2}\sqrt{\frac{4F + N^2 S}{S}} \quad C)\ \bar{f}_1 = \frac{A}{2} - \frac{1}{2}\sqrt{\frac{4F + N^2 S}{S}}. \tag{4.1.5}$$

It is worth to notice that for $F = 0$ we recover the three solutions of (3.2.6) that we have found in the analysis of the $n = 2$ case without external force field (Section 3.2). In order to test the linear stability of these solutions, we study the evolution in time of the perturbations as we performed in subsection 3.2.1. Considering the evolution problem of $(\bar{f} + \delta f)$, and expanding Eq. (4.1.3), up to the first order in δf one obtains:

$$\frac{\delta f_1(t)}{dt} = (6\frac{S}{N} \bar{f_1}^2 - 6S\bar{f_1} + NS - 2\frac{F}{N})\, \delta f_1. \tag{4.1.6}$$

Then the evaluation of the R.H.S. of Eq. (4.1.6) in each equilibrium in (4.1.5) reads:

$$A)\ \frac{\delta f_1(t)}{dt} = -\left(\frac{2F}{N} + \frac{NS}{2} \right) \delta f_1 \tag{4.1.7}$$

$$B)\ \frac{\delta f_1(t)}{dt} = +\left(\frac{4F}{N} + NS \right) \delta f_1 \tag{4.1.8}$$

$$C)\ \frac{\delta f_1(t)}{dt} = +\left(\frac{4F}{N} + NS \right) \delta f_1. \tag{4.1.9}$$

For $N > 0$, $< S \leq 1$ and $F > 0$ the only stable solution for every initial conditions, is the solution $A)$ $\bar{f}_1 = \frac{N}{2}$. Recalling the expression for f_2, the whole equilibrium for the system (4.1.2) is:

$$(\bar{f}_1, \bar{f}_2) = \left(\frac{N}{2}, \frac{N}{2}\right). \tag{4.1.10}$$

This is the same stable solution we obtained in the analysis of the case $n = 2$ without external force field in Section 3.2.1, and it is independent on the external force field. However we will see that this is a peculiar fact for the case $n = 2$, because for $n \geq 3$ simulations show that the stationary solution depends on the magnitude F of the external force field (see subsection 4.1.4).
It is worth stressing that one could have derived the stable equilibrium solution (4.1.10) simply by considering symmetry arguments. Indeed, because the system is subjected to a *uniform* external force field, symmetry in the evolution is conserved. It follows that also the stationary distribution must be symmetric, and then the only possibility for the case $n = 2$ is the uniform distribution, that is independent from the magnitude F of the external force field.

4.1.2 The sensitivity analysis on the initial conditions

In this subsection we analyse the dynamics of the system (4.1.1) subjected to an uniform external force field with fixed magnitude F. Again, simulations focus on the analysis of the system behaviour with initial conditions (3.1.5). The computational analysis aims at analyze how the presence of an external force field modifies the qualitative behaviours and the emergent features of the dynamics, compared to the case where the system is not subjected to an external force field (see section 3.3.3). In particular the role of the thermostat in controlling the system behaviour is stressed out. The sensitivity analysis of the initial conditions is performed following the same scheme we have used to investigate the system behaviour in absence of the external force field in subsection 3.3.3. In particular, the parameters kept at constant values for all simulations are chosen as in subsection 3.3.3. We fix $N = 100$ (total number of pedestrians), we select $n = 7$ (number of gates), the interaction range (3.1.4) is then equal to $m = 5$, and we set $p = 1$ (leader parameter) and $S = 1$ (fluidity parameter). Finally the magnitude of the external force is set to $F = 100$. Figures 4.1, 4.2, 4.3, 4.4, 4.5 show the dynamical evolutions of the system for the initial conditions **U**, **L**, **R**, **C**, **H**, respectively.
The results of the simulations are summarized as follows:

For all the tested initial conditions, the system reaches a non equilibrium stationary state, as shown in Figures 4.1, 4.2, 4.3, 4.4, 4.5. This means that even if pedestrians are subjected to an external event, in a long timescale they manage to organize themselves as they did when no external event is influencing their gate choice. This is in agreement with real situations. The existence of a stationary state is a remarkable result, because it underlines the capability of the thermostat term in mimic the system capacity of self-organization with respect to the environment accordingly to the physical constraints it is subjected. Always referring to Figures 4.1, 4.2, 4.3, 4.4, 4.5, simulations show that the asymptotic state is qualitative always a Gaussian distribution centred in the central gate. Further computational investigations show that the asymptotic state is quantitative the same distribution for the initial conditions **U**, **L**, **R**, **C**, **H**. However it is quantitatively different from the case where no external force field acts on the system. This characteristic will be further investigated in subsection 4.1.4.

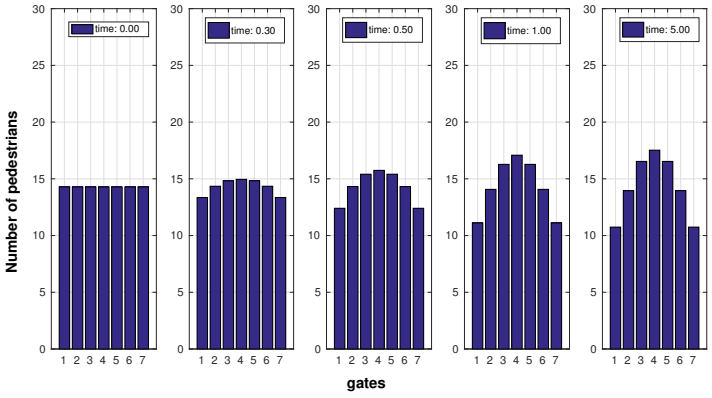

(a)

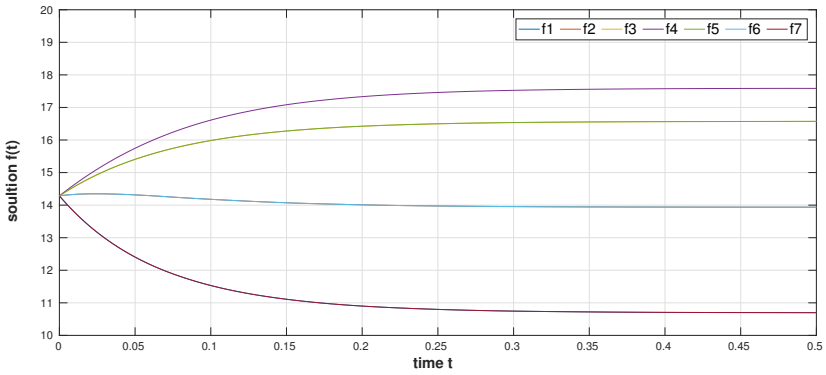

(b)

Figure 4.1: System subjected to an uniform external force field of magnitude $F = 100$. The pedestrians distribution for different instants of time (a), and the whole time evolution of $\mathbf{f}(t)$ for the initial condition $\mathbf{U}$ (b).

The pedestrians dynamics subjected to a constant uniform external force field is faster than the pedestrians dynamics where no external agent is present, in the sense that the system reaches its asymptotic distribution in less time compared to the case where only internal interactions drive the pedestrians dynamics, compare the timescales of Figures 3.8 and 4.1, Figures 3.9 and 4.2, Figures 3.10 and 4.3, Figures 3.11 and 4.4, Figures 3.12 and 4.5.

As shown in Figures 4.1, 4.2, 4.3, 4.4, 4.5, the symmetry with respect to the central gate is kept in the time evolution of the system, exactly as in the case where no external force field acts on the system. This is obviously due to the fact that the presence of an uniform and constant external force field does not introduce any asymmetry in the system structure of 4.1.1.

As expected, the total number of pedestrians N is always conserved in all the performed simulations. The computational analysis then confirm the role of the thermostat term in keeping constant the zero-order moment despite the presence of an external force field, as we purposely set up in the model (3.1.2).

As already mentioned, there are some common features in the scenarios where pedestrians dynamics is driven only by internal interactions and where pedestrians are subjected to an external force field. However two intrinsic changes in the qualitative dynamics emerge from simulations.

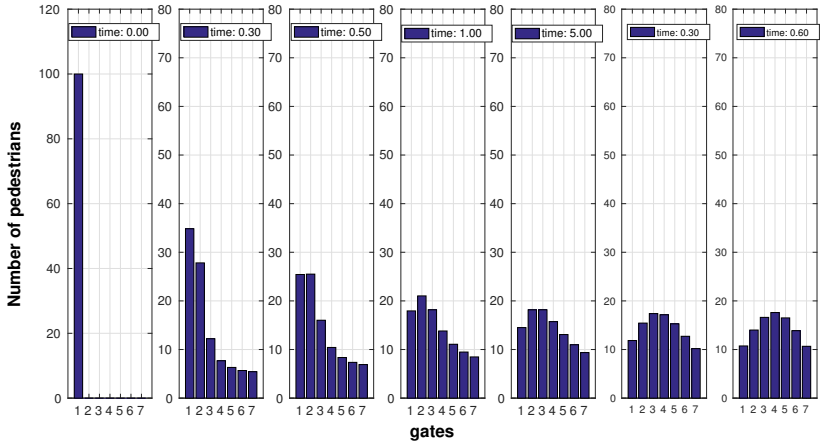

(a)

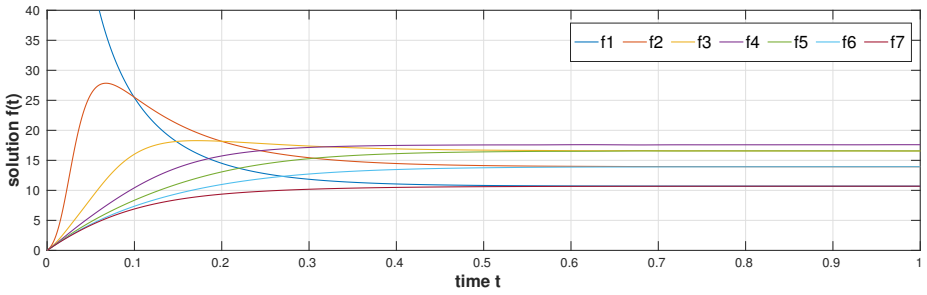

(b)

Figure 4.2: System subjected to an uniform external force field of magnitude $F = 100$. The pedestrians distribution for different instants of time (a), and the whole time evolution of $\mathbf{f}(t)$ for the initial condition $\mathbf{L}$ (b)

Firstly, for the initial conditions $\mathbf{L}$, $\mathbf{R}$, $\mathbf{H}$, there are no more metastable states during the evolution (compare Figures 3.9 (b) and 4.2 (b), Figures 3.10 (b) and 4.3 (b), Figures 3.12 (b) and 4.5 (b)). The presence of an external force field acting on the system prevents the formation of self-organized structures during the evolution of the system that on the contrary would naturally arise from the internal dynamics. Secondly, for all the initial conditions tested pedestrians start to choose all the gates from the beginning of the time evolution (see at time $t = 0$ the evolution in figure (b) of Figures 4.1, 4.2, 4.3, 4.4, 4.5).

Accordingly to the results, the global effect of the uniform external force field acting on the pedestrians system is to force them to choose all the gates from the beginning, and to fill them faster and with a continuous evolution. The scenario agrees qualitatively with what usually happens in a real metro station in situations of hurry or fast evacuation.

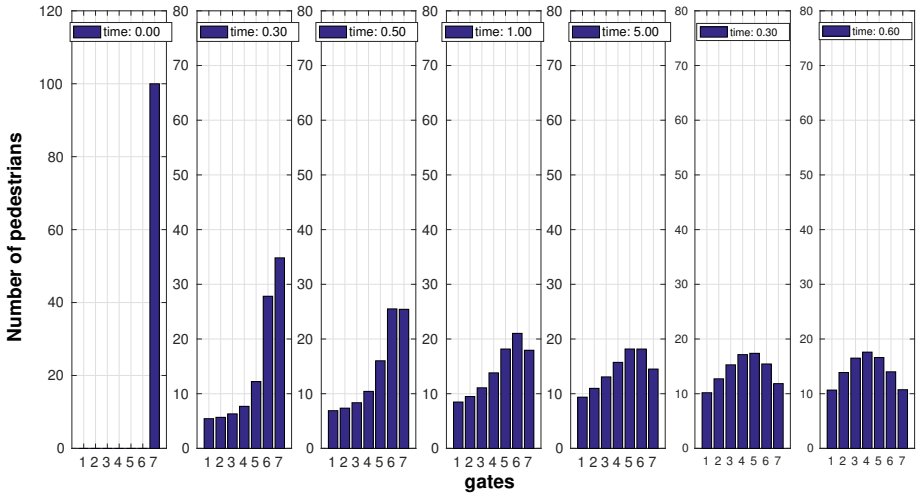

(a)

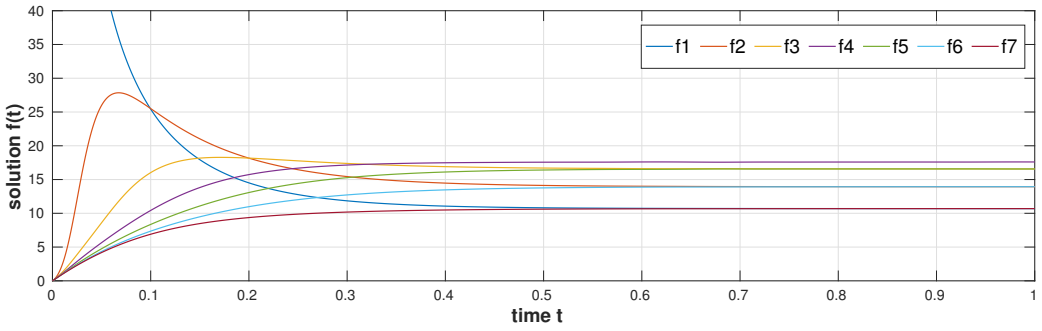

(b)

Figure 4.3: System subjected to an uniform external force field of magnitude $F = 100$. The pedestrians distribution for different instants of time (a), and the whole time evolution of $\mathbf{f}(t)$ for the initial condition $\mathbf{R}$ (b).

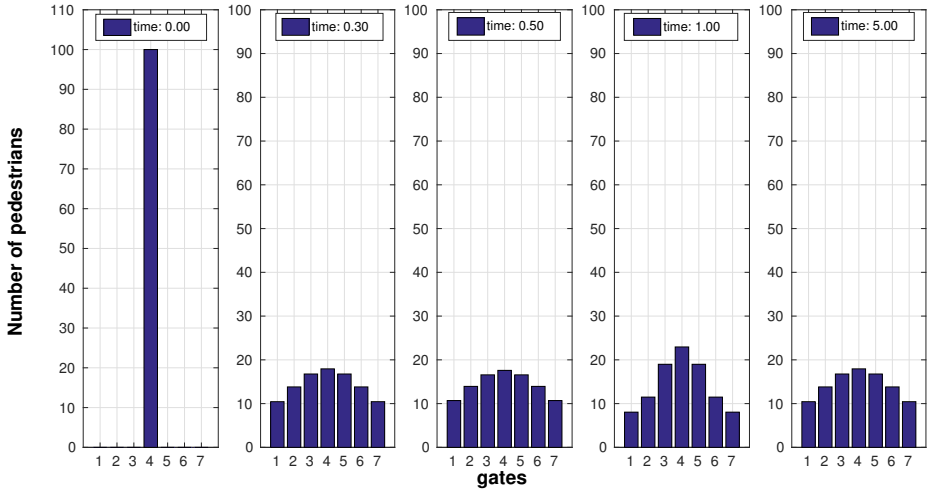

(a)

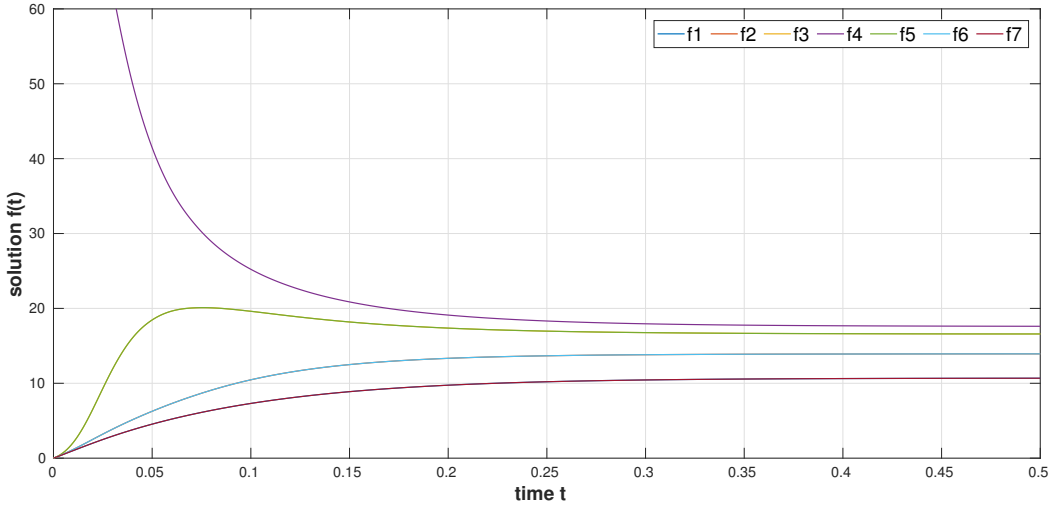

(b)

Figure 4.4: System subjected to an uniform external force field of magnitude $F = 100$. The pedestrians distribution for different instants of time (a), and the whole time evolution of $\mathbf{f}(t)$ for the initial condition $\mathbf{C}$ (b)

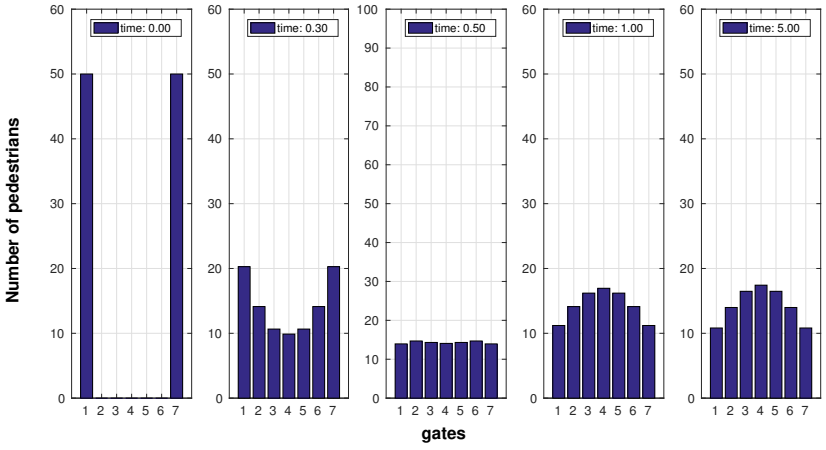

(a)

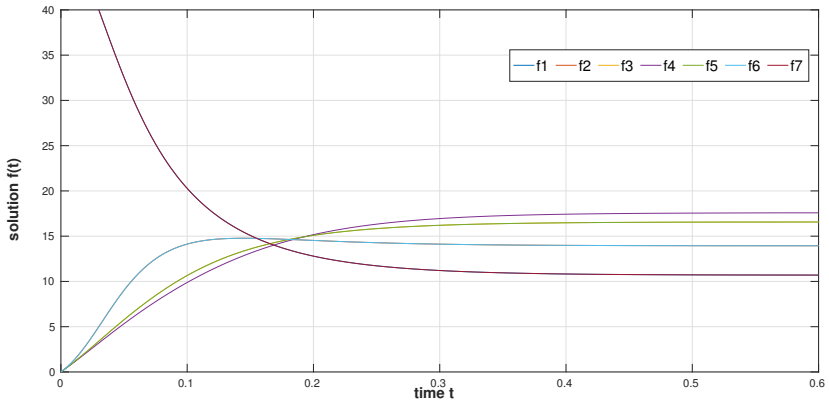

(b)

Figure 4.5: System subjected to an uniform external force field of magnitude $F = 100$. The pedestrians distribution for different instants of time (a), and the whole time evolution of $\mathbf{f}(t)$ for the initial condition $\mathbf{H}$ (b)

4.1.3 Analysis for increasing number of gates n

In this subsection we focus on the analysis of the system dynamics when varying the number of gates n, as we did in 3.3.4 for the case where the system is not subjected to an external force field. After fixing the parameters $N = 100$, $S = 1$, $p = 1$ and $F = 100$, we let again vary the number of gates n from $n = 2$ up to $n = 25$.

The results of the simulations show that the dynamical behaviours and the emergent features described for the case $n = 7$ in the previous subsection remains qualitative the same for all n (and for each initial condition respectively). Figure 4.6 shows the dynamical evolution for the case $n = 15$ with the initial condition $\mathbf{R}$.

The role of the thermostat in controlling the behaviours of the system emerges clearly in the analysis of the convergence time for increasing n. Indeed as shown in Figure 4.7, that reports the convergence time for different n for the initial condition $\mathbf{R}$, the convergence time first increases with n, then it decreases slowly towards saturation. It is worth noticing that this behaviour is qualitative the same for all the initial condition tested, then it is not restrictive to limit our considerations

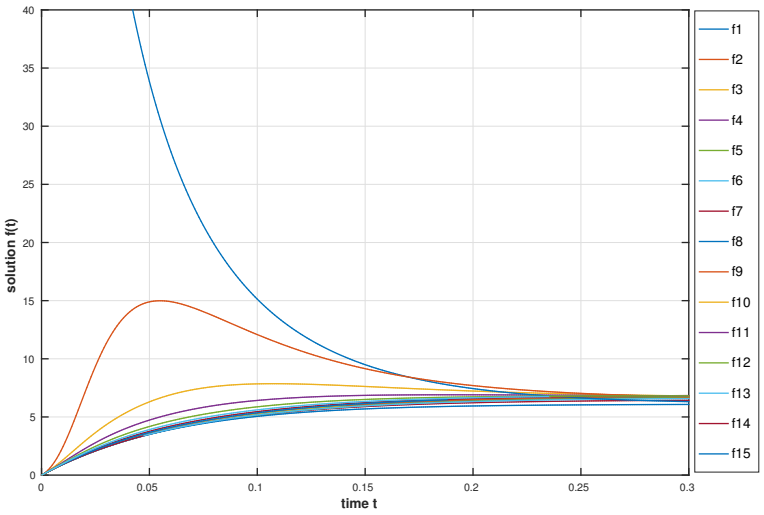

Figure 4.6: System with $n = 15$ subjected to an uniform external force field of magnitude $F = 100$. The whole time evolution of $\mathbf{f}(t)$ for the initial condition $\mathbf{R}$ (b).

to the dynamics with the initial condition $\mathbf{R}$. The convergence time for a system subjected to an external force field is qualitative different from the case in which it is not subjected to an external force field. Indeed, for the latter case, the convergence time increases exponentially with n, for the former the convergence saturates with n (compare Figure 4.7 with Figure 3.14). This behaviour can be addressed to the presence of the thermostat term in Eq. (4.1.1). For increasing values of n, the convergence time saturates because the thermostat term must balance the action of the external force field (that drives the system out of equilibrium) in order to keep constant the zero-order moment. The system is then driven to reach a stationary state out of equilibrium in a finite time, that is lower than the convergence time for the case without the external force field. Moreover as we have pointed out, the convergence time first increases for lower n, and then decreases as n grows. This behaviour can be explained as arising from a competition between the internal dynamics given by the term $\mathbf{J}[\mathbf{f}]$ and the dynamics that arise from the other two terms $\mathbf{F} - \alpha\mathbf{f}$ in the system of equations (3.1.2): the number of pedestrians per gate is higher for low n (being the total number of pedestrians N constant), and then the internal interactions are stronger for lower n than for higher n, because internal interactions depend on the local density and on the leader effect (recall the term (3.1.7) in the table of games). On the other hand the external force term F is always the same for all n, and also the thermostat term can be thought as constant too (in fact in the thermostat term $-\alpha f_i$, the term $\alpha = nF/N$ grows with n, but $f_i(t)$ decreases on average with n). Consequently for low n internal interactions overcome the external action of the force field, and then the convergence time grows qualitative as the case where the system is not subjected to the external field. On the contrary, for higher n, the action of the external force field overcomes the internal interactions, and the convergence time tends to saturates as explained before. These considerations explain then the behaviour of the convergence time in Figure 4.7.

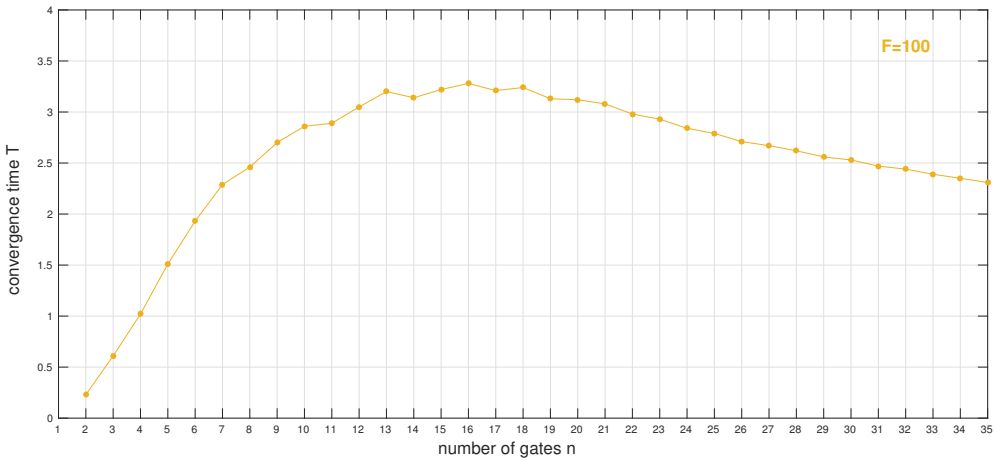

Figure 4.7: Convergence time versus n for $F = 100$, and the initial condition $\mathbf{R}$.

4.1.4 Analysis for increasing values of F

This subsection investigates the role of the magnitude F of the uniform external force field in affecting the pedestrians behaviour. After fixing the parameters $n = 7$, $N = 100$, $S = 1$, $p = 1$, we let vary the magnitude of the force F, and we analyse the evolution of system (4.1.1). Simulations show that the magnitude F of the external force field affects the intrinsic dynamics, the shape of the asymptotic distribution and the convergence time to reach the asymptotic distribution.
The results of the simulations can be summarized as follow:

As shown in Figure 4.8, the convergence time T needed to reach the asymptotic distribution decreases with the value F for all the initial conditions, and it saturates to a non zero value. This behaviour is in agreement with what is expected in a real situation in the metro station: if the external event that affects pedestrians choice is intense, (magnitude F of the uniform external the force field), the pedestrians are driven to quickly choose a gate, and as a consequence, they reach the asymptotic distribution in less time.

Simulations show that by increasing the magnitude of the external force field F there is an increasing spreading in the asymptotic distribution. This spreading fast saturate, and the asymptotic distribution saturates to the uniform distribution, see Figure 4.9. The dispersion σ^2 of the asymptotic distribution as function of the magnitude force F has been calculated in the same way as in (3.3.2), see Figure (4.9). This spreading behaviour can be addressed to the fact that the uniform external force field tends indeed to uniform the behaviour of all pedestrians, acting against the natural concentration of pedestrians towards the center of the gate side that on the contrary occurs when the system is not subjected to an external force field (see Section 3.3).

It is worth stressing that the saturation effects on the convergence time T and on the behaviour of the asymptotic distribution emerging on simulation, can be addressed to the thermostat term. Indeed the thermostat induces the action of the external force field to saturate because of the bounds imposed on the system: the fixed number of gates n (limited space) induces the saturation of the asymptotic distribution, while limited mean velocity and time reaction of pedestrians induce the saturation of the convergence time. The thermostat term reproduces the bounded real conditions of pedestrians displacing at the entrance of a metro station, and this translate in the saturation of the external force field effects.

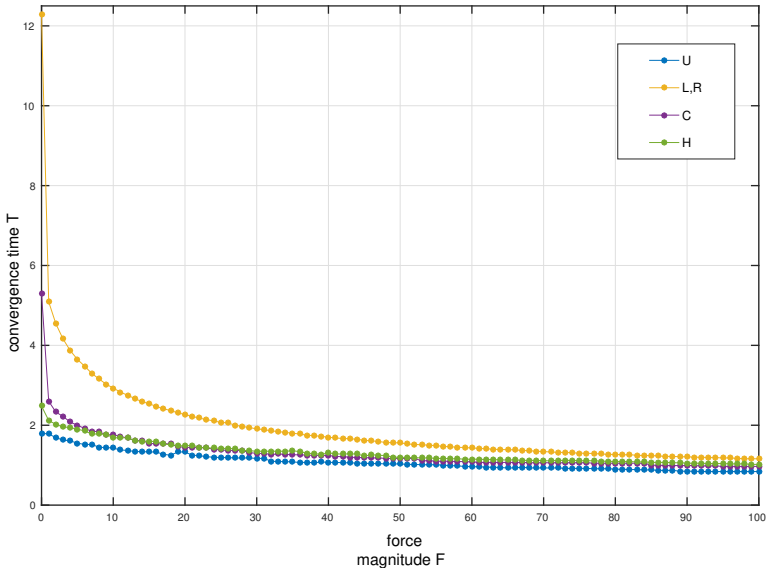

Figure 4.8: Convergence time T versus the magnitude of the external force field F for the initial conditions **U**, **L**, **R**, **C**, **H**.

As additional analysis, Figure 4.10 shows the convergence time T and for different values of the number of gates n for different magnitudes F. For each value of the magnitude F of the external force field, the behaviour of the convergence time T is qualitative the same as the one depicted in the previous subsection for the case $F = 100$. However as F increases, the convergence time globally decreases for all n (shifting and crushing of the curve towards lower value of the convergence time), and the maximum convergence time corresponds to smaller values of n (shifting of the curve maximum towards lower value of number of gate n). This behaviour is consistent with the results we obtained in this subsection and in the previous one. Indeed as F increases, the convergence time globally decreases (recall Figure 4.8) and the number of gate n at which the action of the external force field overcomes internal interactions decreases (see the previous subsection (4.1.3)).

4.2 The case of constant non uniform external force field

In this section we focus on the qualitative analysis of the pedestrians dynamics subjected to the action of a *constant non uniform* external force field. In the context of pedestrians dynamic in a metro station, a constant and non uniform external force field can model an event where there are preferential gates to take (for season tickets holders, for specific exit gates that allow to reach remarkable places to visit, and so on). The external force field then acts only on these gates that pedestrians are lead to choose. The analysis of the system (3.1.2) subjected to a non uniform external force field is important because it allows to realise how a non symmetric external event (in our model the symmetry is considered with respect to the center of the gates side) can break the possible symmetry of the internal evolution and then of the asymptotic distribution, giving rise to a very heterogeneous dynamic depending strongly on the initial condition. Specifically in this analysis we limit ourselves to the case of an external force field **F** acting only on the first gate:

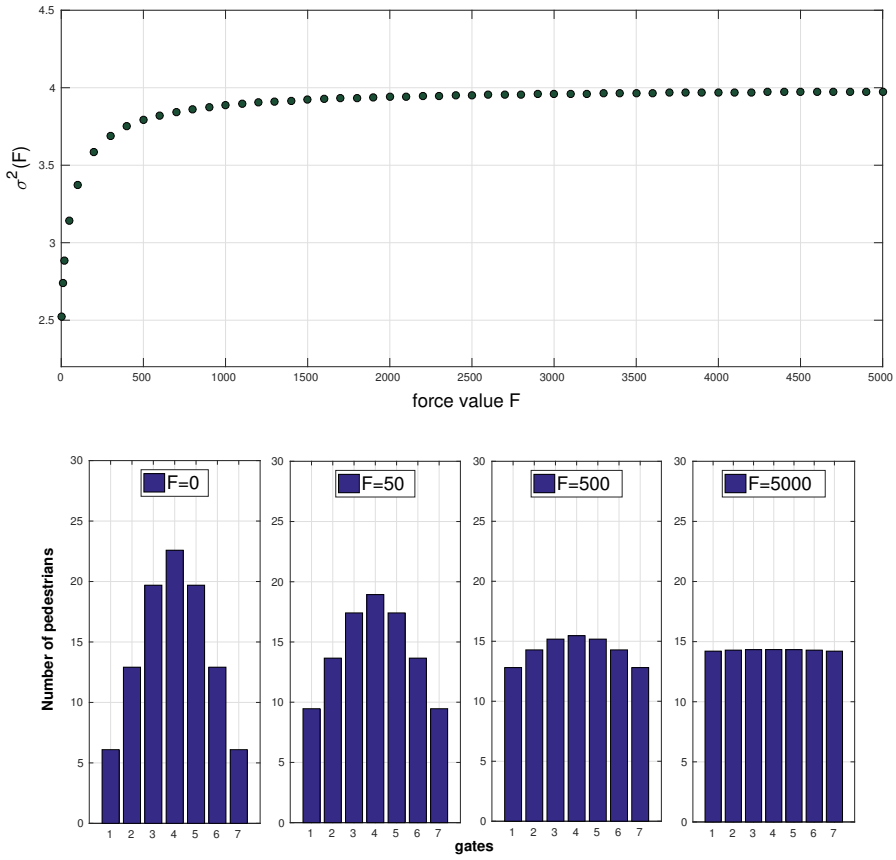

Figure 4.9: Dispersion of the asymptotic distribution with increasing magnitude F of the external force field.

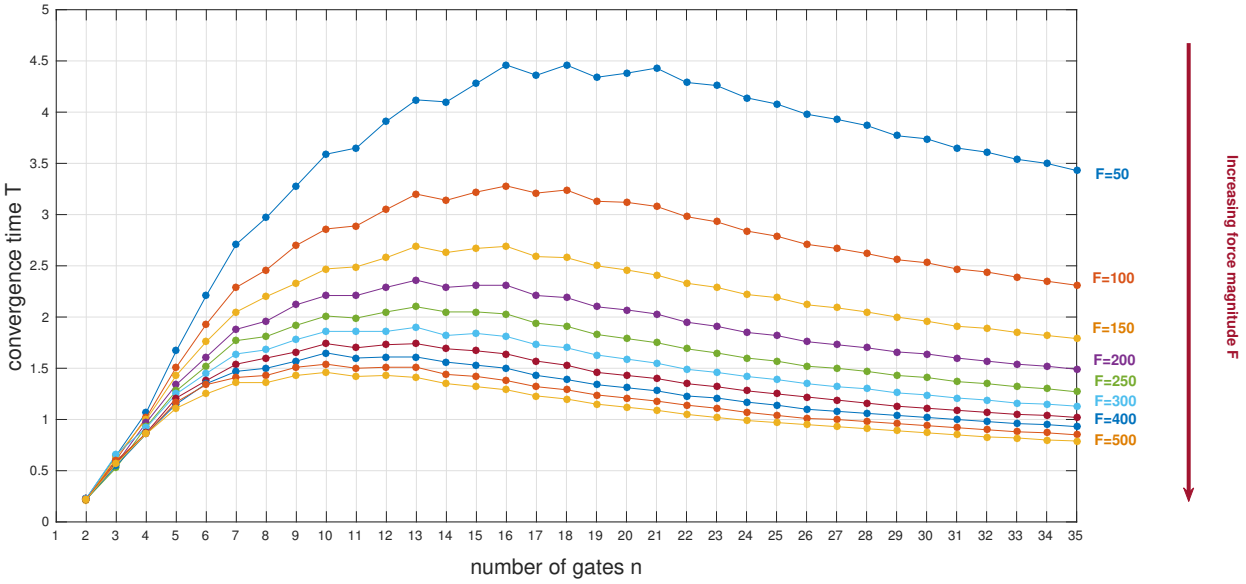

Figure 4.10: Saturation of convergence time with n for different magnitude F of the external force field.

$$\mathbf{F} = \begin{cases} F > 0 & \text{if } i = 1 \\ \\ 0 & \text{else} \end{cases} \tag{4.2.1}$$

The thermostat term (2.1.5) in this case is symply given by $\alpha = \frac{F}{N}$. Bearing in mind the functional form of the external force field (4.2.1), the Cauchy problem for the pedestrians dynamic in a metro station (3.1.2) rewrites:

$$\begin{cases} \dfrac{df_i}{dt} = J_i[\mathbf{f}] + F - \left(\dfrac{F}{N}\right) f_i & \text{if } i = 1 \\ \\ \dfrac{df_i}{dt} = J_i[\mathbf{f}] - \left(\dfrac{F}{N}\right) f_i & \text{else} \\ \\ f(0) = f^0 \end{cases} \tag{4.2.2}$$

It is worth stressing that even if the external force field acts only on the first gate, the thermostat term $-\alpha f_i$ is present in all the equations of the system (4.2.2). Limiting ourselves to the analysis of case in which the external force field acts only on the first gate is not reductive. Indeed, we will see that the emerging features and the dynamical behaviours arising from the analysis of system (4.2.2) are representative and predictive for many others cases where the system is subjected to an arbitrary constant and non uniform external force field.
The analysis of the case of a system subjected to a constant non uniform external force field is presented in two parts: in the first subsection we perform the sensitivity analysis on the initial conditions (3.1.5) for the system (4.2.2), by focusing on the asymmetry in the dynamic introduced by the external force field (4.2.1), and by discussing the very heterogeneous dynamics that arises; then in the second subsection we extend the analysis of the first subsection to the case of an arbitrary constant non uniform external force field, by considering other specific examples and we infer the typical emergent features and dynamical behaviour for the the system (3.1.2) when subjected to a constant non uniform external force field. Again, the role of the thermostat in controlling the dynamics and in allowing the system to reach a stationary state of non-equilibrium is stressed out.

4.2.1 The sensitivity analysis on the initial condition

As mentioned in the introduction of this section, a non uniform external force field gives rise to a very heterogeneous and asymetric dynamic depending strongly on the initial condition. However in the following sensitivity analysis on the initial conditions we will see that the dynamic reaches the same (asymetric) asymptotic state for all the initial conditions (3.1.5). The sensitivity analysis on the initial condition is perfomed as in Section 3.3.3 and in Section 4.1.2. Specifically, we fix $N = 100$, $n = 7$, $S = 1$, and $p = 1$, and the magnitude of the external force field acting on the first gate has been taken equal to $F = 500$.
The results of the simulations are summarized for each initial condition as follows:

Initial condition U. As shown in Figure 4.11 (b), pedestrians entering uniformly the gate zone (initial condition 3.1.8) and subjected to the external force field (4.2.1) behave as follows: the external force field acting only on the first gate, obliges pedestrians to choose the first

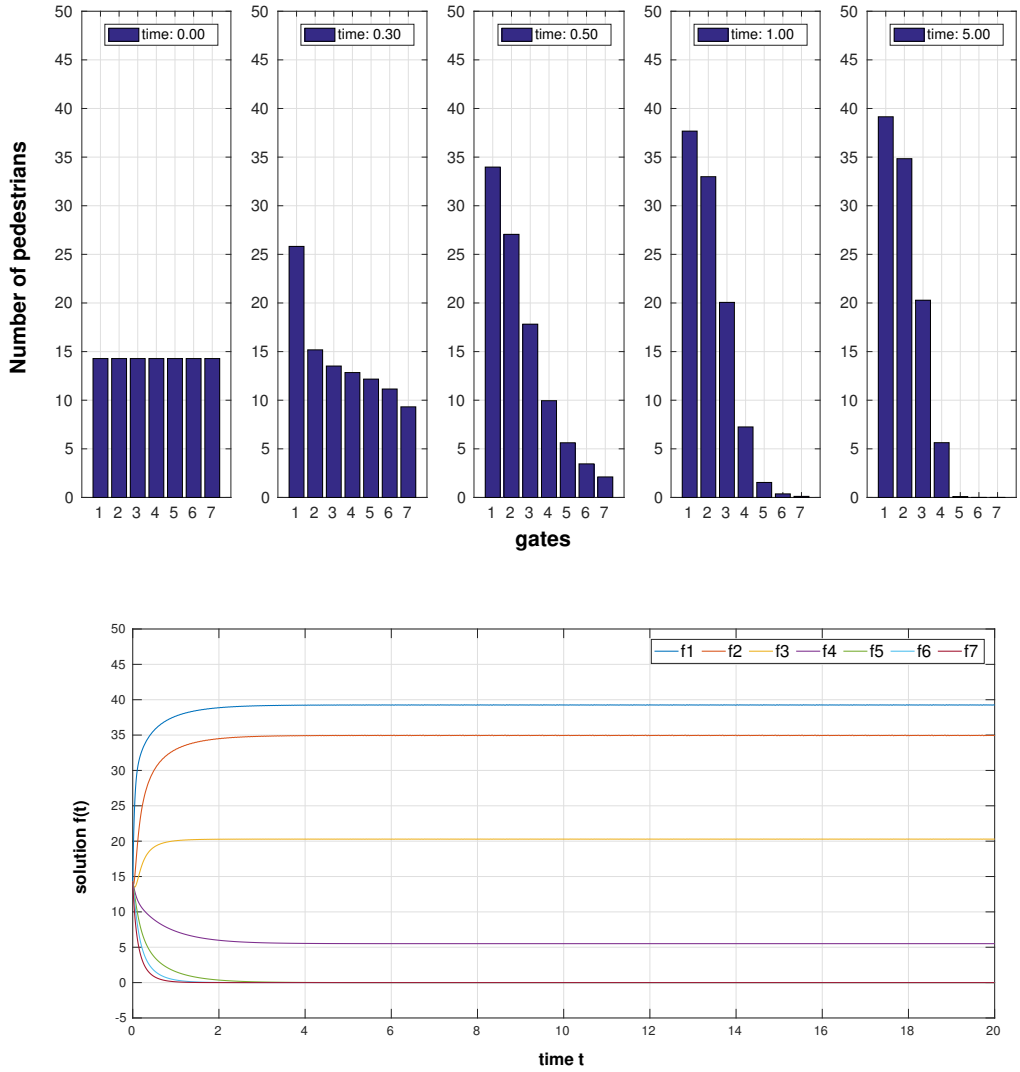

Figure 4.11: System subjected to an external force field of magnitude $F = 500$ acting only on the first gate $i = 1$: the pedestrians distribution at consecutive fixed instants of time, and the whole time evolution of $\mathbf{f}(t)$ in time of the system with the initial condition $\mathbf{U}$.

gate $i = 1$ from the beginning of the evolution ($t = 0$). Then evolving in time, the flux of pedestrians is overbalanced towards the left part of the gates side: gates $i = 1$, $i = 2$, $i = 3$ are preferred in time by pedestrians, with descendent preference from $i = 1$ up to $i = 3$ (compare the mean number of pedestrians in time of these gates). The evolution is not symmetric with respect to the gate $i = 4$, contrary to the case of the constant uniform external force field (4.1). The symmetric internal leader-follower dynamics is biased by the presence of the external force field, and the pedestrians flux behaves as if the leaders where choosing gates only in the left part of the gates side (see Figure 4.11 (a)). Note that the asymmetric evolution is clear from the fact that all the 7 lines representing each $f_i(t)$ are distinguishable in Figure 4.11 (b). The evolution continues with the described trend just until pedestrians reach a stationary state of non-equilibrium. As shown in the last histogram of Figure 4.11 (a), the asymptotic state reached is asymetric: as expected the maximum of

the distribution corrspond to $i = 1$ and the distribution monotonically decreases from gate $i = 2$ up to gate $i = 4$. Gates $i = 5$, $i = 6$ and $i = 7$ are empty, and then they are not chosen by pedestrians in the asymptotic limit. It is worth stressing that the asymptotic state is given by the balance between the action of the external force field $\mathbf{F}$ plus the thermostat term $-\alpha\mathbf{f}$, and the internal dynamic $\mathbf{J}[\mathbf{f}]$. The action of the internal dynamics $\mathbf{J}[\mathbf{f}]$ exactely prevents the systestem to reach an asymptotic distribution where all pedestrians choose the gate $i = 1$, as one could expect by considering an external force field acting only on gate $i = 1$. Indeed the internal dynamics tends naturally to drive pedestrians to reach an asymptotic distribution where all the gates are partially filled. (For example, recall the last hisogram of Figure **??** (a)). The action of the external force field force pedestrians to choose specific gates, driving the system to reach an asymptotic state with some gates that are even not chosen. We will see that the effect of lefting some gate empty in the asymptotic limit is strictly linked to the intensity F of the external force field. Finally, it is worth stressing that the thermostat term allows the system to reach a stationary state of non-equilibrium just described, and it ensures the conservation of the total number of pedestrians as expected.

Initial condition L. The evolution of pedestrians choice under the action of an external force field acting only on gate $i = 1$ in the case where all pedestrians enter from the left side of the gates zone (initial condition 3.1.9), is similar to the analogous case where no external force field acts on the system. In fact, if one compares Figure 4.12(b) to Figure 3.9 (b), the system evolution in the former case is similar to the latter: for the case where the system is subjected to the external force field (4.2.1), the gates are chosen progressively and metastable states are reached during the evolution (but in this case they are not symmetric). This similarity in the evolution is due to the fact that the initial condition (3.1.9) already promotes the action of the external force field 4.2.1, giving rise to a more controlled dynamics with respect to the cases with initial condition **U**, **R**, **C**, **H** . As for the previous case with the initial condition **U**, also in this case the role of the internal interactions $\mathbf{J}[\mathbf{f}]$ is remarkable in influencing the asymptotic distribution: even if all pedestrians enter from the left side of the gates zone, and the external force field forces pedestrians to choose the first gate, in long time scales pedestrians will not all choose the first gate. As for the uniform initial condition **U** just discussed, the internal interactions of leader-dynamic prevents the static solution where all pedestrians choose the first gate.

Initial condition R. This is the first case we analyze where the dynamics of pedestrians entering all from the right side of the gates zone, is not symmetric to the case where all the pedestrians enter from the left side of the gates zone, as it happens for the case where the system is not subjected to an external force field (3.3), or it is subjected to a constant and uniform external force field (4.1). This fact is obviously due to the asymmetry introduced in the system by the non uniform external force field. As shown in Figure 4.13 (b), in the case where all pedestrians enter from the right side of the entrance side (initial condition **R**) the external force field on the first gate forces some pedestrians to choose the first gate from the beginning of the evolution ($t = 0$). Then a continue flux of pedestrians moving from the right side of the gates zone (gate $i = 7$) towards the left side of the gates zone (gate $i = 1$) occurs as the evolution in time goes by. Both the action of the external force field and the role of the leader-follower internal dynamic emerge clearly in the evolution. Indeed on the one hand, in

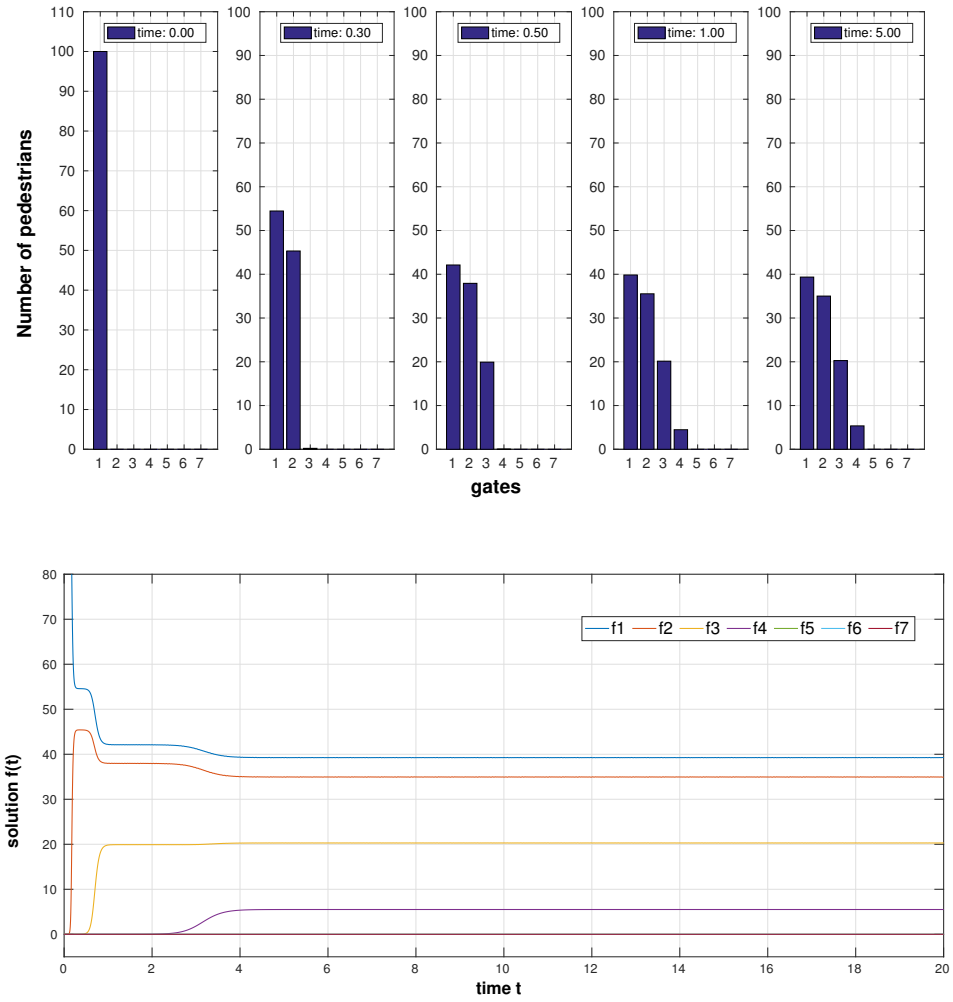

Figure 4.12: System subjected to an external force field of magnitude $F = 500$ acting only on the first gate $i = 1$: the pedestrians distribution at consecutive fixed instants of time, and the whole time evolution of $\mathbf{f}(t)$ in time of the system with the initial condition $\mathbf{L}$.

the right part of the gates side a leader-follower dynamic is established from the beginning (compare the dynamics in Figure 3.10 whithout external force field with the dynamics for gates $i = 5$, $i = 6$, $i = 7$ in Figure 4.13). On the other hand in the left part of the gates side, the external force field obliges pedestrians to move quickly towards the gate $i = 1$. The combination of these two phenomenons give rise to the asymetric pedestrian flux in Figure 4.13. Finally, the asymptotic state reached by the system fills the first four gates and left empty the last three ones. (see the last histogram of Figure 4.13 (a)). Further computational analysis shows that the asymptotic state is the same asymptotic state that the system reaches when evolves with initial condition $\mathbf{U}$ and $\mathbf{L}$.

Initial condition C. The evolution of the system when all pedestrians enter the gates zone from the center (initial condition (3.1.12)), locally reproduces the evolution of the previous case where all pedestrians enter from the right side of the gates zone (initial condition $\mathbf{U}$). As shown in Figure 4.14, pedestrians are forced to choose the first gate from the beginning of

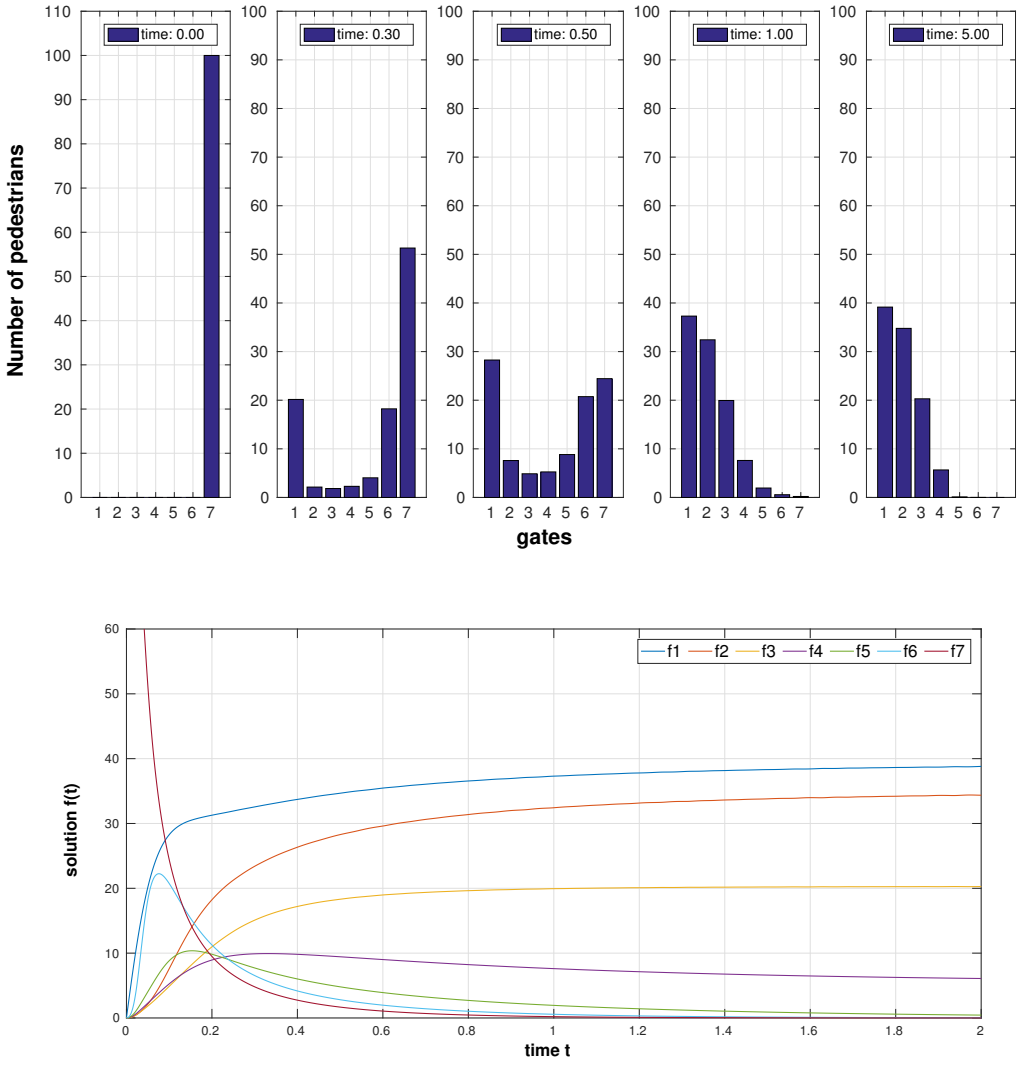

Figure 4.13: System subjected to an external force field of magnitude $F = 500$ acting only on the first gate $i = 1$: the pedestrians distribution at consecutive fixed instants of time, and the whole time evolution of $\mathbf{f}(t)$ in time of the system with the initial condition $\mathbf{R}$.

the evolution, and this behaviour overlaps to the leader-following dynamics, that is totally unbalanced towards the left side of the gates zone because of the external force field acting on gate $i = 1$. The asymptotic state reached by the system is always the same as in the previous three cases we have analysed (initial conditions $\mathbf{U}$, $\mathbf{L}$, $\mathbf{R}$.)

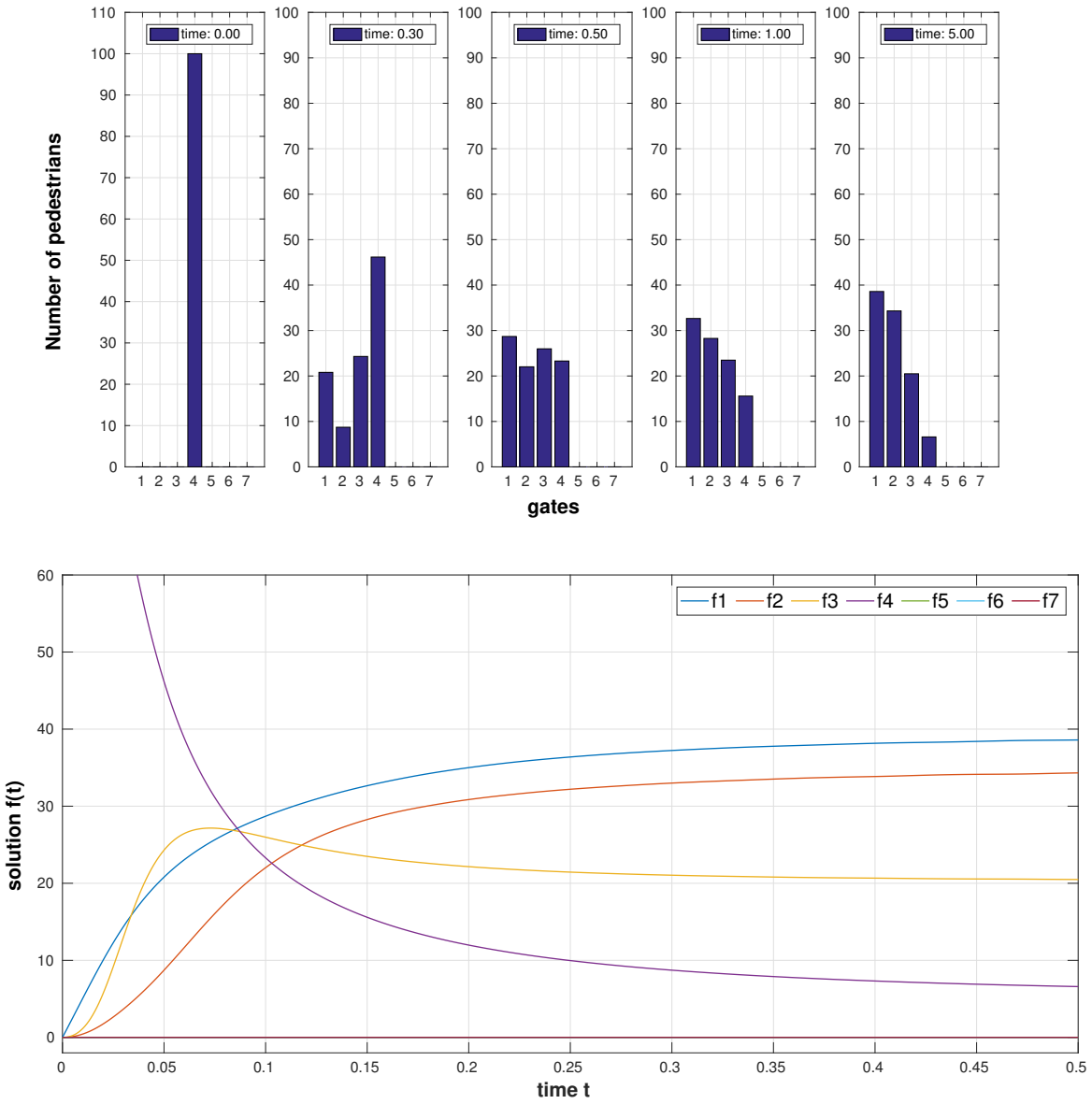

Figure 4.14: System subjected to an external force field of magnitude $F = 500$ acting only on the first gate $i = 1$: the pedestrians distribution at consecutive fixed instants of time, and the whole time evolution of $\mathbf{f}(t)$ in time of the system with the initial condition **C**.

Initial condition H. As for the initial condition **C**, for pedestrians entering the gates zone half of them from the right side and the other half from the left side (initial condition (3.1.13)), the dynamics is similar to the case where all pedestrians enter from the right side of the gates zone (initial condition **U**), see Figure 4.15 and Figure 4.13. However for the initial condition **H**, the number of pedestrians that choose the first gate decreases at the beginnig, reproducing locally the dynamics where all pedestrians enter from the left side of the gates zone (see Figure 4.12). Then the number of pedestrians that choose the first gate interchanges this trend, and it increases until it reaches its asymptotic value. This behaviour is due to the action of the internal dynamics and of the external force field, that act in opposite ways: at the beginning of the evolution some pedestrians in gate $i = 1$ choose the empty gates on their

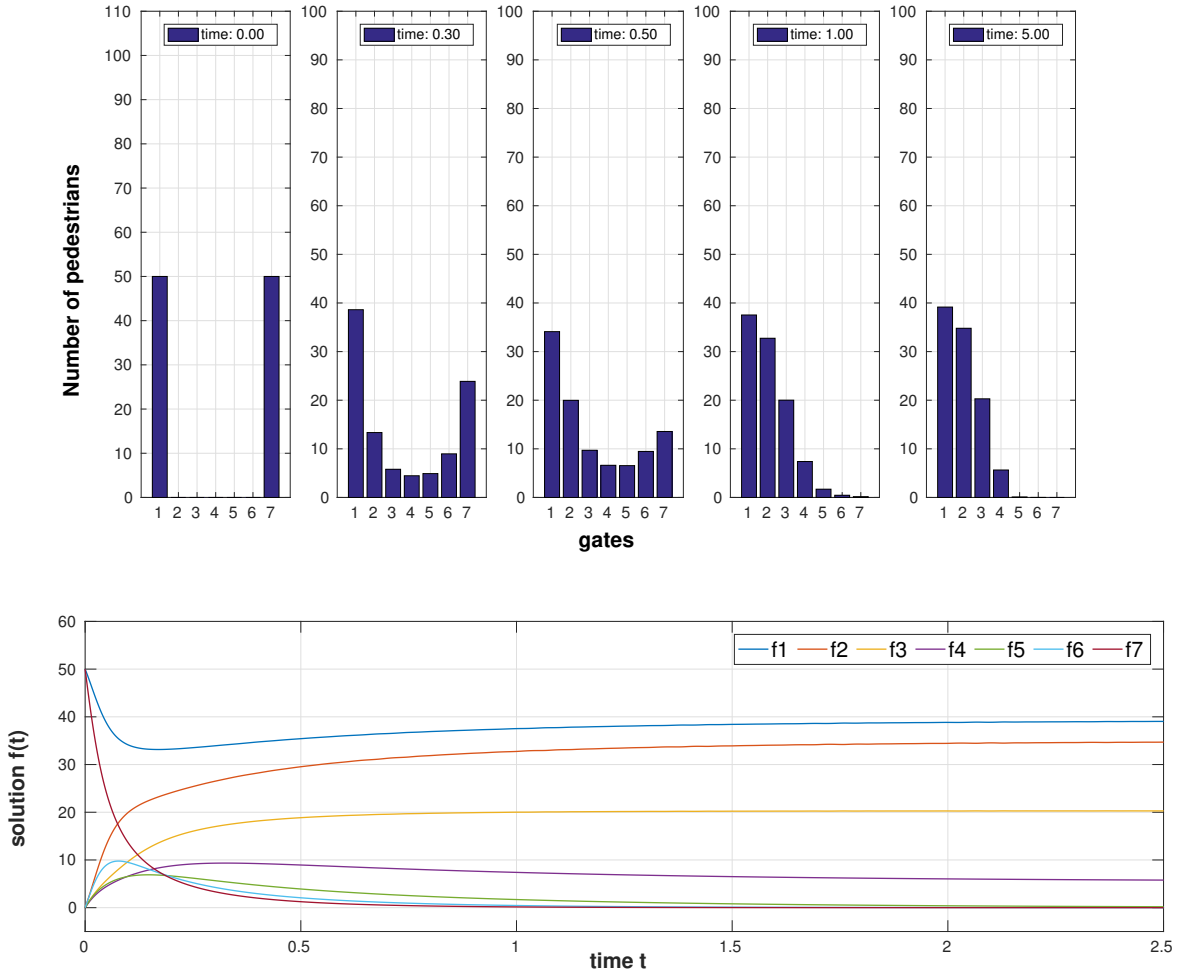

Figure 4.15: System subjected to an external force field of magnitude $F = 500$ acting only on the first gate $i = 1$: the pedestrians distribution at consecutive fixed instants of time, and the whole time evolution of $\mathbf{f}(t)$ in time of the system with the initial condition $\mathbf{H}$.

right and follow some leader by choosing gate $i = 2$ and $i = 3$ (internal dynamics); this trend is then inverted when the last three gates start to empty, because the external force field and the biased leader-follower dynamics force pedestrians to consider in their choice only the left part of the gates side. The asymptotic distribution reached by pedestrians is the same asymptotic distribution of the four previous cases we have analysed (initial condition $\mathbf{U}, \mathbf{L}, \mathbf{R}, \mathbf{C}$). The system (4.2.2) reaches the same asymptotic distribution for all the five initial conditions (3.1.5).

4.2.2 Discussion and other non uniform cases

This subsection is devoted to the extension of the the analysis we performed in the previous subsections to the case of an arbitrary constant non uniform external force field. Besides the results obtained for the case where the external force field acts only on the first gate, we consider other specific examples, and from them we infer the typical emergent features and the dynamical behaviour for the system (3.1.2) when subjected to an arbitrary constant non uniform external

force field.

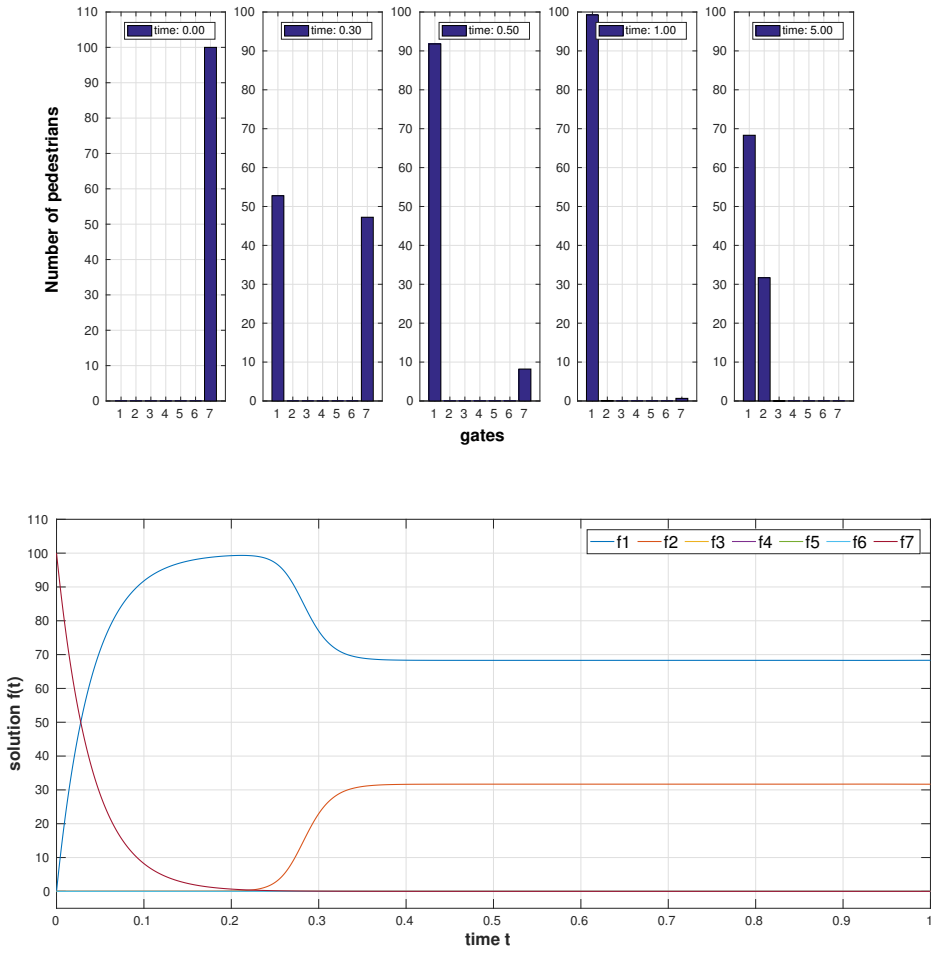

Figure 4.16: System subjected to an external force field of magnitude $F = 2500$ acting only on the first gate $i = 1$: the pedestrians distribution at consecutive fixed instants of time, and the whole time evolution of $\mathbf{f}(t)$ in time of the system with the initial condition $\mathbf{R}$.

The most important feature that emerges from the sensitivity analysis on the initial conditions performed in Section 4.2.1, is the balance between the action of the external force field and the action of the internal dynamics, that are mediated by the role of the thermostat that ensures the conservation of the total number of pedestrians N. As expected simulations performed with the parameters setting of Section (4.2.1), but with higher magnitude F of the external force field, show that the balance between the action of the external force field and the action of the internal dynamics depends on F. Figure 4.16 depicts the dynamics for the initial condition $\mathbf{R}$ for $F = 2500$,, the force field strongly overcomes the action of the internal dynamics. In the specific case of Figure 4.16, the action of the external force field is so strong that all pedestrians move directly from gate $i = 7$ to gate $i = 1$, and the internal leader-follower dynamics even does not take place. Moreover further simulations show that the convergence time towards the asymptotic state decreases with F, as in the case of the system subjected to an uniform external force field.

The shape of the asymptotic distribution also changes with the magnitude F of the external force field on the first gate, as Figure 4.17 shows. The asymmetry respect to the central gate $i = 4$

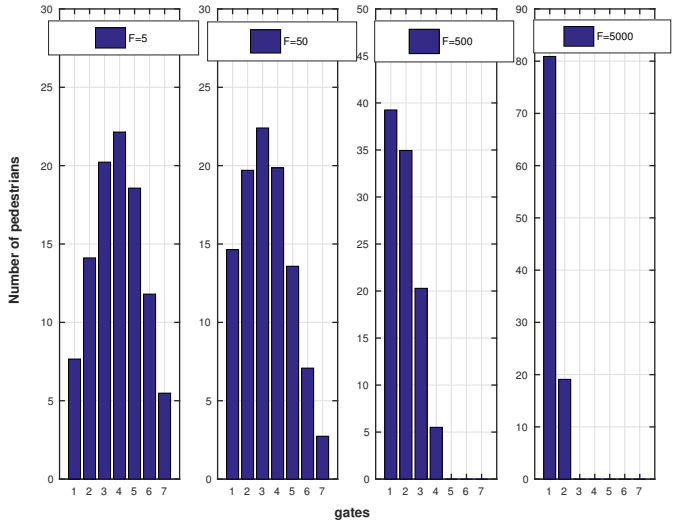

Figure 4.17: The asymptotic distribution for different magnitude F of the external force field acting only on gate $i = 1$.

in the asymptotic distribution increases with F, and the number of gates that are chosen in long times scales reduces at maximum up to two (gate $i = 1$ and $i = 2$). It is worth stressing that even with very high values of the magnitude F, the internal dynamic is never totally overcome by the action of the external force field. Indeed the asymptotic distribution does not include only the first gate, but at least two of them (see the last histogram in Figure 4.17). Additional computational analysis also points out that, for a fixed value of F, the asymptotic state is quantitatively the same for all the initial conditions (3.1.5).

For what concerns the functional form of the external force field $\mathbf{F}$, let us consider the two following examples. Figure 4.18 shows the evolution with the initial condition $\mathbf{H}$ for the case with $n = 7$ gates with a constant non uniform external force field acting on gate $i = 2$, $i = 3$, and $i = 4$ with magnitude $F = 500$ on all of them. The evolution of the system is driven by the balance between the action of the external force field and the internal dynamics. The system evolves towards an asymptotic state that is locally symmetric with respect to the gate $i = 3$. The shape of the asymptotic state locally reproduces the asymptotic state for the case of the constant uniform force field (recall the anaysis in Sec 4.1). Indeed, if we consider only the gates $i = 2$, $i = 3$, $i = 4$, locally we have a uniform external force field acting on the system. However for the action of the internal dynamic, also gate $i = 1$ and $i = 5$ are chosen on a long time scale, because the external force field is not strong enough to oblige pedestrians to choose only gates $i = 2$, $i = 3$, $i = 4$ on long time scales. As shown in Figure 4.19, for the case $n = 7$ with the external force field acting with magnitude $F = 500$ only on odd gates (i.e. on gates $i = 1$, $i = 3$, $i = 5$, $i = 7$), the system evolves from the initial condition $\mathbf{H}$ to an asymptotic state that respect the symmetry of the external force field: on odd gates there is an equal number of pedestrian choosing gates $i = 1$, $i = 3$, $i = 5$, $i = 7$, while in even gates $i = 2$, $i = 4$, $i = 6$ we can identify a symmetric distribution centred on gate $i = 4$. This local symmetric distribution is due to the effect of internal interactions that naturally leads pedestrians to concentrate towards the center. The formation of such a structure is possible because the external force field is not strong enough to overcome completely the action

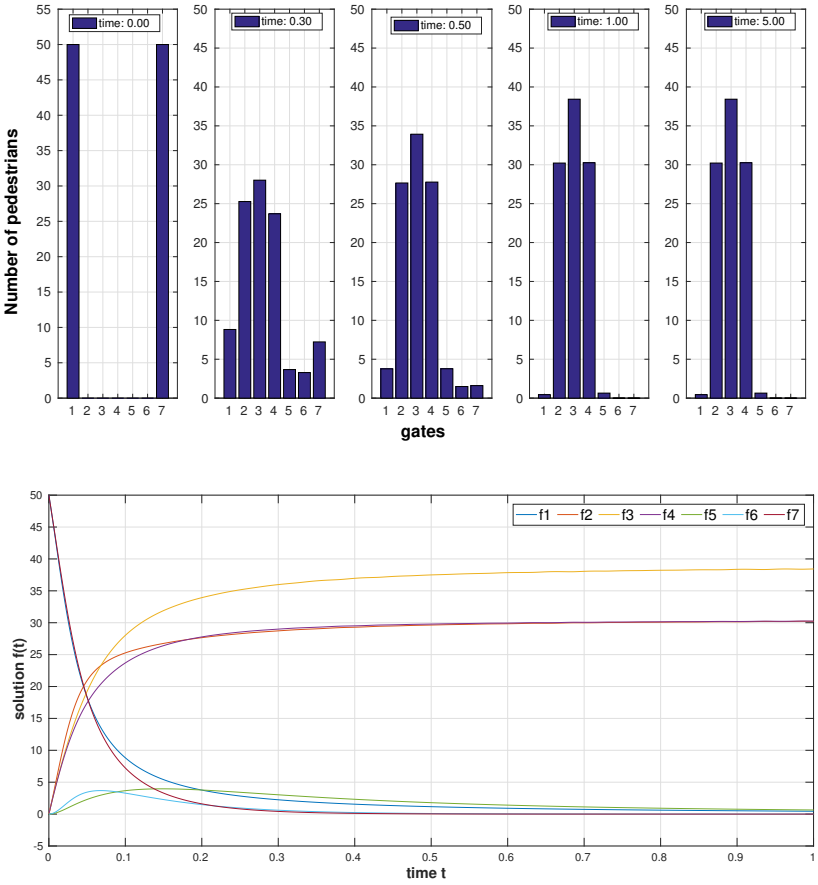

Figure 4.18: System subjected to an external force field of magnitude $F = 500$ acting only on gates $i = 2$, $i = 3$, $i = 4$: the pedestrians distribution at consecutive fixed instants of time, and the whole time evolution of $\mathbf{f}(t)$ with the initial condition $\mathbf{H}$.

of the internal interactions.

By varying the number of gates n, the functional form of the constant non uniform external force field $\mathbf{F}$ and the magnitude F, we can infer from simulations that the dynamics and the shape of the asymptotic state depends continuously on the combination of these parameters. For example Figure 4.20, shows that for the case $n = 10$ with an external force field acting on the first gate with magnitude $F = 500$, the dynamics is similar to the case of $n = 7$ in the same conditions (see Figure 4.13). However by comparing the asymptotic distribution for the case $n = 7$ and the asymptotic distribution for the case $n = 10$, they are different. Compare the last histogram of Figure 4.20 (a) with the last histogram of 4.13 (a). This means that the asymptotic distribution does non depend only on the magnitude F of the external force field, but it is also sensitive to the number of gates n.

Even if the emerging phenomenons described in the previous analysis is heterogeneous, as we have seen it is in a certain way always predictable, if we bear in mind the considerations about the balance between the external force field and the internal interactions controlled by the magnitude F of the external force field, the symmetry of the external force field respect to the gates side, the role of the thermostat and finally the role of the number of gates n.

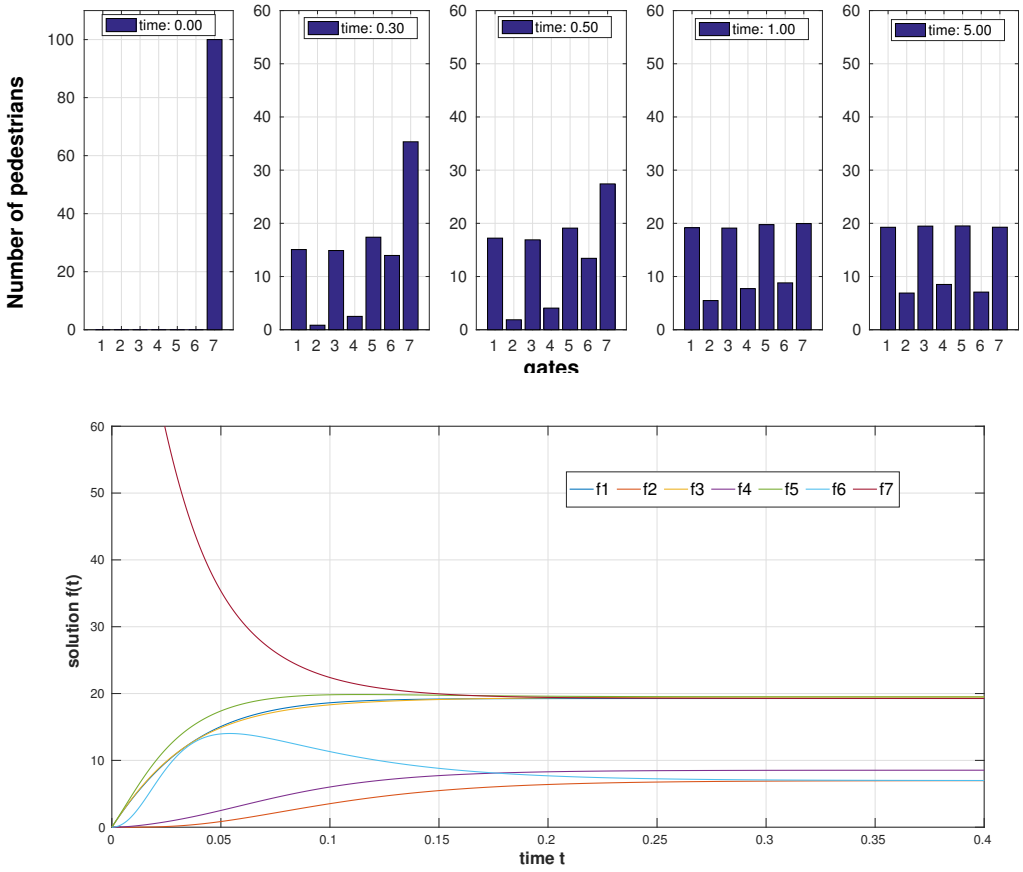

Figure 4.19: System subjected to an external force field of magnitude $F = 500$ acting only on odd gates $i = 1$, $i = 3$, $i = 5$, $i = 7$. The pedestrians distribution at consecutive fixed instants of time, and the whole time evolution of $\mathbf{f}(t)$ with the initial condition $\mathbf{R}$.

4.3 Time dependent external force field

This section deals with the qualitative analysis of the system (3.1.2) when subjected to an explicit *time dependent* external force field $\mathbf{F}(t)$. For the model depicting the dynamics of pedestrians in a metro station, the time dependent external force field can represent an event where there are recurrent announcements in the metro zone (periodic external force field), or an alarm situation that fades during time (external force field decreasing in time). In the analysis we will limit ourselves to the case of a uniform time dependent external force field. This is not a reductive choice, because by bearing in mind the analysis performed in Sec. 4.1, and Sec. **??** the case of a uniform time dependent force field can be easily extended to the non unifom case.
In the case of a uniform time dependent external force field, pedestrians are then subjected to the action of a external force field $\mathbf{F}$ which has the same functional form for all the gates, i.e. $F_i = F(t)$, $\forall i$. It is worth stressing that we must have $F(t) \geq 0$ $\forall t \geq 0$, because the external force field must be always positive in the thermostatted kinetic framework we are dealing with (See 2.1). The thermostat term (2.1.1) in this case symply reads $\alpha = \frac{nF(t)}{N}$, and the related Cauchy problem for the pedestrian dynamics in a metro station (3.1.2) rewrites:

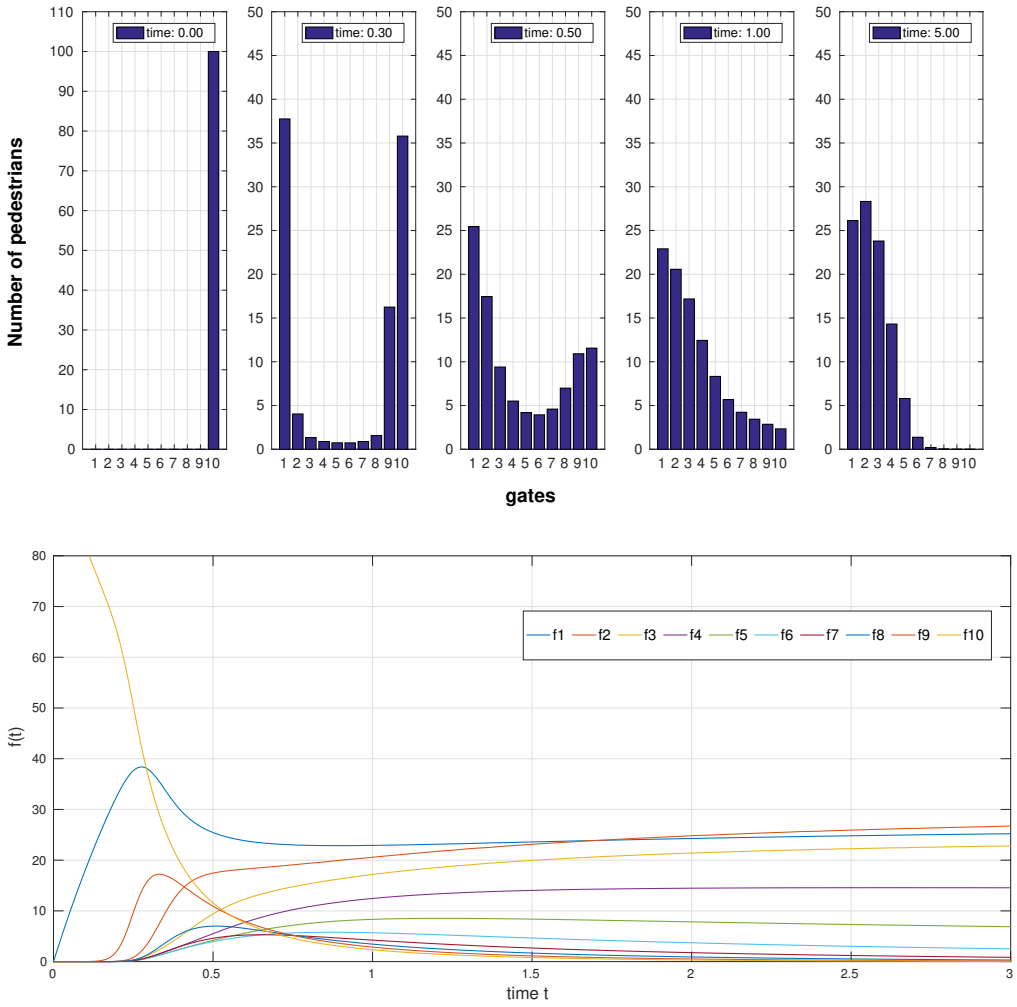

Figure 4.20: System with $n = 10$ subjected to an external force field of magnitude $F = 500$ acting only on the first gate $i = 1$. The pedestrians distribution at consecutive fixed instants of time, and the whole time evolution of $\mathbf{f}(t)$ with the initial condition $\mathbf{H}$.

$$\begin{cases} \dfrac{df}{dt} = J_i[\mathbf{f}] + F(t) - \left(\dfrac{n}{N}F(t)\right) f_i \\ \\ f(0) = f^0 \end{cases} \tag{4.3.1}$$

It is worth noticing the time dependance of the thermostat term, $\alpha(t)$. Indeed as the system is subjected to a time dependent external force field $\mathbf{F}(t)$ the thermostat controls the system evolution exactly at each time t. We will see in the following analysis that this time dependence will allow us to see clearly the role of the thermostat in keeping constant the total number of pedestrians N during the evolution of the system.

In the computational analysis of the system (4.3.1) we focus on a general discussion of the time evolution of the system for specific functional forms of the external force field $\mathbf{F}(t)$, and expecially we remark the role of the thermostat in controlling the system dynamic. Specifically, as we did in the previous sections, we fix $N = 100$, $n = 7$, $p = 1$ and $S = 1$. For the uniform external force field, we choose the following functional forms:

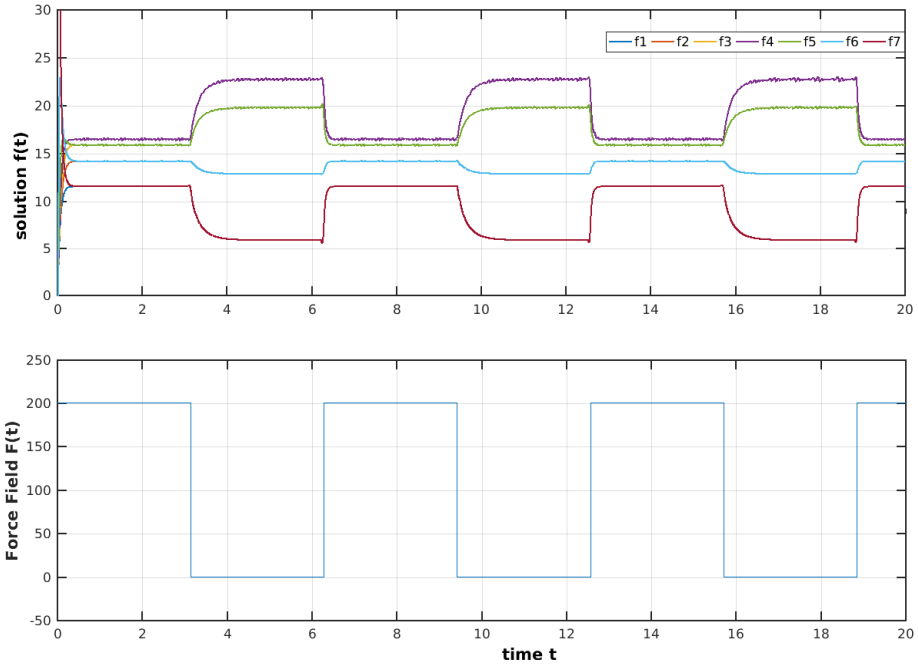

Figure 4.21: Evolution of the system with initial condition **C** under the action of the uniform time dependent external force field A) with $F = 500$.

$$A) \quad F(t) = \begin{cases} F > 0 & \text{if} \quad kT < t < (k+1)T \quad T > 0,\, k \in \mathbb{N} \\ 0 & \text{else} \end{cases} \tag{4.3.2}$$

$$B) \quad F(t) = Ae^{-\frac{t}{b}} \qquad A,\, b > 0 \tag{4.3.3}$$

The case A) represents a square wave periodic external force field, with period T. The case B) is the exponential decreasing external force field. The values of the parameters F, T, A, b are set casewise in the simulations.

The results of the simulations are summarized as follows:
For what concerns the periodic external force field A), after a first transitorial evolution that depends on the initial condition, the system undergoes oscillations, as shown in Figures 4.21. For the case A) of the time square periodic external force field, when the external force field is equal to $F(t) = F$, the system go rapidly towards the asymptotic state that correspond to the case where an uniform external force field acts on the system (see Section 4.1), while when the force field stops acting on the system, the system goes slowly towards the asymptotic state that corresponds to the case where no external force field acts on the system (see Section 3.3). Also in the case B) of the exponential decreasing external force field, at each time t, the system tries to reach the asymptotic state that corresponds to the asymptotic distribution for case where the external force field acts on the system with magnitude $F(t)$, and then as $F(t)$ decreases the asymptotic state concentrates slowly towards the central gate $i = 4$. It is worth stressing the fact that the system adapts continuously itself to the action external of force field due to the control role of the thermostat term. Moreover, the role of the thermostat term in allowing the system to conserve the total number of pedestrians N all the system can never be in phase with the external force field $F(t)$: some f_i must increase and some must decreases.

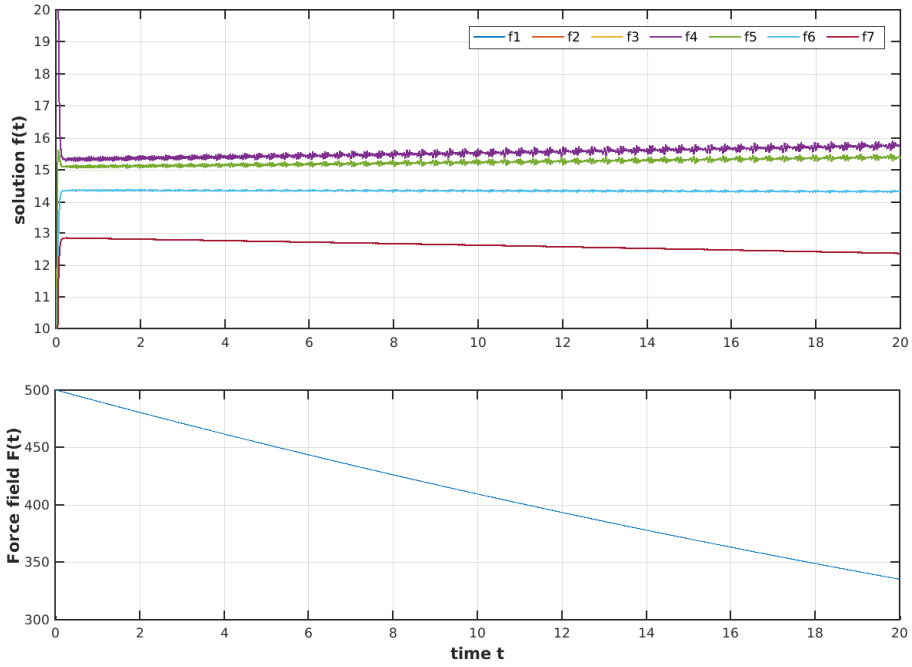

Figure 4.22: Evolution of the system with initial condition **C** under the action of the uniform time dependent external force field B) $F(t) = Be^{-t/b}$, with $B = 500$, $b = 50$.

4.4 Summary

In this chapter we have analysed the pedestrians dynamics subjected to the action of an external force field. In particular, the analysis focused on the model (3.1.2) for specific external force fields, whose functional forms are defined in order to have a physical meaning for the pedestrians model under consideration. The investigation on the system dynamics has been performed through numerical simulations that focus on how the internal dynamics of the system is affected by the presence of an external force field, and on the role of the thermostat in allowing the system to reach a stationary state and in controlling other characteristic of the system. Specifically, the system has been analysed in three cases: in the case of a constant an uniform external force field, that can represent an event where pedestrians are in a hurry to reach the gates (early morning, evacuation alarm); in the case of a constant non uniform external force field, that can represent an event where there are preferential gates to take (for season tickets holders, specific exit gates that allows to reach remarkable place to visit); in the case of a uniform time dependent force field, that can represent an event where there are recurrent announcement in the metro zone, or an alarm situation that fades during time. The results of the numerical simulations can be summarized as follow:

- In the case of an uniform external force field acting on the system (see section 4.1), the thermostat term allows the system to reach a non equilibrium stationary state. Two intrinsic changes emerge from simulations respect to the scenarios where pedestrians dynamics is driven only by internal interactions. Firstly the presence of an external force field prevents the formation of self-organized structures (periods of stuck in time) during the evolution of the system that on the contrary arise considering only the internal dynamics. Secondly, the

pedestrians start to choose all the gates from the beginning of the time evolution. Moreover by increasing the magnitude of the external force field F, the convergence time T needed to reach the asymptotic distribution decreases with F, while the spreading of the asymptotic distribution increases with F. Both these behaviours are in agreement with what is expected. Indeed if the external event that affects pedestrians choice is intense, (magnitude F of the uniform external the force field), the pedestrians are driven to quickly choose a gate, and they reach the asymptotic distribution in less time. The spreading of the asymptotic distribution on the contrary is addressed to the fact that the uniform external force field uniform the behaviour of all pedestrians, acting against the natural concentration of pedestrians towards the center of the gate side. Moreover both the convergence time T and the spread of the asymptotic distribution show a saturation point with respect to the increment of F, that can be addressed to the controlling role of the thermostat term.

- The analysis of the system subjected to a non uniform external force field (see section 4.2) stresses out how a non symmetric external event can break the symmetry of the internal evolution and then of the asymptotic distribution, giving rise to a very heterogeneous dynamics depending strongly on the initial condition. The time evolution of the system is driven by the balance between the action of the external force field and the action of the internal leader-follower dynamics, that is mediated by the magnitude F of the external force field. The thermostat term ensures the conservation of the total number of pedestrians and allows the system to reach an asymptotic state, whose form depends on the functional form of the external force field and its magnitude F, and on the number of gates n. However once fixed these three condition, simulations show that the asymptotic state is qualitative and quantitative the same for all the initial condition we have considered (3.1.5).

- In the case of a time dependent force field (see section 4.3), the system does not reach a stationary state, but it adapts continuously itself to the action of the external force field. Indeed the system try to reach at each instant t the asymptotic state that correspond to the case of a constant external force field of magnitude $F(t)$. This behaviour is controlled by the thermostat term that must ensure the conservation of the total number N of pedestrians. For example, under the action of a periodic external force field, the whole system cannot be in phase with the external force field, because of the conservation of N.

Accordingly to the above results and considerations, the scenario agrees qualitatively with what happens in a real metro station when pedestrians are subjected to the action of an external event (situations of hurry, of evacuation from specific gates, periodic sounds alarms and so on). The time evolution of the system is driven by the balance between the action of the external force field and the action of the internal leader-follower dynamics, that is mediated by the magnitude of the external force field. The thermostat term allows the system to reach a stationary state even this means that even if pedestrians are subjected to an external event, in a long timescale they manage to organize themselves, and this is in agreement with real situations. The existence of a stationary state underlines the capability of the thermostat term in mimic the system capacity of self-organization with respect to the environment accordingly to the physical constraints it is subjected. It is important to underline that the simulations, with their phenomenological interpretations do not cover the whole variety of conceivable pedestrian dynamical situations that can be observed at the entrance of a metro station.

Conclusions

The first part of this thesis work (Chapter 2) has been concerned with the derivation of a new discrete thermostatted kinetic framework for active particles whose microscopic state depends only on the activity variable. The proposed framework is designed to take into account, in addition to the interactions among the individuals of the system, also the effects of external actions that move the system out of equilibrium. For this purpose, the external force field is coupled to a dumping term (thermostat) in the equations, in order to allow the system to reach a stationary state of non-equilibrium. Moreover the thermostat term is designed in order to conserve a general p-order moment of the system during the time evolution. As mentioned in the introduction, this new thermostatted framework is suitable to describe complex systems in life sciences characterized by the fact that the microscopic state is identified by a discrete variable rather than a continuous one, especially when the low number of individuals weakens the assumption of continuity of the distribution function.

The analysis developed for the proposed thermostatted discrete framework refers to the local and global existence and uniqueness of solution of the related Cauchy problem. The proof of the existence of solution has been gained by employing the fundamental theorem of existence of solution for ordinary differential equations, and not strong assumptions have been considered for the internal interactions and for the external force field. It is worth stressing that the well-posedness of the problem is an important topic in the derivation of mathematical frameworks. Indeed if the framework is well-posedness, it can be considered as a paradigm for the derivation of specific models in the applied sciences and a computational analysis can be performed.

From the research perspective viewpoint, many improvements can be considered. An important research perspective is also the mathematical proof of the existence of the non-equilibrium stationary state, which can be pursued by employing fixed point arguments ([56]). Moreover the modeling approach proposed in the present work is based on the assumption that the system is homogeneous in the space and velocity variables. For nonhomogeneous systems, the framework needs to be further generalized for taking into account the role of boundary conditions in bounded and unbounded domains. From the mathematical point of view, the analysis of such a framework appears a hard problem considering the difficulty of the quadratic nonlinearity. It is worth pointing out that the external force field introduced in the framework proposed in this work acts at the macroscopic scale. Further developments of the framework include the possibility to model the interaction with the force field at the microscopic scale. In this context the force field is considered as a known functional subsystem which interacts with the active particles of the main system.

In the second part of this thesis work (Chapter 3 and Chapter 4), we have derived a specific model for pedestrians dynamics in a metro station in the framework of the thermostatted kinetic

theory proposed in Chapter 2. The model is proposed for analysing the time distribution of a finite group of pedestrians approaching at the gates (turnistiles) at the entrance of a metro station. In particular we are interested to analyse the pedestrian dynamics when pedestrian are subjected to an external event that can affect their internal dynamics (sound signals, collective hurry, evacuation alarm). The purpose of the proposed model is to reproduce emerging features of this dynamics, once fixed the interactions among individuals, the initial distribution of pedestrians, and the definition of an external force field coupled with the thermostat term. In the pedestrian modeling we are dealing with the activity variable represents the gate choice performed by a generic pedestrian. The thermostat term is defined in order to keep the number of pedestrians (zero-order moment) constant during the time evolution of the system.

The microscopic interactions among pedestrians are modeled starting by some reasonable phenomenological hypothesis on the pedestrians behaviour that aims to characterize the pedestrians interactions in an essential way. We have considered binary local interactions according to a leader-follower dynamics that depend on the local density of pedestrians. In the analysis we focus on some functional forms of the external force field that have a physical meaning for the pedestrians model under consideration (pedestrians are in a hurry to reach the gates in early morning, preferential gates to take for season tickets holders, specific exit gates that allows to reach remarkable place to visit, recurrent announcement).

Because of the analytical complexity of the model, the system has been investigated by means of numerical analysis. Firstly, simulations have been addressed to the sensitivity analysis of the parameters of the model and on selected initial conditions that have a specific meaning for the model and its applications. Then we have analysed the system when subjected to different magnitudes and functional forms of the external force field. Further computational analysis has been performed for investigating the dynamics for increasing number of gates of the metro.

The first part of the computational analysis (Chapter 3) focus on the internal dynamics of the system (external force field, and consequently the thermostat term, are set to zero). The simulations show that the emergents features arising from the interactions at the microscales reproduce qualitatively some known behaviours of pedestrians when they are approaching to the entrance gates: the flow imposed by the leader dynamics, the concentration of pedestrians in time towards the central gate, the trend to choose progressively all the gates available, and the formation of periods of stuck in time (metastable local states during the time evolution), i.e. instants where pedestrians are thinking about their next choice, or just waiting to see if the situation in front of the gates changes. Some of these emerging behaviours could have been predicted by the looking at the interactions at the microscale, and thus they verify the model (symmetry in the evolution, pedestrian flow imposed by leader dynamics), other of them are emerging collective behaviour (formation of metastable local state, concentration of pedestrian towards the central gate) that underline the complex nature of the system.

The second part of the computational analysis (Chapter 4) has been addressed to analyse pedestrians dynamics when affected by the presence of an external force field. The scenario depicted by the simulations agrees qualitatively with what happens in a real metro station when pedestrians are subjected to the action of an external event. The time evolution of the system is driven by the balance between the action of the external force field and the action of the internal leader-follower dynamics, and this balance is controlled by the magnitude of the external force field. In particular the analysis of the system subjected to a non uniform external force field stresses out

how a non symmetric external event can break the symmetry of the internal evolution and then of the asymptotic distribution, giving rise to a very heterogeneous dynamics depending strongly on the initial condition. The main result shown by simulations is how the thermostat term allows the system to reach a non-equilibrium stationary state and how it keeps the total number of pedestrians constant. The existence of a stationary state for the model then underlines the capability of the thermostat term in mimic the system capacity of self-organization with respect to the environment accordingly to the physical constraints it is subjected to. Indeed, if pedestrians are subjected to an external event, in a long timescale they manage to organize themselves, and this is in agreement with real situations. It is worth stressing that the simulations results with their phenomenological interpretations, do not cover the whole variety of conceivable pedestrian dynamical situations that can be observed at the entrance of a metro station. Moreover only the validation of the model could stress the goodness of these predictively results.

From the research perspective viewpoint, many refinements and improvements can be considered. The microscopic interactions can be modeled differently, by taking into account others characteristic of pedestrians behaviour (for the heterogeneity of pedestrians behaviour see [17], [45]). It is worth stressing that a priori all the modeling are possible, but only the simulations and the subsequent validation of the model can test the model capability to reproduce efficiently the dynamics and the emerging features of the real time distribution of pedestrians in approaching the gates at the entrance of a metro station. Further improvements can be performed by considering by taking into account multiple interactions ([49]).

The modeling approach proposed is based on the assumption that the system is homogeneous in the space and velocity variables. An important research improvement for the proposed model would be the introduction of the mechanical variable of space and velocity. The introduction of the mechanical variables would allow a more realistic modeling of pedestrian dynamics in a metro station, by taking into account the velocity of the pedestrians and their movements within the metro zone ([68]). For example events like evacuations could be suitable modeled with this approach ([67]). Moreover macroscopic observable quantities such as local density or the flux of pedestrians can be introduced for the studying of the model, by analogy with some traffic models ([66]). However, as pointed out in the previous section, for nonhomogeneous systems the thermostatted framework needs to be further generalized. Finally the model should be validate. The validation of the model can be based on a suitable comparison between predictions of the model and empirical data ([69]).

Bibliography

[1] C. Bianca, N. Bellomo, *Towards a Mathematical Theory of Complex Biological Systems*, Series in Mathematical an Biological Medicine, Vol. 11, World Scientific, 2011.

[2] R. Erban, H. G. Othmer, *From individual to collective behaviour in bacteria chemotaxis*, SIAM Journal of Applied Mathematics 65 (2004), 361-391.

[3] S.L. Levin, *Complex adaptive systems: exploring the known, the unknown and the unknowable*, American Mathematical Society Bulletin 40 (2002), 3-19.

[4] F. Schweitzer, *Brownian Agents and Active Particles*, Springer- Verlag, Berlin, 2003.

[5] D. Helbing, *Stochastic and Boltzmann-like models for behavioural changes, and their relation to game theory*, Physica A 269 (1999), 511-526.

[6] C. Bianca, *Onset of nonlinearity in thermostatted active particles models for complex systems*, Nonlinear Analysis: Real World Applications 13, (2012) 2593-2608.

[7] N. Bellomo, C. Bianca, M. Delitala, *Complexity analysis and mathematical tools towards the modelling of living systems*, Physics of Life Reviews 6 (2009), 144-175.

[8] E. De Angelis , M. Delitala, *Modelling complex systems in applied sciences; methods and tools of the mathematical kinetic theory for active particles*, Mathematical and Computer Modelling Volume 43 (2006), 1310–1328.

[9] M.L. Bertotti, M. Delitala *From discrete kintetic and stochastic game theory to modeling complex systems in applied sciences*, Mathematica Models and Methods in Applied Sciences, Vol. 14, No. 7 (2004) 1061-1084.

[10] N. Bellomo, A. Bellouquidb, *On the mathematical kinetic theory of active particles with discrete states: The derivation of macroscopic equations*, Mathematical and Computer Modelling Volume 44 (2006), 397–404.

[11] A. Chauviere, I. Brazzoli, *On the discrete kinetic theory for active particles. Mathematical tools.*, Mathematical and Computer Modelling: An International Journal archive, Volume 43 (2006), 933-944.

[12] G. Ajmone Marsan, N. Bellomo, M. Egidi, *Towards a mathematical theory of complex socio-economical systems by functional subsystems representation*, Kinetic and Related Models 2008, 1:249-278.

[13] B. Perthame, *Transport equation in biology*, Basel:Birtkäuser; 2007.

[14] G.F. Webb, *Theory of non-linear age dependent population dynamics*, New York: Marcel Dekker, 1985.

[15] N. Bellomo, M. Delitala, V. Coscia, *From the mathematical kinetic, and stochastic game theory to modelling mutations, onset, progression and immune competition of cancer cells*, Physics of Life Reviews 2008, 5:183-206.

[16] B. Kerner, *The Physics of Traffic: Empirical Freeway Pattern Features, Engineering Applications, and Theory*, Springer, Berlin, 2004.

[17] H. Timmermans, *Pedestrian Behavior: Models, Data Collection and Applications*, Emerald Group Publishing Limited, Bingley (UK), 2009.

[18] M. Ballerini, N. Cabibbo, R. Candelier, A. Cavagna, E. Cisbani, I. Giardina, et al, *Interaction ruling animal collective behaviour depends on topological rather than metric distance: Evidence from a field study.* Proc Natl Acad Sci 105 (2008), 1232-1237.

[19] E. Bonabeau, G. Theraulaz, J.L. Deneubourgs, *Mathematical model of self-organizing hierarchies in animal societies*, Bull Math Biol 58 (1996), 661-717.

[20] D.J. Krause, G.D. Ruxton, *Living in groups*, Oxford: Oxford University Press, 2002.

[21] C. Bianca, *Mathematical Modeling for Keloid Formation triggered by virus: malignant effects and immune system competition*, Mathematical Models and Methods in Applied Sciences 2011, 21: 389-419.

[22] C. Bianca, *Kinetic theory for acive particles modelling coupled to Gaussian Thermostats*, Applied Mathematical Science,6 (2012) 651-660.

[23] T. Chou, K. Mallick, R. K. P. Zia, *Non-equilibrium statistical mechanics: From a paradigmatic model to biological transport*, Reports on Progress in Physics, v74, 116601, (2011).

[24] D. L. DeAngelis, J. C. Waterhouse, *Equilibrium and Nonequilibrium Concepts in Ecological Models*, Ecological Monographs Vol. 57, No. 1 (Mar., 1987), pp. 1-21.

[25] Š. Volner, *The importance of non-equilibrium in the development of economic system (thermodynamic approach)*, Foresight,(2015) Vol. 17 Iss: 1, pp.74 - 84.

[26] C., M. Marsili, A. Vespignani, *Nonequilibrium Phase Transition in a Model for Social Influence*, Phys. Rev. Lett. 85, 3536, 2000.

[27] J. Kachroo, *Pedestrian Dynamics: Mathematical Theory and Evacuation Control*, CRC Press, Boca Raton-FL, 2009.

[28] D.J. Evans, G.P. Morris, *Statistical Mechanics of Nonequilibrium Liquids*, Academic Press, New York, 1990.

[29] X. Yong, L.T. Zhang *Thermostats and thermostat strategies for molecular dynamics simulations of nanofluidics*, Journal of Chemical Physics, 138 :084503 (2013).

[30] C. Huang, A. Varghese, G. Gompper, R. G. Winkler, *Thermostat for non-equilibrium multiparticle collision dynamics simulations*, Phys. Rev. E 91, 013310 (2015).

[31] O.G. Jepps, L. Rondoni, *Deterministic thermostats, theories of nonequilibrium systems and parallels with the ergodic condition*, J. Phys. A: Math. Theor. 43 (2010) 133001.

[32] C. Lanczos, *The Variational Principles of Mechanics, Dover, New York,1979*

[33] L.V. Woodcock, *Isothermal molecular dynamics calculation for liquid salts*, Chemical Physics Letters 10 (1971), 257-261.

[34] M. Delitala, A. Tosin, *Mathematical modeling of vehicular traffic: a discrete kinetic theory approach*, Mathematical Models and Methods in Applied Sciences, 2008, 18:1193-1216.

[35] M.L. Bertotti, M. Delitala, *Conservation laws and asymptotic behaviour of a model of social dynamics*, Nonlinear Analysis RWA 2008, 9:183-196.

[36] N. Bellomo, B. Carbonaro, *On the complexity of multiple interactions with additional reasoning about Kate, Jules and Jim*, Mathematical and Computer Modeling, 2008, 47:160-171.

[37] B. Carbonaro, C. Giordano, *A second step towards mathematical models in psychology: a stochastic description of human feelings*, Mathematical and Computer Modeling, 2005, 41:587-614.

[38] M. Loschiavo, *The modeling of political dynamics by generalized kinetic (Boltzmann) models*, Mathematical and Computer Modeling, 2003, 37:261-281.

[39] M. Loschiavo, *A dynamical model of electoral competition*, Mathematical and Computer Modeling, 2006, 43:1288-1309.

[40] L. Arlotti, E. De Angelis *On the initial value problem of a class of models of the kinetic theory for active particles*, Applied Mathematics Letters 24 (2011), 257-263.

[41] G.P. Morris, C.P. Dettmann, *Thermostats: analysis and application*, Chaos 8 (1998), 321-333.

[42] K.F. Gauss, *Uber ein Neues Allgemeines Grundesatz der Mechanik*, Journal für die Reine und Angewandte Mathematik 4 (1829), 232-235.

[43] C.Bianca, *Thermostated kinetic equations as models for complex systems in phyisics and life sciences*, Physics of life Rewievs 9, (2012) 359-399.

[44] C. Mogno, C. Bianca, *Qualitative analysis of a discrete thermostatted kinetic framework modeling complex adaptive systems*, submitted.

[45] K.Rio, W.H. Warren, *A data driven model of pedestrian following and emergent crowd behaviour*, Department of Cognitive, Linguistic, and Psychological Sciences Brown University Providence, RI, USA. 2012.

[46] L. Arlotti, E. De Angelis, L.Fermo, M. Lachowicz, N.Bellomo, *On a class of integro-differential equations modelling complex systems with nonlinear interactions*, Applied Mathematics Letters 25 (2012), 490-495.

[47] N. Bellomo, C.Bianca, M.S. Mongiovì, *On the modeling of nonlinear interactions in large complex systems*, Applied Mathematics Letters 23 (2010), 1372-1377.

[48] F. Fasso, *Dispense per il corso di Istituzioni di Fisica Matematica.*,CLEUP, Padova, 2013.

[49] C. Bianca, *New Research Perspectives on Thermostatted Kinetic Models*, Journal of Mathematics and Statistics 2015, 11 (1): 16.20.

[50] Dormand, J. R. and P. J. Prince, *A family of embedded Runge-Kutta formulae*, J. Comp. Appl. Math., Vol. 6, 1980, pp. 19–26.

[51] Shampine, L. F. and M. W. Reichelt, *The MATLAB ODE Suite*, SIAM Journal on Scientific Computing, Vol. 18, 1997, pp. 1–22.

[52] C. Daganzo, *Requiem for second order fluid approximations of traffic flow*, Transportation Research B 29B (1995), 277-286.

[53] C. Dogbe, *On the modelling of crowd dynamics by generalized kinetic models*, Journal of Mathematical Analysis and Applications 387 (2012), 512-532.

[54] L. Gramani, *On the modeling of granular traffic flow by the kinetic theory for active particles. Trend to equilibrium and macroscopic behaviour*, International Journal of Nonlinear Mechanics 44 (2009), 263-268.

[55] C. Bianca, *New research perspectives on thermostatted kinetic models*, Journal of Mathematics and Statistics 11 (2015), 16-20.

[56] C. Bianca, *Existence of stationary solutions in kinetic models with Gaussian thermostats*, Mathematical Methods in the Applied Sciences 36 (2013), 1768-1775.

[57] Z. Zhang, D. Bi, *Bifurcation analysis in a delayed computer virus model with the effect of external computers*, Advances in Difference Equations, 317, (2015).

[58] Y. Kuang, *Delay Differential Equations with Applications in Population Dynamics*, vol. 191 of Mathematics in Science and Engineering, Academic Press, Boston, Mass, USA, 1993.

[59] T. Erneux, *Applied Delay Differential Equations*, Springer, New York, NY, USA, 2009.

[60] M. J. Piotrowska, *A remark on the ODE with two discrete delays*, Journal of Mathematical Analysis and Applications 329 (2007), 664-676.

[61] C.G. Li, M. Kostic, M. Li, S. Piskarev, *On a class of time-fractional differential equations*, Fractional Calculus and Applied Analysis 15 (2012), 639-668.

[62] S. Sivasundaram, J. Uvah, *Controllability of impulsive hybrid integro-differential systems*, Nonlinear Analysis: Hybrid Systems 2 (2008), 1003-1009.

[63] Y. Dolak, C. Schmeiser, *Kinetic models for chemotaxis: Hydrodynamic limits and spatio-temporal mechanisms*, J Math Biol 51 (2005), 595-615.

[64] C. Bianca, C. Dogbe, *Kinetic models coupled with Gaussian thermostats: Macroscopic frameworks*, Nonlinearity 27 (2014), 2771-2803.

[65] C. Bianca, C. Dogbe, *On the Boltzmann gas mixture equation: Linking the kinetic and fluid regimes*, Communications in Nonlinear Science and Numerical Simulation 29 (2015), 240-256.

[66] C. Bianca, V. Coscia *On the coupling of steady and adaptive velocity grids in vehicular traffic modelling*, Appl. Math. Lett., 24(2):149-155, 2011.

[67] J. P. Agnelli, F. Colasuonno, and D. Knopoff, *A kinetic theory approach to the dynamics of crowd evacuation from bounded domains*, Math. Models Methods Appl. Sci. 25, 109 (2015).

[68] *Mathematical Modeling of Crowds Dynamics: Complexity and Kinetic Approach*, Nonlinear Studies. 2012, Vol. 19 Issue 3, p371-380.

[69] N. Bellomo, C. Bianca, V. Coscia, *On the modeling of crowds dynamics: an overview and research perspectives*, SeMA Journal(2011) 54:25-46.

[70] S. Buchmuller and U. Weidman, *Parameters of pedestrians, pedestrian traffic and walking facilities*, ETH Report Nr.132, October, (2006).